

Precision Spectroscopy of Pionic Atoms at RIBF and Deduction of Chiral Condensate at Nuclear Density

**RIKEN Nishina Center
Kenta Itahashi**

published 2023/3

nature physics

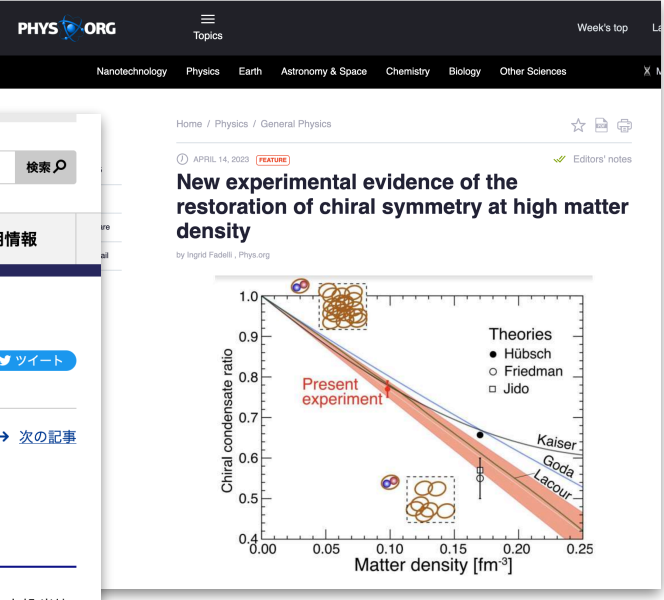
T. Nishi, K.I. et al., Nat. Phys. 19, 788(2023)

Article

<https://doi.org/10.1038/s41567-023-02001-x>

**Chiral symmetry restoration at high matter
density observed in pionic atoms**

- Nature Physics **19**, 788 (2023/3/23)
Article DOI: 10.1038/s41567-023-02001-x
- Nature Physics **19**, 764 (2023/3/23)
News and Views "Modified in Medium"



PHYS. ORG

P

Nature Physics 19, 764 (2023/3/23)
News and Views "Modified in Medium"

naturephysics

Explore content ▾ About the journal ▾ Publish with us ▾

nature > nature physics > news & views > article

News & Views | Published: 23 March 2023

Nuclear physics

Modified in medium

Sean Freeman✉

Nature Physics 19, 764–765 (2023) | [Cite this article](#)

411 Accesses | 2 Altmetric | [Metrics](#)

The strong interaction is modified in the presence of nuclear matter. An experiment has now quantified with high precision and accuracy the reduction of the order parameter of the system's chiral symmetry, which is partially restored.

The vacuum state of quantum chromodynamics (QCD) sounds dull, boring and empty. However, due to the strength of the strong force underlying QCD, it turns out to be extremely complex and is teeming with pairs of virtual particles that cannot be directly observed.

プレスリリース

理化学研究所

理研について 研究室紹介 研究成果（プレスリリース） 広報活動 産学連携 採用情報

Home > 研究成果（プレスリリース） > 研究成果（プレスリリース）2023

2023年3月27日 前の記事 一覧へ戻る 次の記事
理化学研究所

“π”で探る真空の秘密

—真空に隠された構造「クォーク凝縮」の精密測定に成功—

理化学研究所（理研）仁科加速器科学研究センター 加速器基盤研究部の西 隆博 研究員、中間子科学研究室の板橋 健太 専任研究員（開拓研究本部 岩崎 中間子科学研究室 専任研究員）、奈良女子大学 理学部 数物科学科の比連崎 恒 教授、鳥取大学 農学部 生命環境農学科の池野 なつ美 講師、大阪大学 核物理研究センター 核物理理論研究部門の野瀬-外川 直子 協同研究員らの国際共同研究グループは、 π （パイ）中間子^[1]が原子核に束縛された π 中間子原子の精密測定を行い、真空が空っぽの空間ではなく、見えない構造を隠し持つことを示す実験結果を得ることに成功しました。

一般に真空は、「空（から）」の空間を意味しますが、現代物理学の理論によると、宇宙がビッグバン以降広がりながら冷えていく過程で、クォーク^[2]と反クォーク^[2]の対が空間に凝縮（クォーク凝縮^[3]）し、真空を満たした状態です。この理論は物質の質量の起源に関する基礎的理論である一方、実験的な実証が課題でした。クォーク凝縮は直接には観測できませんが、環境の温度や物質密度によって変化し、クォーク凝縮の量が変化したことの影響は

Nishina Center nta Itahashi

published 2023/3

naturephysics

T. Nishi, K.I. et al., Nat. Phys. 19, 788(2023)

Article

<https://doi.org/10.1038/s41567-023-02001-x>

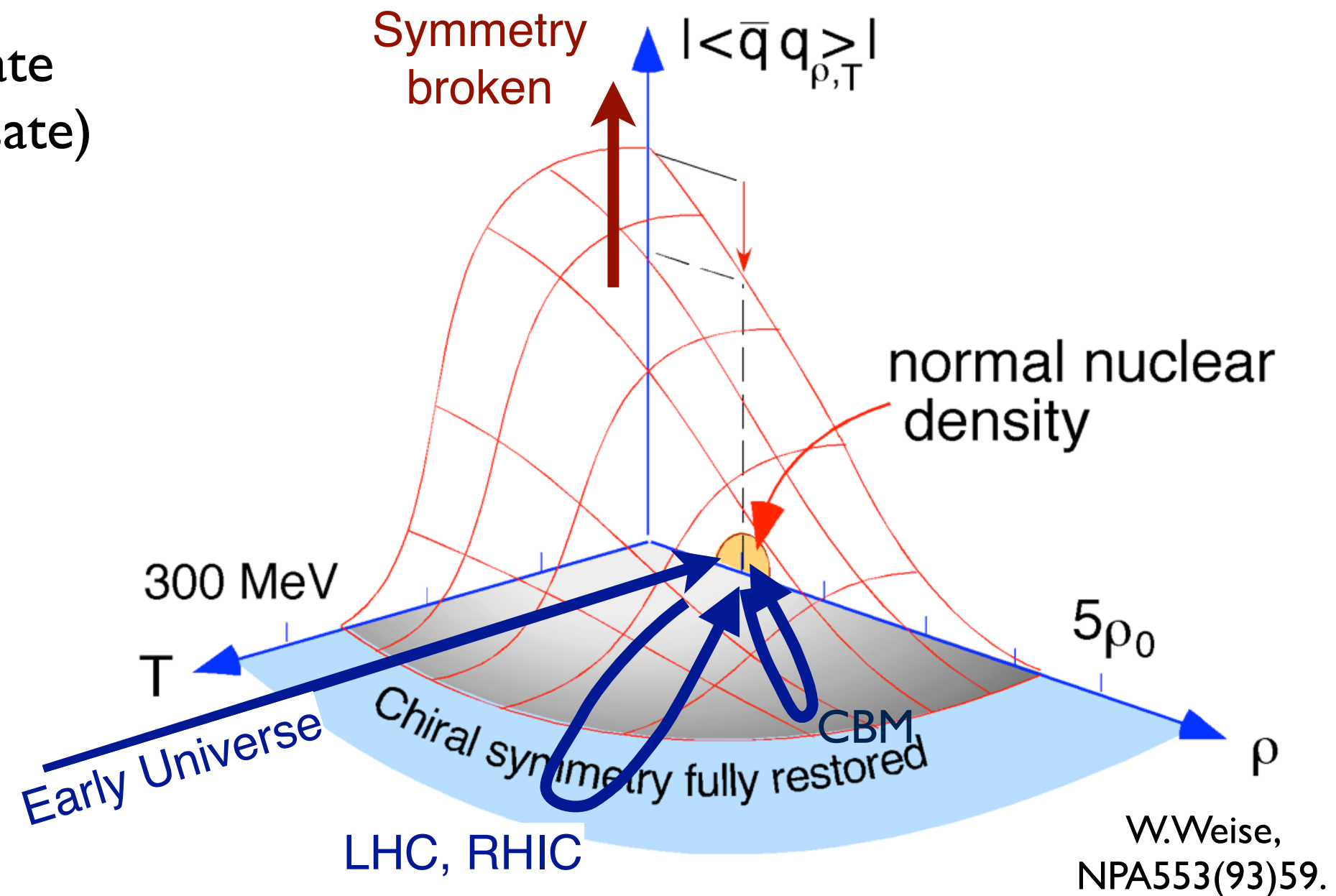
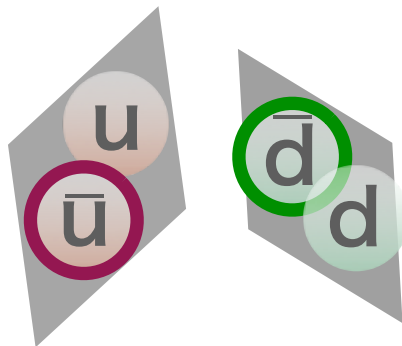
Chiral symmetry restoration at high matter density observed in pionic atoms

- Nature Physics 19, 788 (2023/3/23)
Article DOI: 10.1038/s41567-023-02001-x
- Nature Physics 19, 764 (2023/3/23)
News and Views "Modified in Medium"

Chiral Condensate

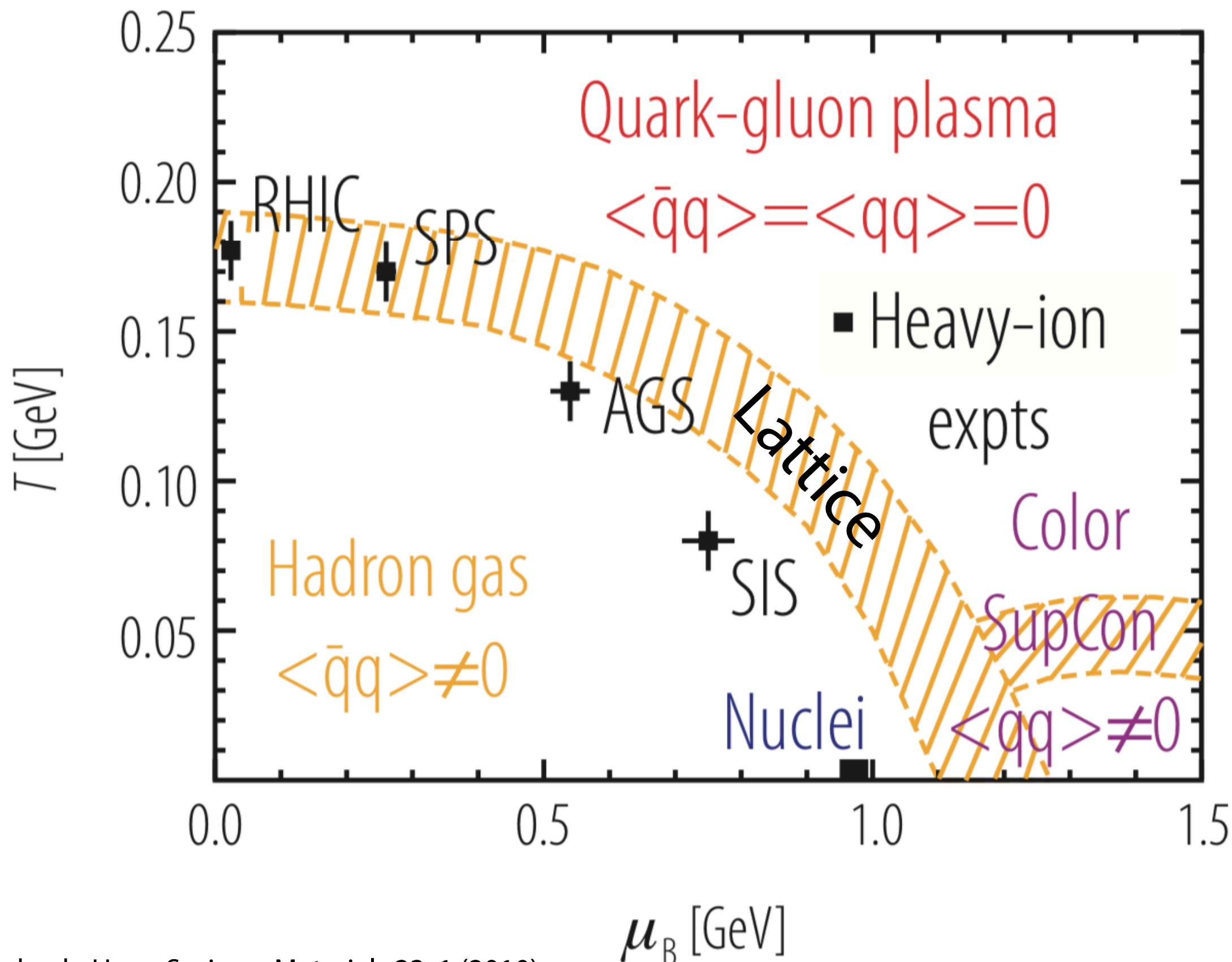
Order parameter of chiral symmetry depends on T and ρ

Chiral condensate
(= quark condensate)



Analysis of material properties
of QCD vacuum

QCD phase and chemical freezeout points



Chiral transition & Quark confinement

Correlation between Confinement and CSB is suggested by
Simultaneous Phase Transition of
Deconfinement and Chiral Restoration.

Lattice QCD results at finite temperature F. Karsch, Lect. Notes Phys. (2002)

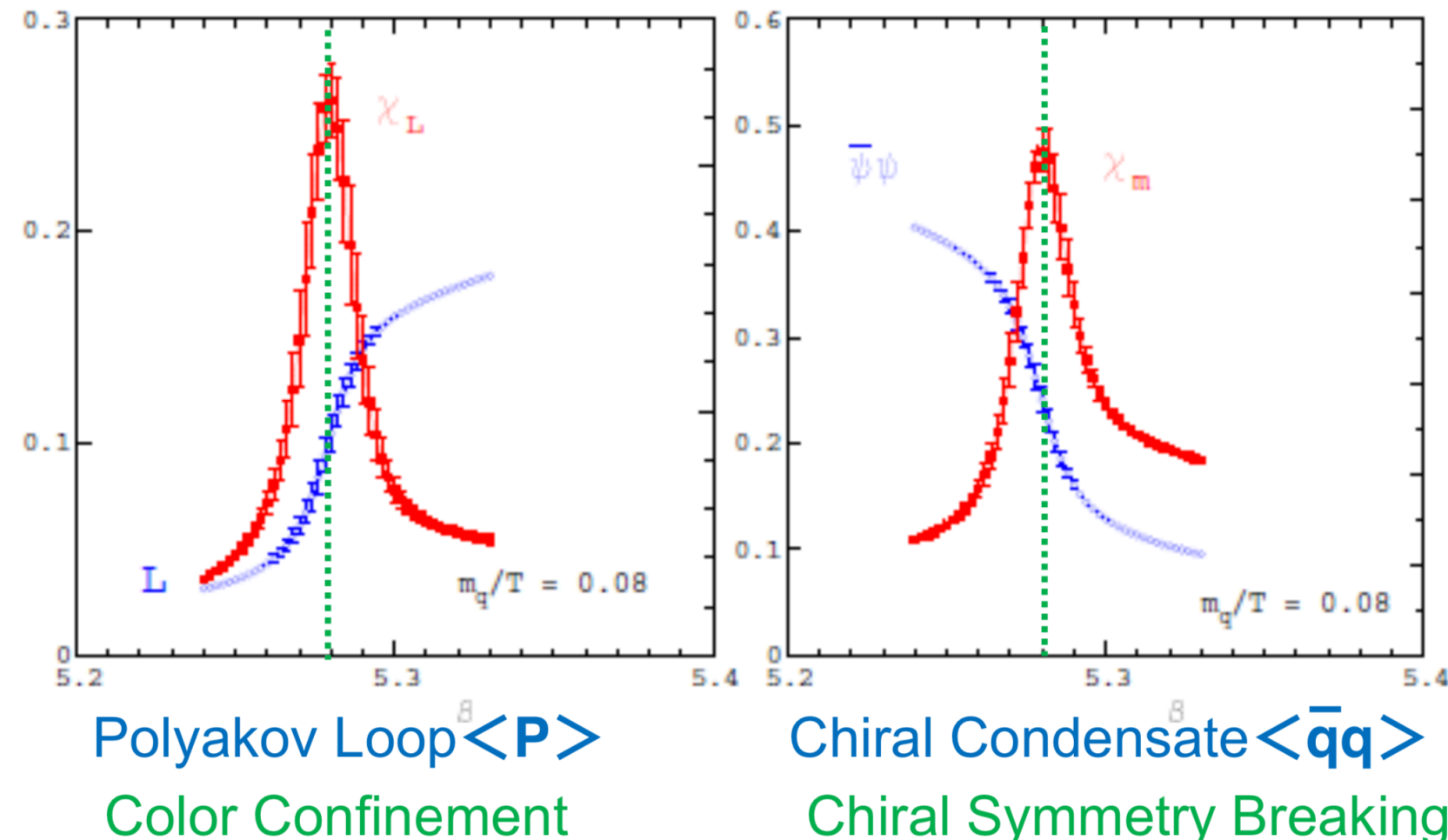


Fig. 2. Deconfinement and chiral symmetry restoration in 2-flavour QCD: Shown is $\langle L \rangle$ (left), which is the order parameter for deconfinement in the pure gauge limit ($m_q \rightarrow \infty$), and $\langle \bar{\psi} \psi \rangle$ (right), which is the order parameter for chiral symmetry breaking in the chiral limit ($m_q \rightarrow 0$). Also shown are the corresponding susceptibilities as a function of the coupling $\beta = 6/g^2$.

Chiral transition & Quark confinement

Correlation between Confinement and CSB is suggested by
Simultaneous Phase Transition of
Deconfinement and Chiral Restoration.

Lattice QCD results at finite temperature F. Karsch, Lect. Notes Phys. (2002)



Color confinement and CSB

Existence of correlation is obvious however
the details are not yet known

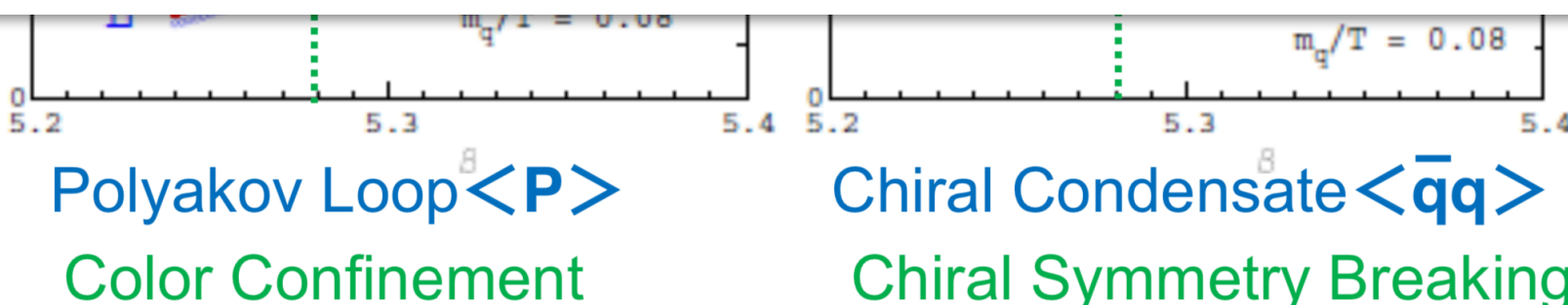
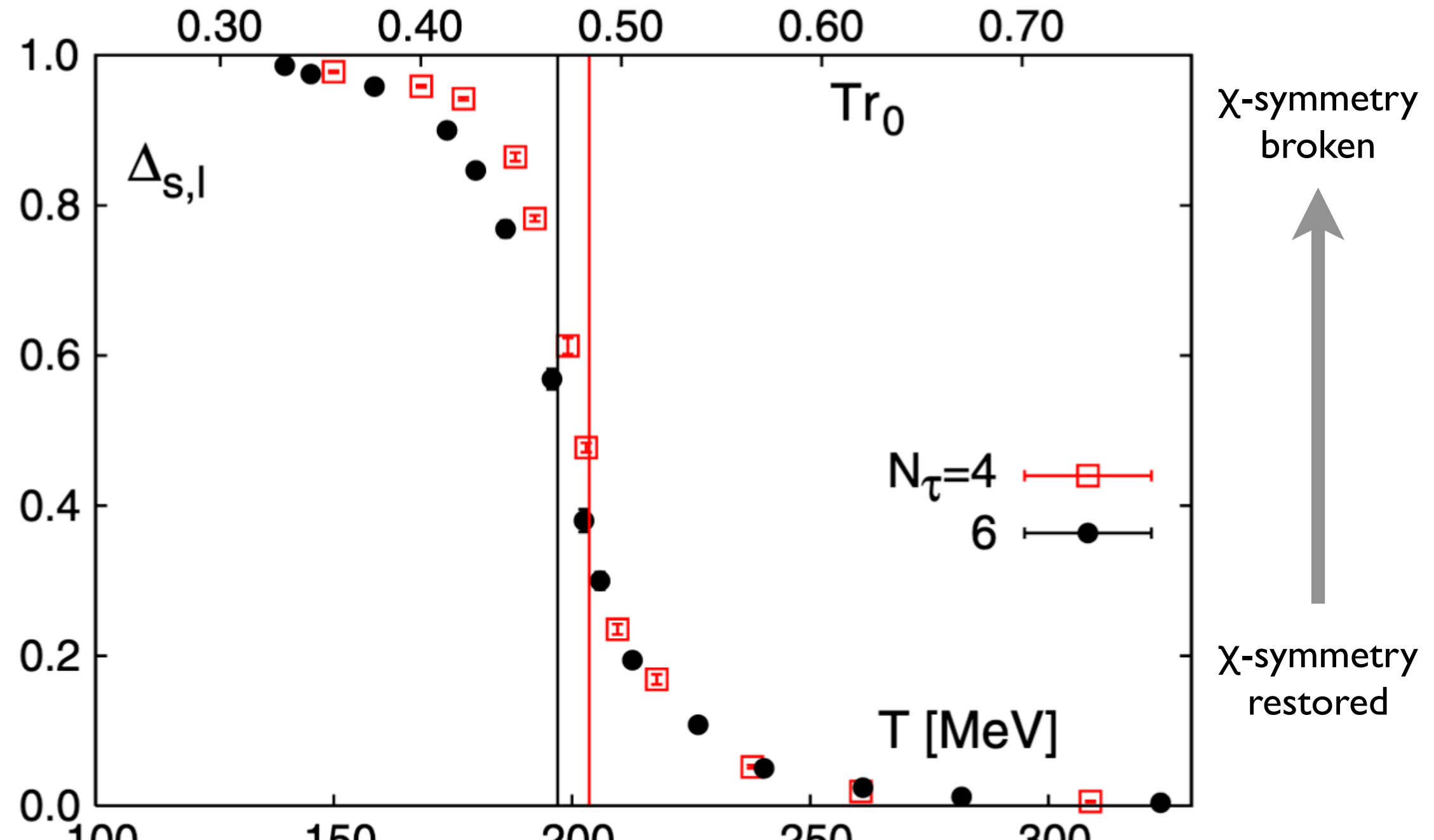


Fig. 2. Deconfinement and chiral symmetry restoration in 2-flavour QCD: Shown is $\langle L \rangle$ (left), which is the order parameter for deconfinement in the pure gauge limit ($m_q \rightarrow \infty$), and $\langle \bar{\psi}\psi \rangle$ (right), which is the order parameter for chiral symmetry breaking in the chiral limit ($m_q \rightarrow 0$). Also shown are the corresponding susceptibilities as a function of the coupling $\beta = 6/g^2$.

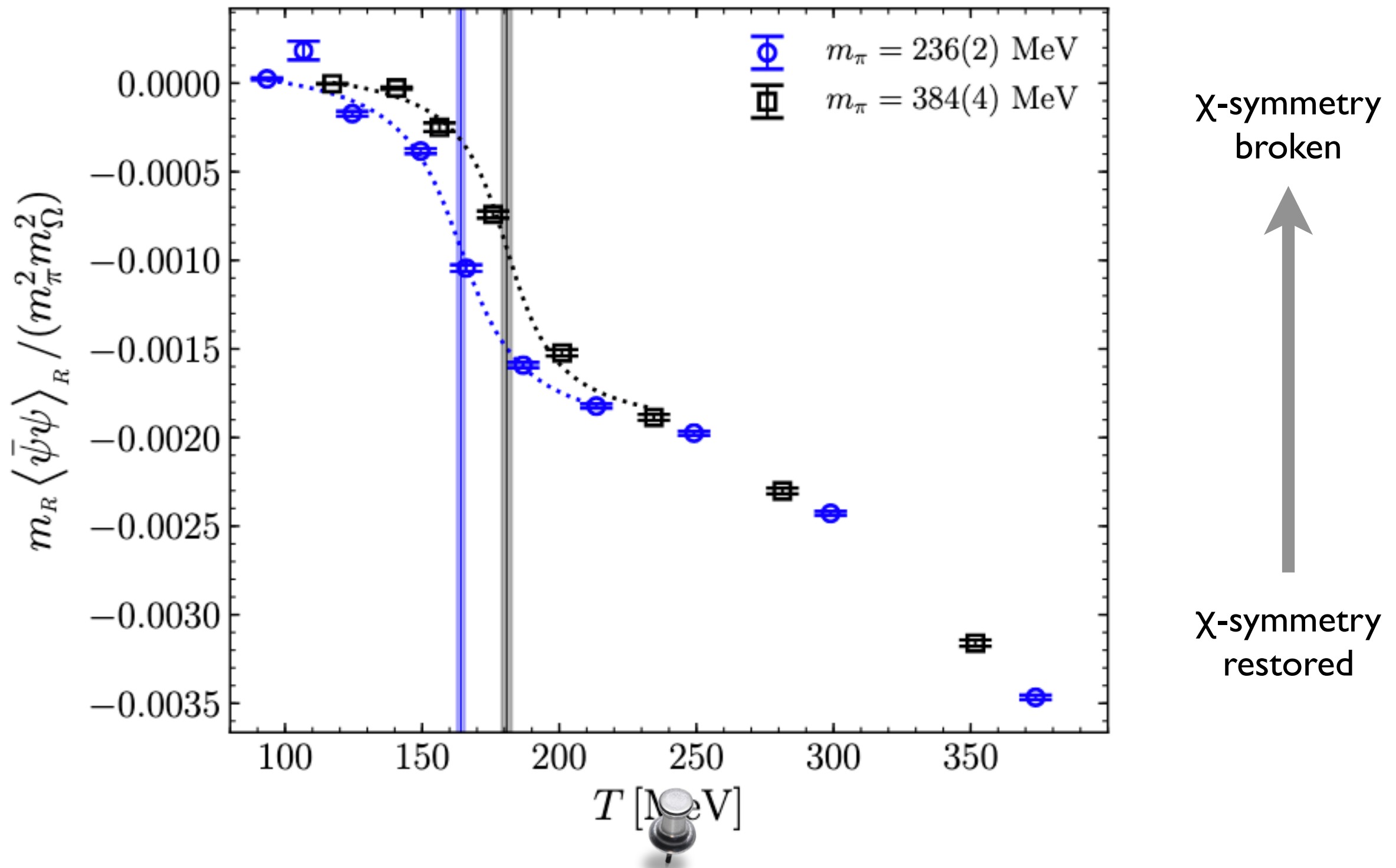
Lattice QCD calculated T dependence of chiral condensate



Temperature dependence of the chiral condensate from lattice

QCD with 2 + 1 quark flavours and almost physical quark masses

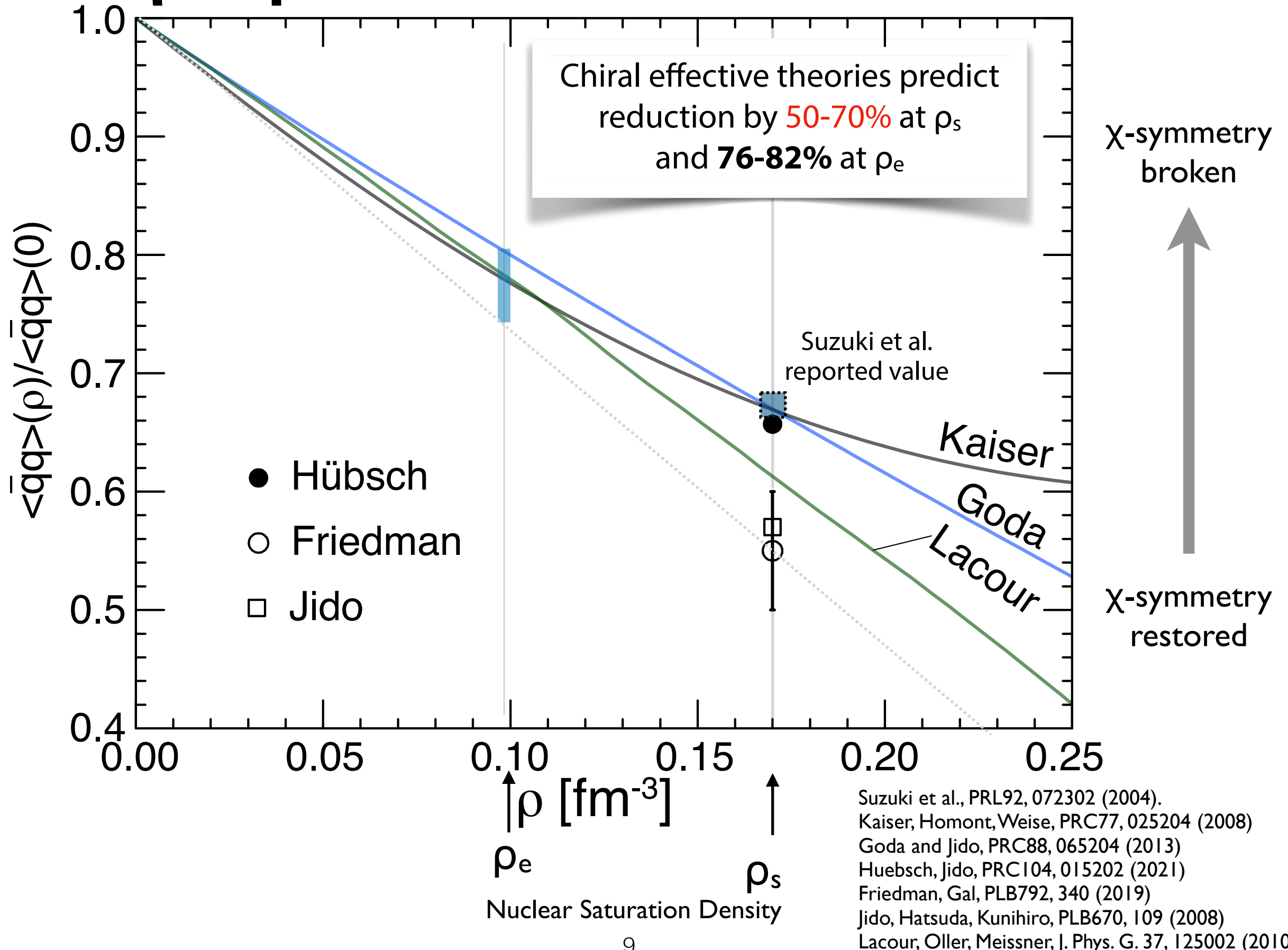
Lattice QCD calculated T dependence of chiral condensate



Remark: sign problem makes it difficult
for lattice to approach non-zero ρ region

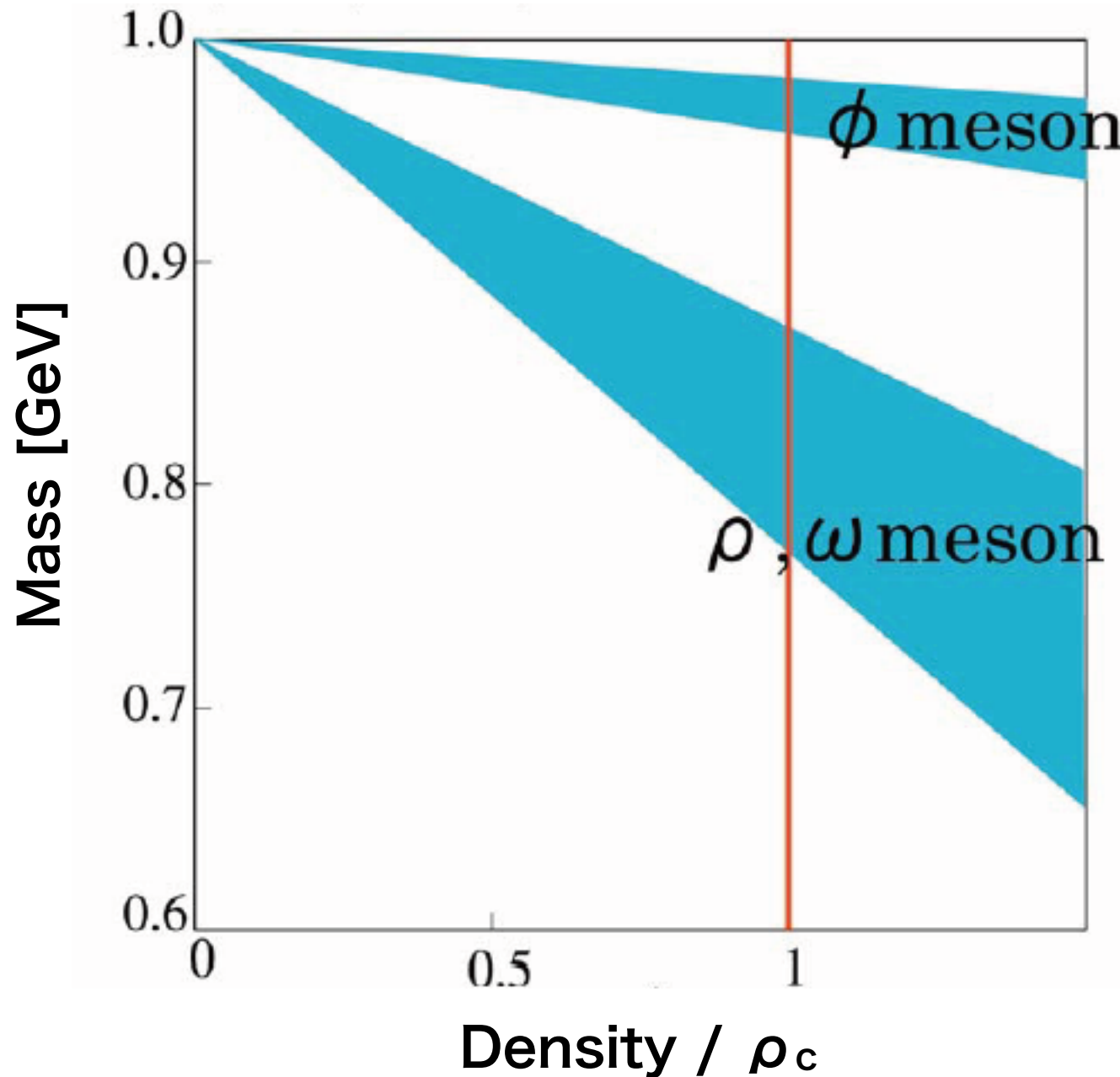
Jon-Ivar Skullerud
PRD105(2022)034504

ρ dependence of chiral condensate



Meson masses and QCD medium effect

Vector meson mass modification in QCD sum rule (J-PARC E16)



$\phi(1020)$

$I^G(J^{PC}) = 0^-(1^{--})$
Mass $m = 1019.455 \pm 0.020$ MeV (S = 1.1)
Full width $\Gamma = 4.26 \pm 0.04$ MeV (S = 1.4)

$\phi(1020)$ DECAY MODES

	Fraction (Γ_i/Γ)	Scale factor/ Confidence level	p (MeV/c)
$K^+ K^-$	(48.9 \pm 0.5) %	S=1.1	127
$K_L^0 K_S^0$	(34.2 \pm 0.4) %	S=1.1	110
$\ell^+ \ell^-$	—		510
$e^+ e^-$	$(2.954 \pm 0.030) \times 10^{-4}$	S=1.1	510
$\mu^+ \mu^-$	$(2.87 \pm 0.19) \times 10^{-4}$		499

$\rho(770)$ [h]

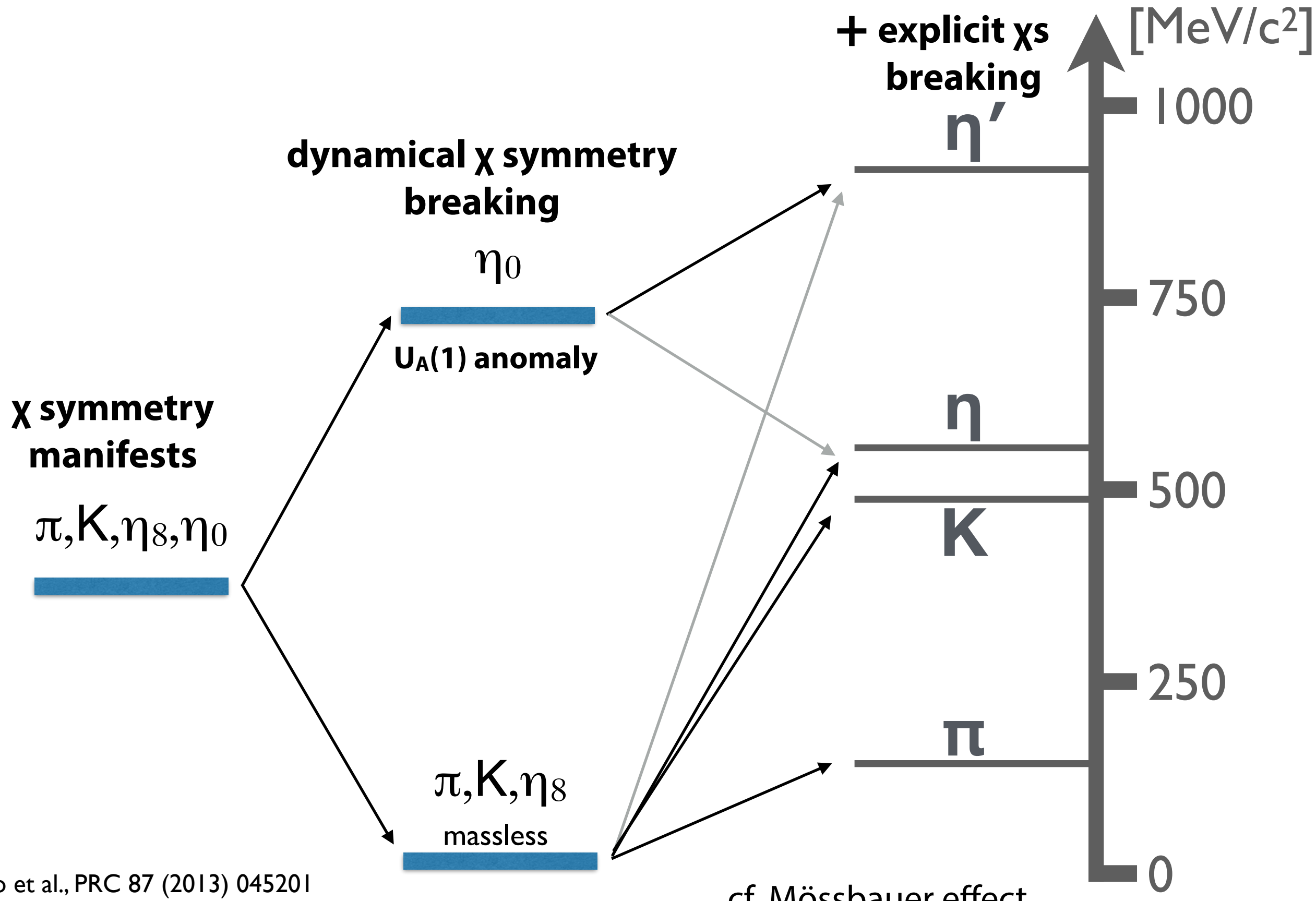
$I^G(J^{PC}) = 1^+(1^{--})$
Mass $m = 775.49 \pm 0.34$ MeV
Full width $\Gamma = 149.1 \pm 0.8$ MeV
 $\Gamma_{ee} = 7.04 \pm 0.06$ keV

$\omega(782)$

$I^G(J^{PC}) = 0^-(1^{--})$
Mass $m = 782.65 \pm 0.12$ MeV (S = 1.9)
Full width $\Gamma = 8.49 \pm 0.08$ MeV
 $\Gamma_{ee} = 0.60 \pm 0.02$ keV

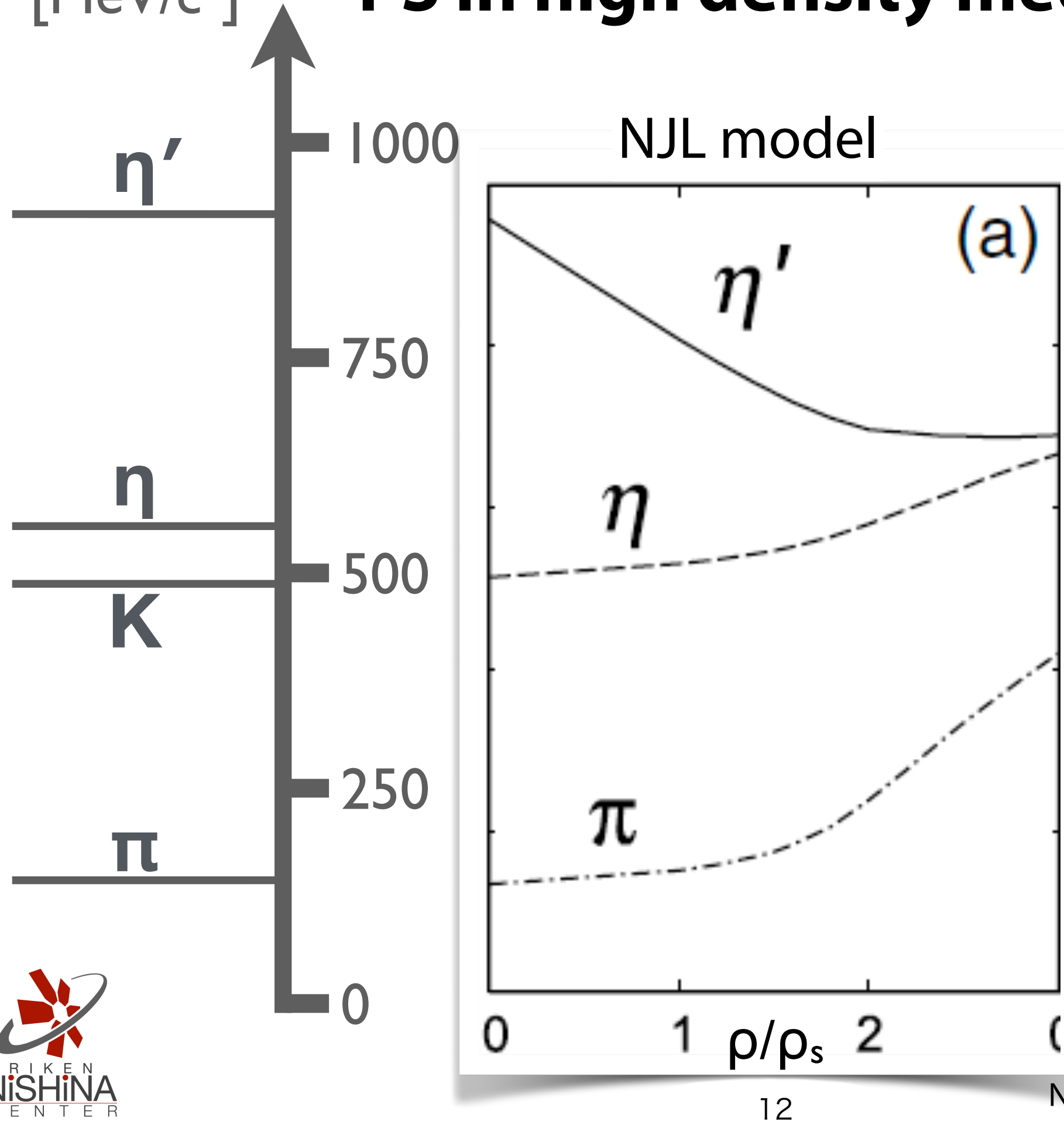
Masses of Pseudo-Scalar Mesons

with various symmetry breaking patterns



[MeV/c²]

PS in high density medium

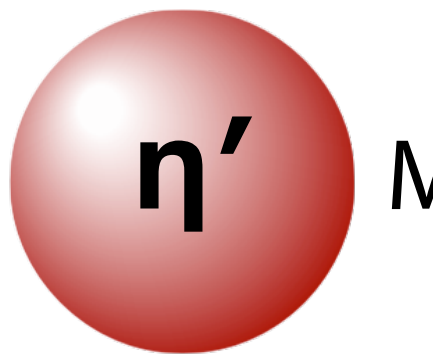


REMARK

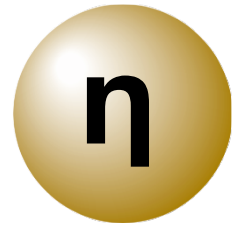
Systematic measurement
is important.

Pseudo-scalar mesons

(in the lowest-mass nonet)



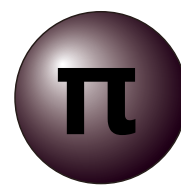
$M=958 \text{ MeV}/c^2$



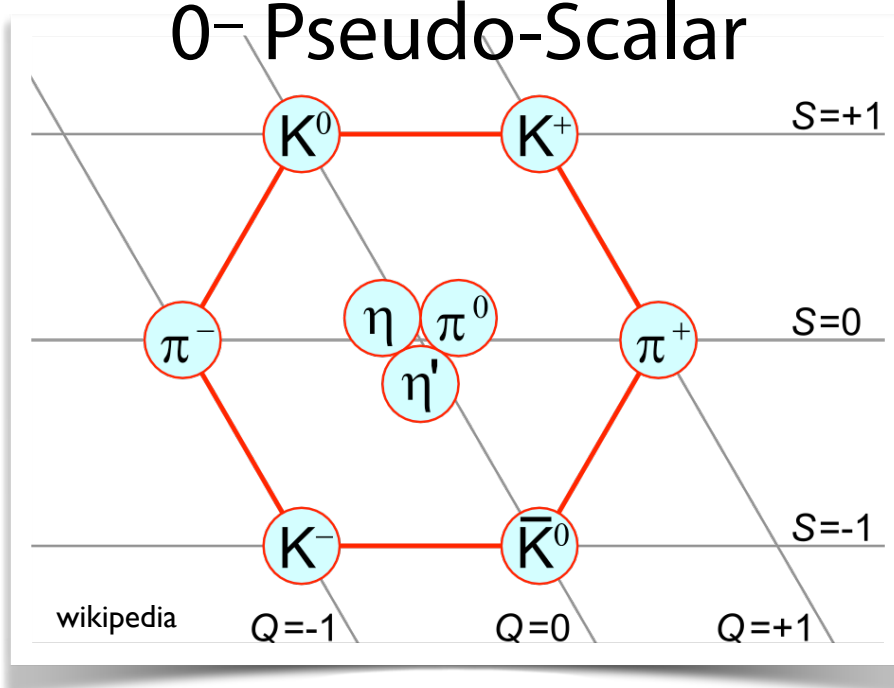
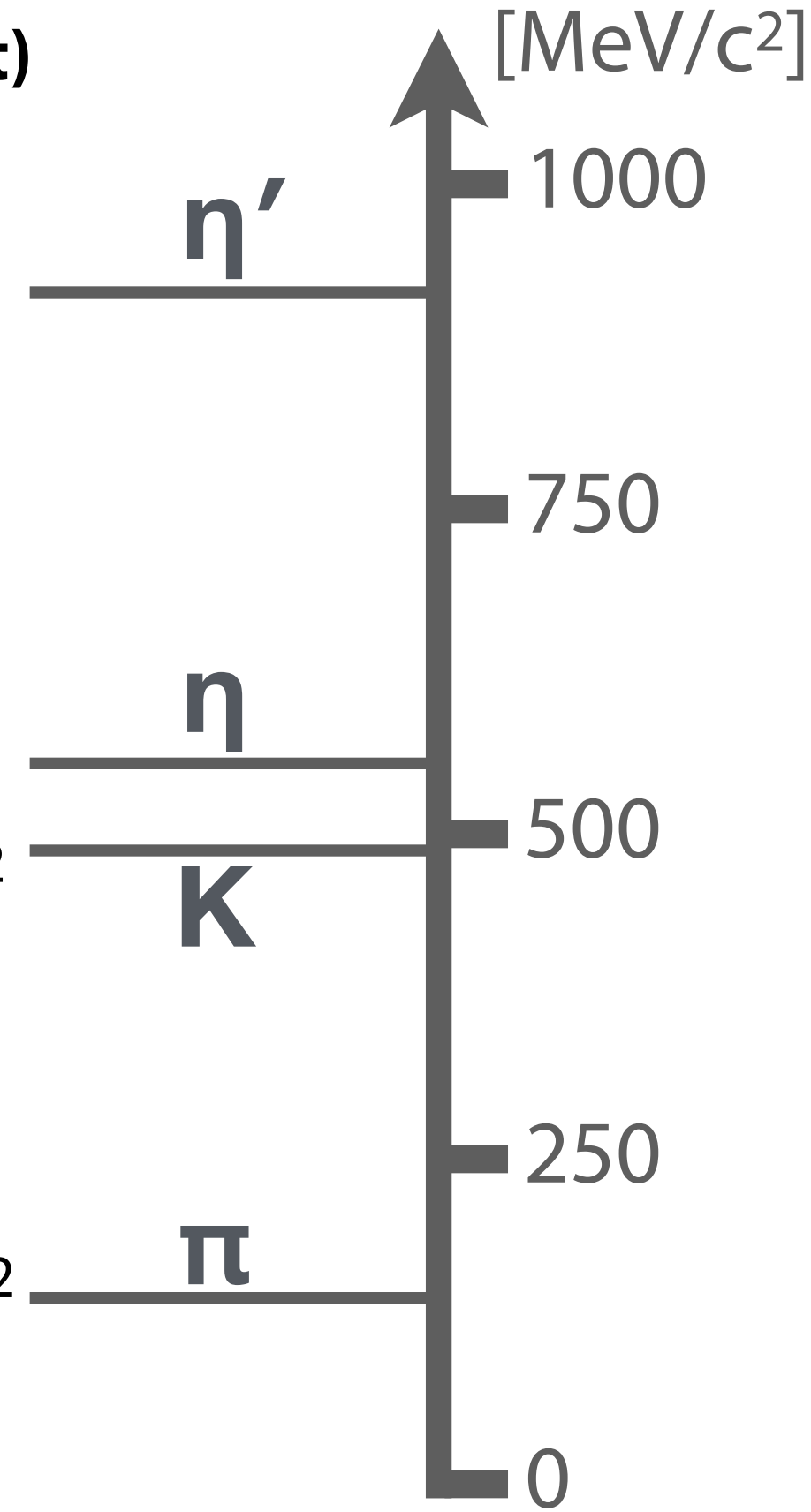
$M=548 \text{ MeV}/c^2$



$M=498 \text{ MeV}/c^2$



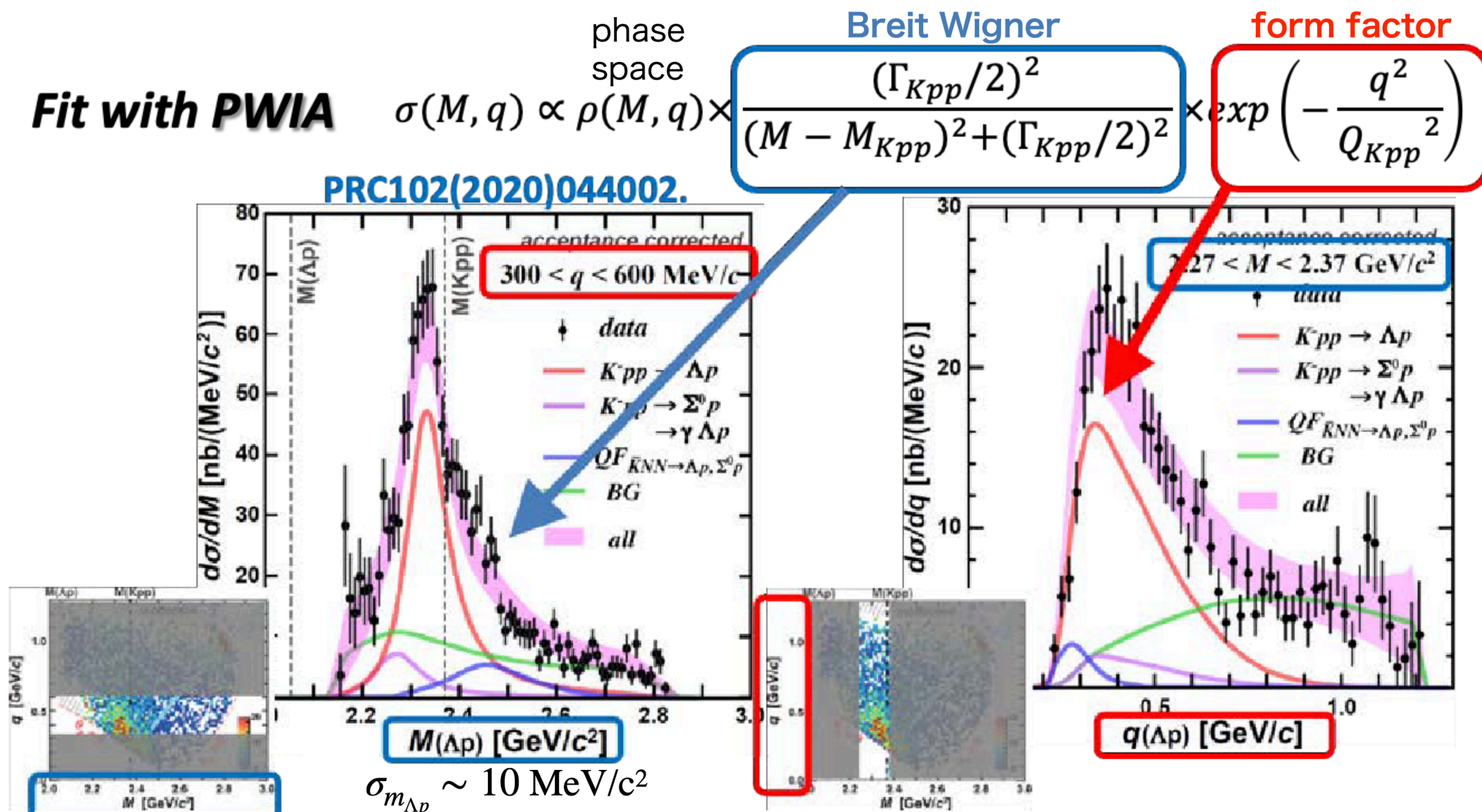
$M=140 \text{ MeV}/c^2$



Spectroscopy of $K\text{-}pp$ bound states

2D Fit for the “ $\bar{K}NN$ ” state

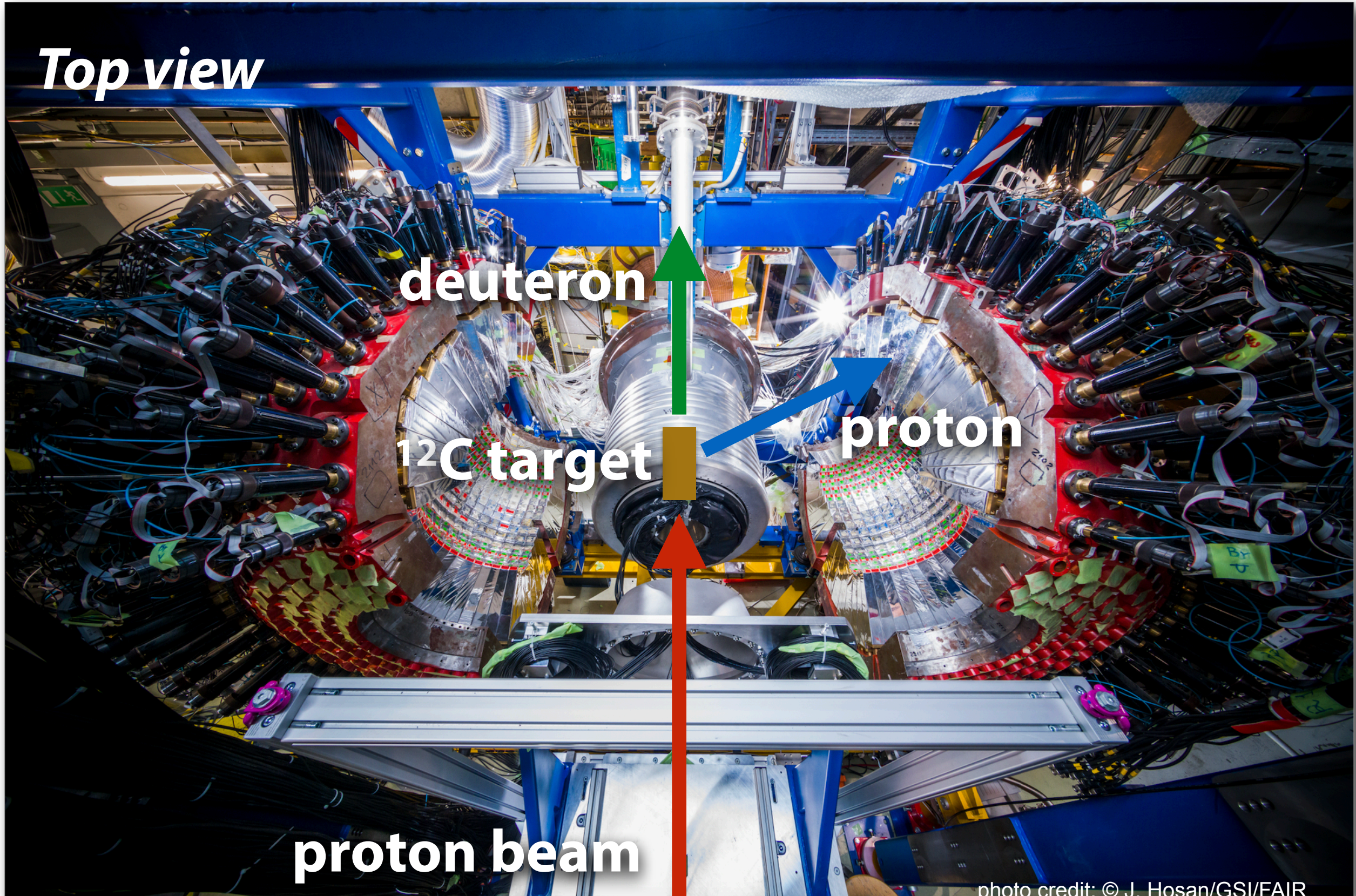
$0.3 < q_x < 0.6 \text{ GeV}/c$: Signals are well separated from other process



$B_{Kpp} \sim 40 \text{ MeV}$, $\Gamma_{Kpp} \sim 100 \text{ MeV}$
 \rightarrow large binding energy

$Q_{Kpp} \sim 400 \text{ MeV}$ (c.f. $Q_{QF} \sim 200 \text{ MeV}$)
 \rightarrow wide momentum transfer

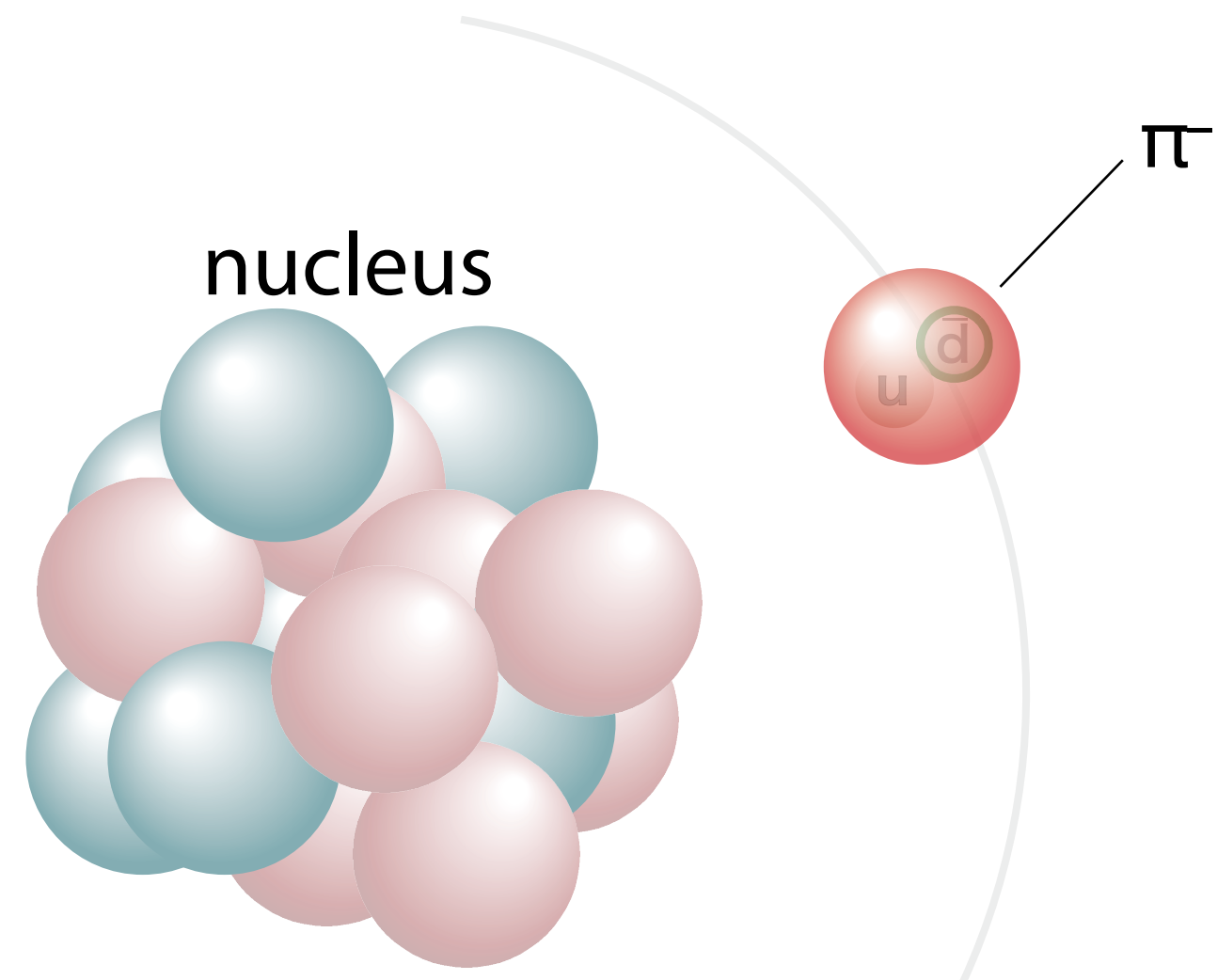
GSI-S490 WASA at FRS for η' mesic nuclei(2022)



S490 Spokesperson: KI
co-Spokesperson: Y.K. Tanaka

D-candidate: R. Sekiya

Pionic atoms

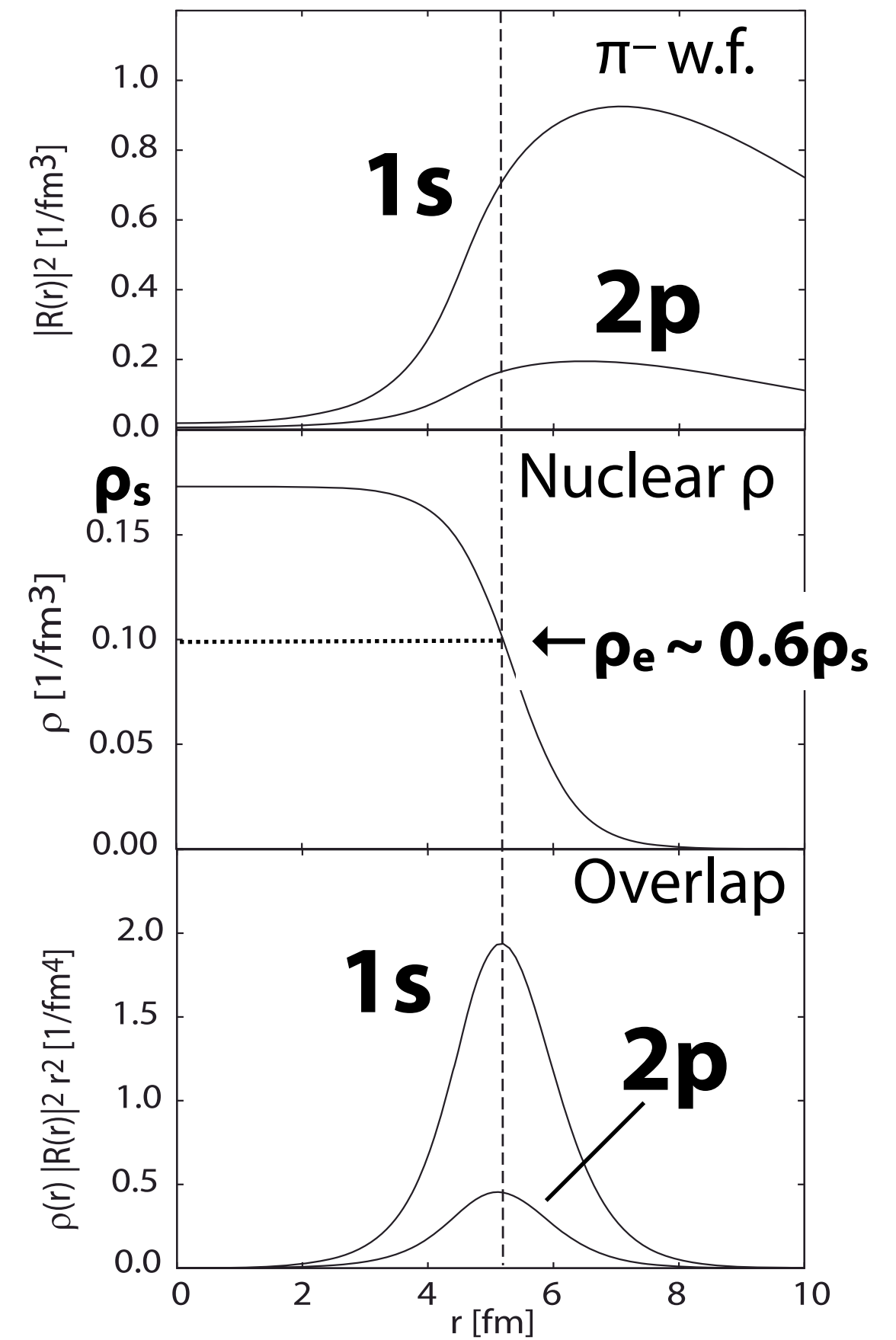


Ericson-Ericson potential

$$U_{\text{opt}}(r) = U_s(r) + U_p(r),$$

$$U_s(r) = b_0 \rho + b_1 (\rho_n - \rho_p) + B_0 \rho^2$$

$$U_p(r) = \frac{2\pi}{\mu} \vec{\nabla} \cdot [c(r) + \varepsilon_2^{-1} C_0 \rho^2(r)] L(r) \vec{\nabla}$$



Pion-nucleus interaction

Overlap between
pion w.f. and nucleus
 $\rightarrow \pi$ works as a probe
 at $\rho_e \sim 0.6\rho_s$



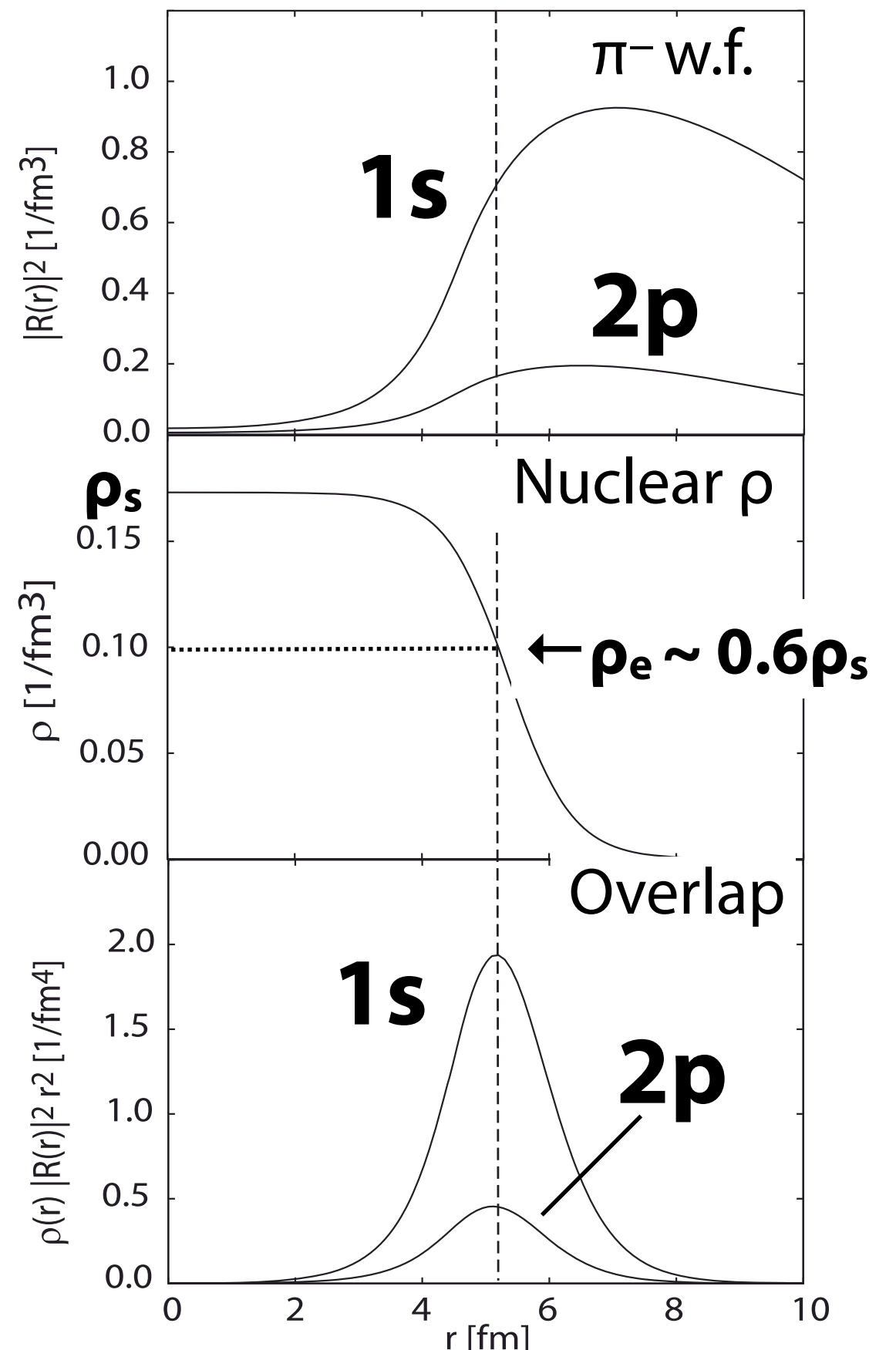
π -nucleus interaction is changed
 for wavefunction renormalization
 of medium effect

Ericson-Ericson potential

$$U_{\text{opt}}(r) = U_s(r) + U_p(r),$$

$$U_s(r) = b_0 \rho + b_1 (\rho_n - \rho_p) + B_0 \rho^2$$

$$U_p(r) = \frac{2\pi}{\mu} \vec{\nabla} \cdot [c(r) + \varepsilon_2^{-1} C_0 \rho^2(r)] L(r) \vec{\nabla}$$



Pion-nucleus interaction and chiral condensate

Overlap between
pion w.f. and nucleus
 $\rightarrow \pi$ works as a probe
at $\rho_e \sim 0.6\rho_s$



π -nucleus interaction is changed
for wavefunction renormalization
of medium effect

In-medium Glashow-Weinberg relation

$$\frac{\langle \bar{q}q \rangle^*}{\langle \bar{q}q \rangle} \simeq \left(\frac{b_1^v}{b_1} \right)^{1/2} \left(1 - \gamma \frac{\rho}{\rho_0} \right)$$

$$\gamma = 0.184 \pm 0.003$$

Jido, Hatsuda, Kunihiro, PLB670, 109 (2008)

Ericson-Ericson potential

$$U_{\text{opt}}(r) = U_s(r) + U_p(r),$$

$$U_s(r) = b_0 \rho + \mathbf{b}_1 (\rho_n - \rho_p) + B_0 \rho^2$$

$$U_p(r) = \frac{2\pi}{\mu} \vec{\nabla} \cdot [c(r) + \varepsilon_2^{-1} C_0 \rho^2(r)] L(r) \vec{\nabla}$$

Pion-nucleus interaction and chiral condensate

Gell-Mann-Oakes-Renner relation

$$f_\pi^2 m_\pi^2 = -2m_q \langle \bar{q}q \rangle$$

Tomozawa-Weinberg relation

$$b_1 = -\frac{m_\pi}{8\pi f_\pi^2}$$

$$\frac{\langle \bar{q}q \rangle_\rho}{\langle \bar{q}q \rangle_0} \approx \frac{b_1^{\text{free}}}{b_1(\rho)}$$

M. Gell-Mann *et al.*, PR175(1968)2195.

Y. Tomozawa, NuovoCimA46(1966)707.

S. Weinberg, PRL17(1966)616.

In-medium Glashow-Weinberg relation

$$\frac{\langle \bar{q}q \rangle^*}{\langle \bar{q}q \rangle} \simeq \left(\frac{b_1^{\text{v}}}{b_1} \right)^{1/2} \left(1 - \gamma \frac{\rho}{\rho_0} \right)$$

$$\gamma = 0.184 \pm 0.003$$

Jido, Hatsuda, Kunihiro, PLB670, 109 (2008)

Pion-nucleus interaction and chiral condensate

Gell-Mann-Oakes-Renner relation

$$f_\pi^2 m_\pi^2 = -2m_q \langle \bar{q}q \rangle$$

Tomozawa-Weinberg relation

$$b_1 = -\frac{m_\pi}{8\pi f_\pi^2}$$

$$\frac{\langle \bar{q}q \rangle_\rho}{\langle \bar{q}q \rangle_0} \approx \frac{b_1^{\text{free}}}{b_1(\rho)}$$

In-medium Glashow-Weinberg relation

$$\frac{\langle \bar{q}q \rangle^*}{\langle \bar{q}q \rangle} \simeq \left(\frac{b_1^v}{b_1} \right)^{1/2} \left(1 - \gamma \frac{\rho}{\rho_0} \right)$$

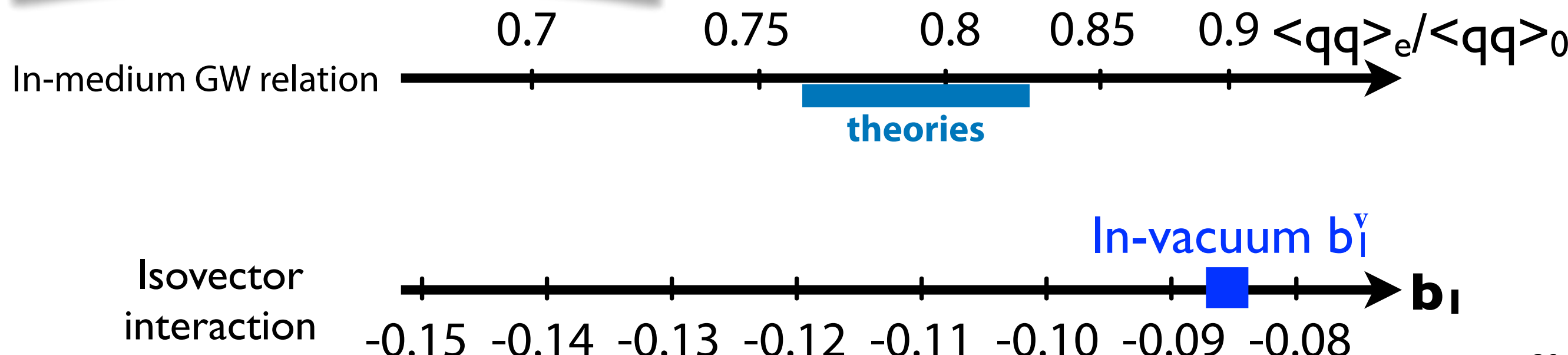
$$\gamma = 0.184 \pm 0.003$$

Jido, Hatsuda, Kunihiro, PLB670, 109 (2008)

Pionic hydrogen and deuterium

$$b_1^v = 0.0866 \pm 0.0010$$

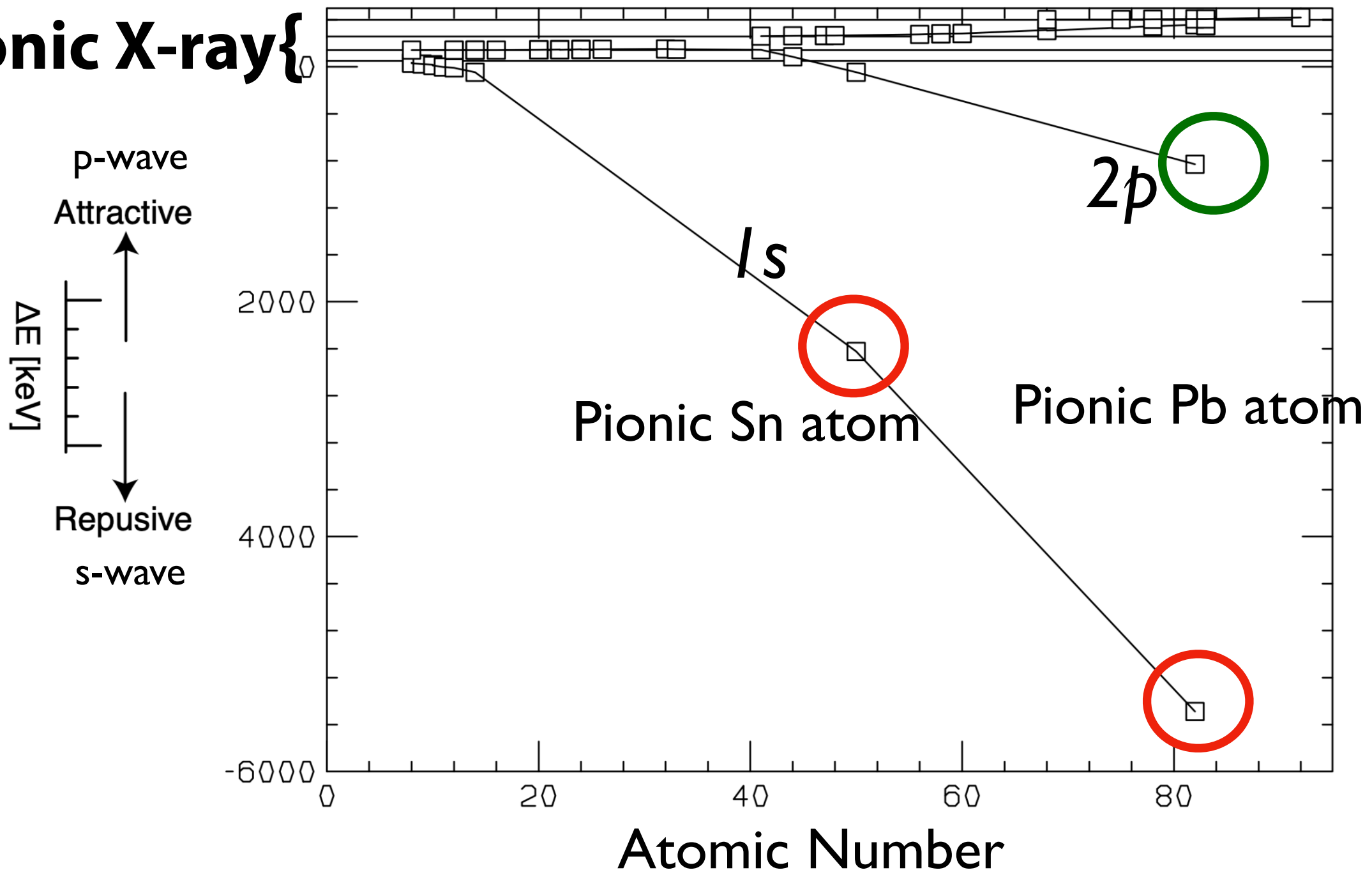
Hirtil et al., EPJA57, 70 (2021)



Deeply bound pionic atoms

Level shifts

Pionic X-ray {



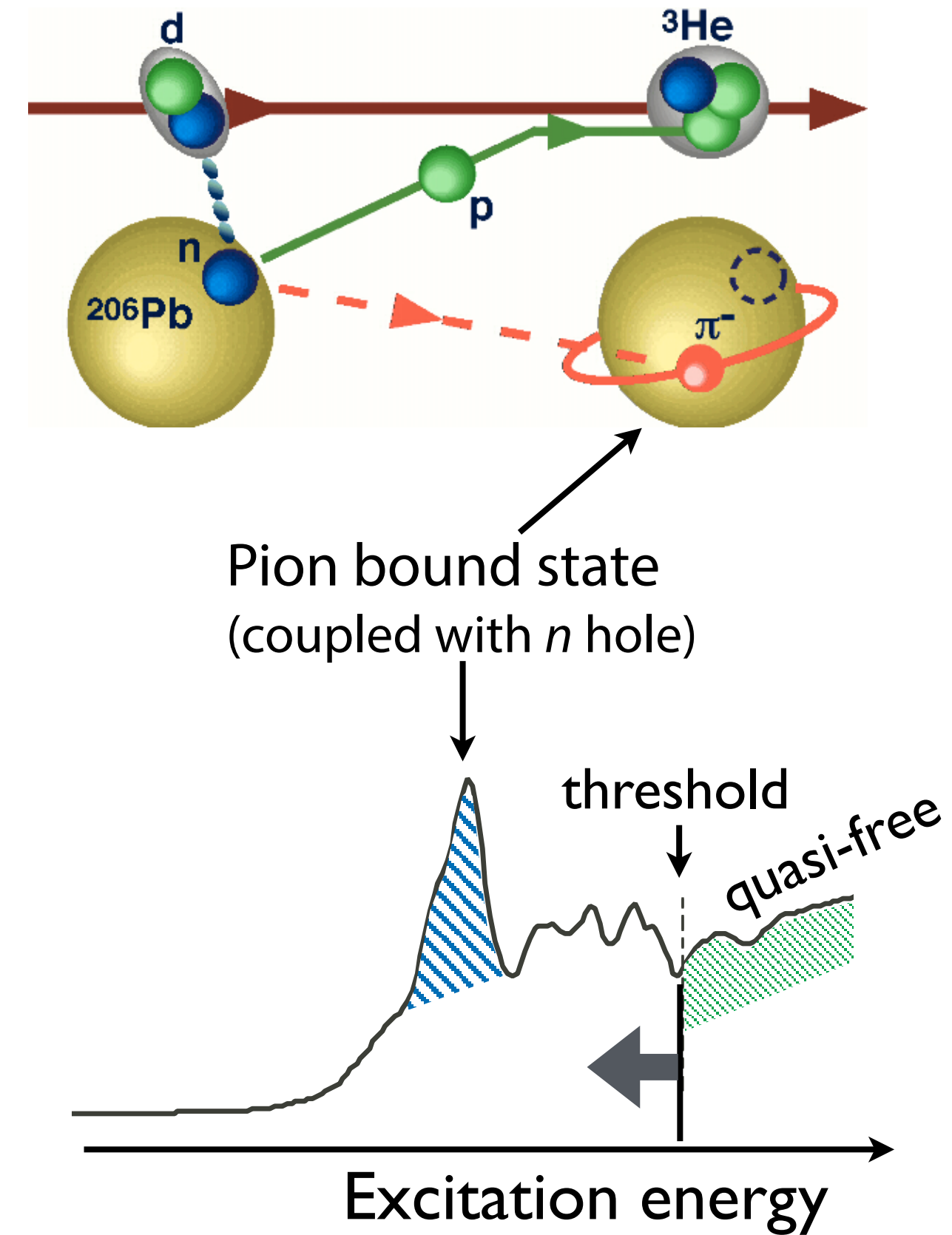
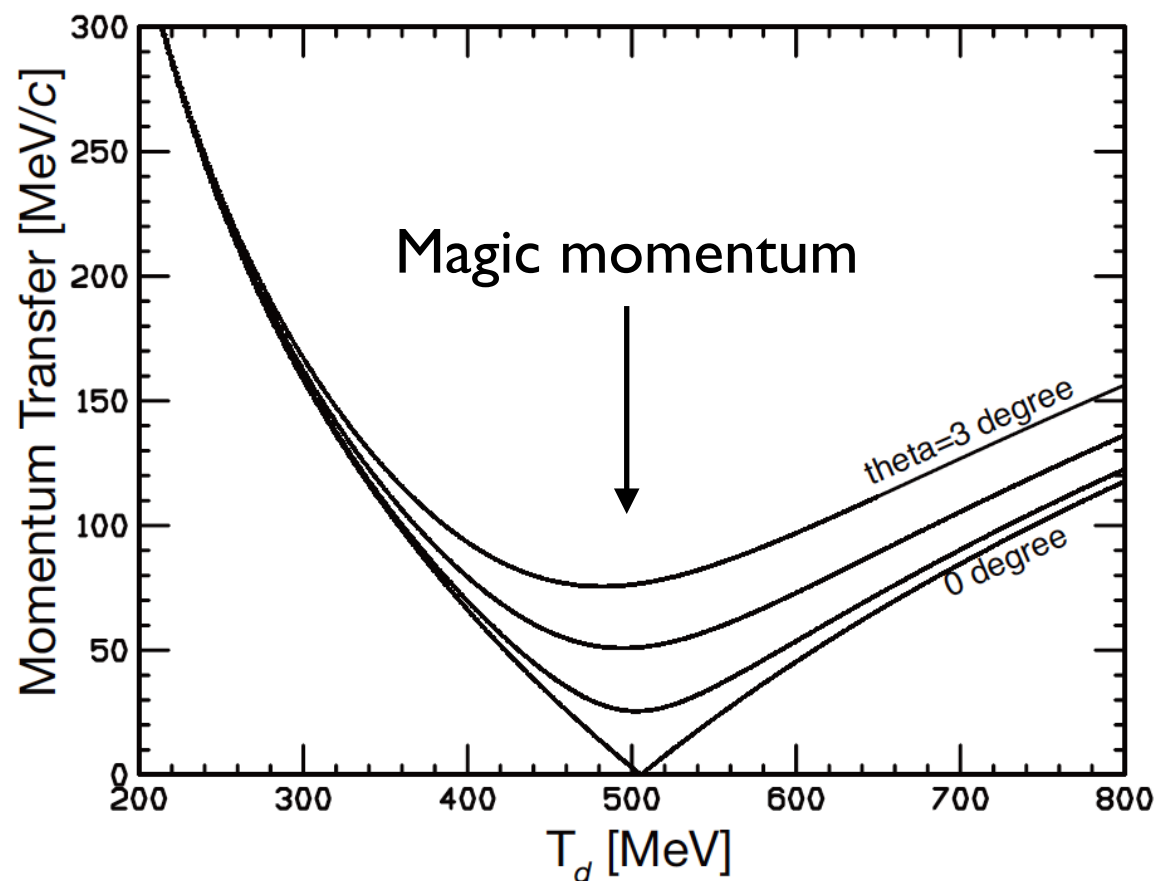
Deeply bound atoms have "super" repulsive shifts
and provide s-wave information

Spectroscopy of pionic atoms in $(d, {}^3\text{He})$ reactions

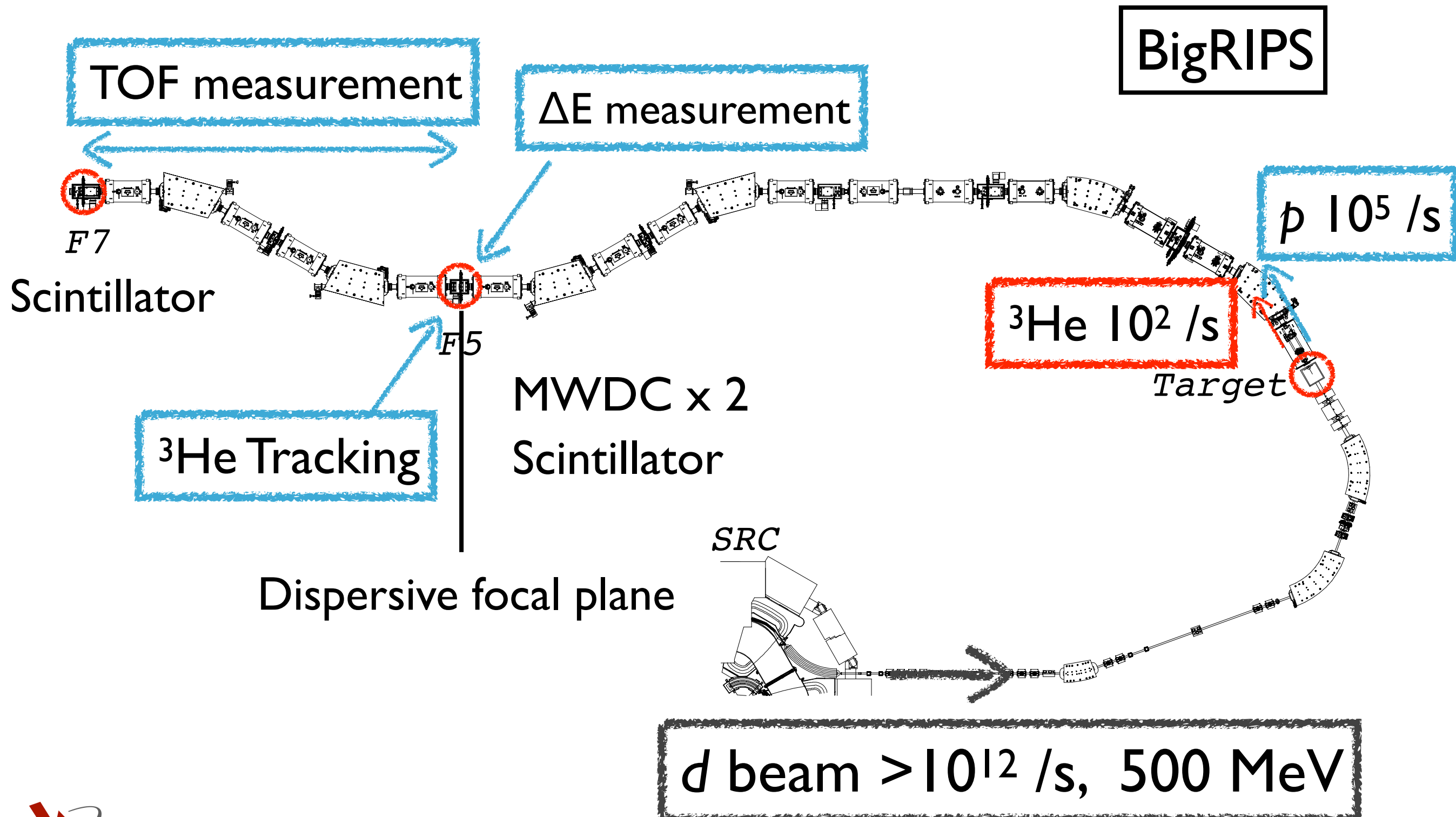
Missing mass spectroscopy to measure excitation spectrum of pionic atoms

Direct production of pionic atoms

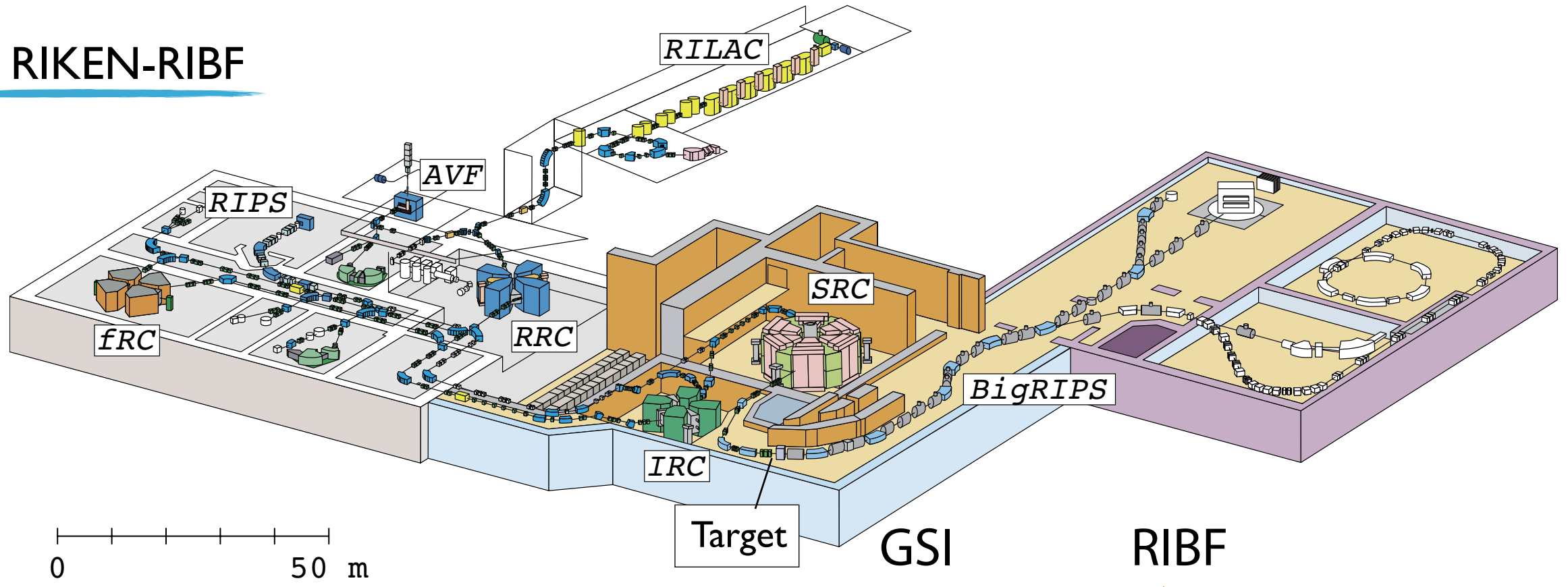
Momentum transfer



(d,³He) Reaction Spectroscopy in RIBF



RI Beam Factory



d beam Intensity

$10^{11}/\text{spill}$

$>10^{12}/\text{s}$

$\times 50!!$

Target

20 mg/cm^2 10 mg/cm^2

$\Delta p_d/p_d$ (FWHM)

0.02%

0.04%

Resolution (FWHM)

400 keV

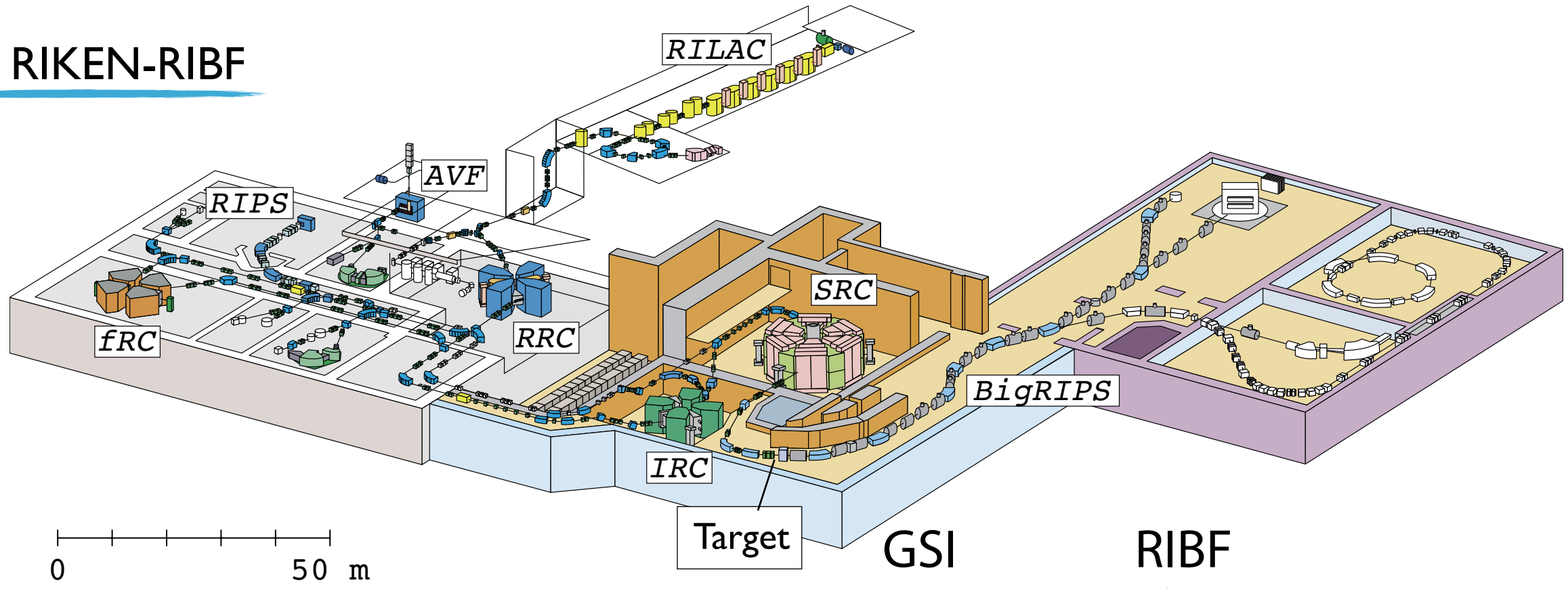
$\sim 800 \text{ keV}$

Acceptance (mrad)

15H, 10V

40H, 60V

RI Beam Factory



d beam Intensity

$10^{11}/\text{spill}$

$>10^{12}/\text{s}$

$\times 50!!$

Target

20 mg/cm^2 10 mg/cm^2

$\Delta p_d/p_d$ (FWHM)

0.02%

0.04%

Resolution (FWHM)

400 keV

< 300 keV

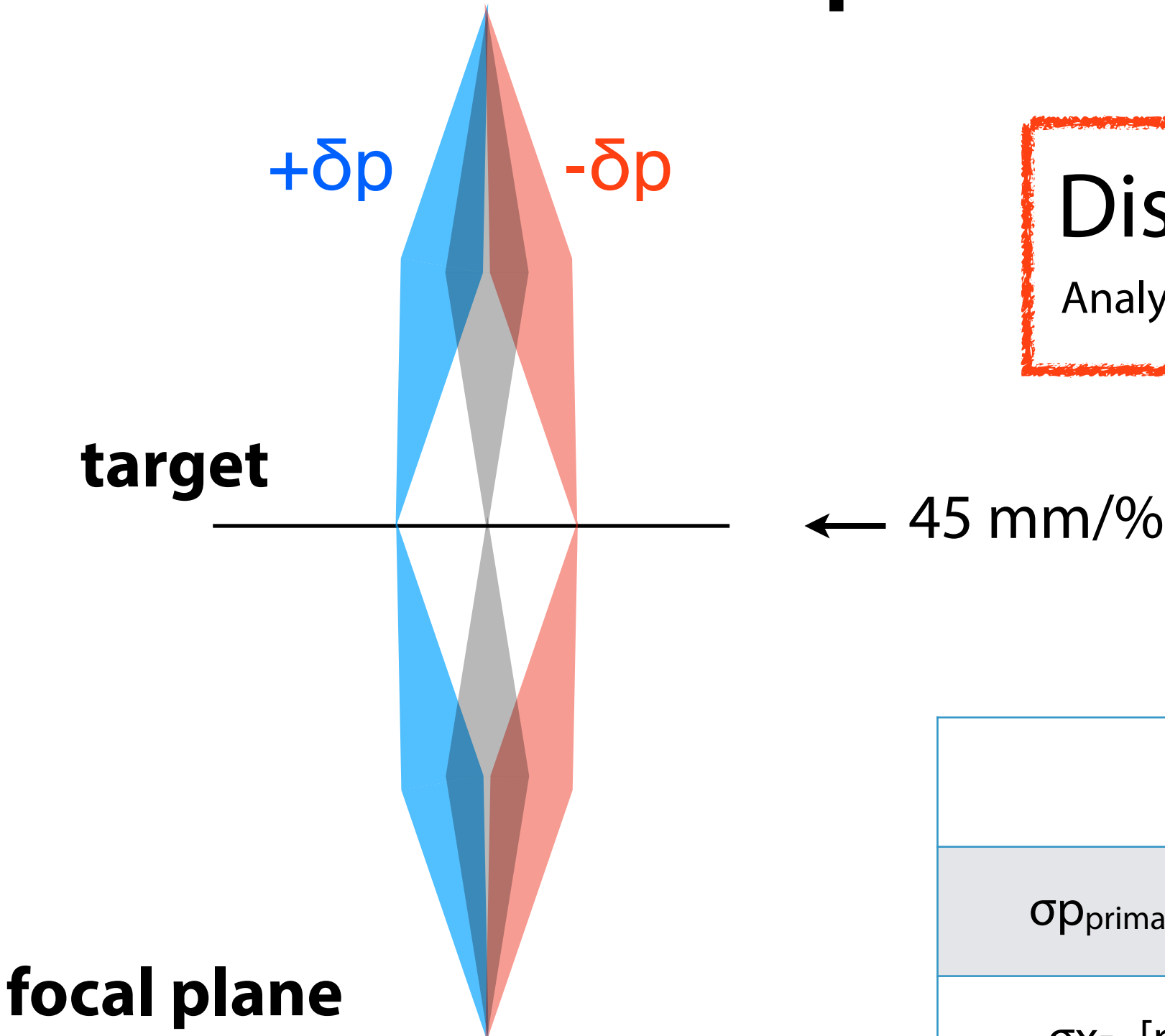
Acceptance (mrad)

15H, 10V

40H, 60V

SRC tuning +
Dispersion matching
required

Resolution improvement technique



Dispersion matching

Analysis of beam energy in the beam line

	Pilot (2010)	Standard
$\sigma p_{\text{primary}} [\%]$	0.04	0.04
$\sigma x_{F0} [\text{mm}]$	0.7	1
$\text{resolution}_{\text{exp}} [\text{keV}]$	500	800

Dispersion matching of primary beam

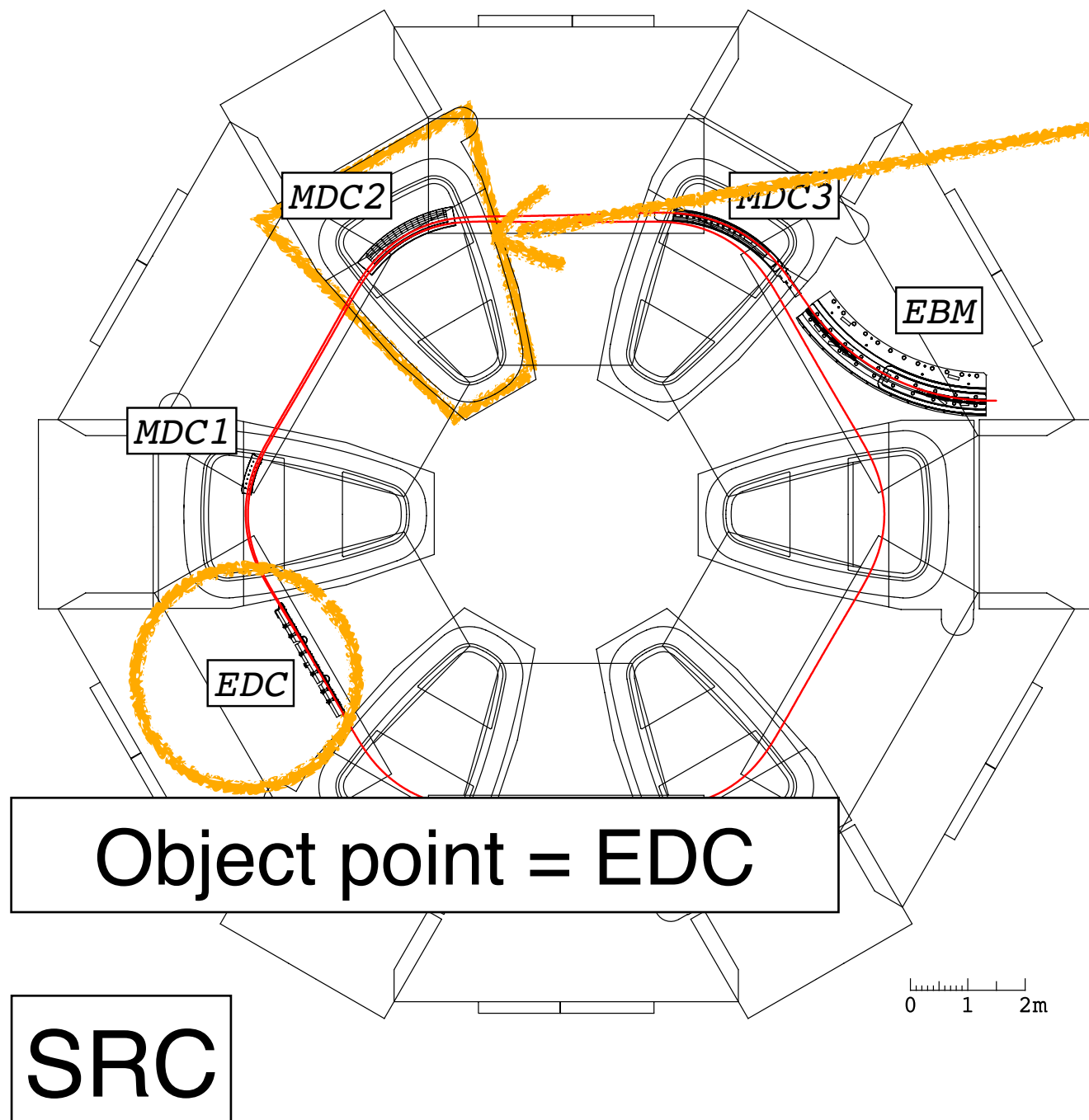
Dispersion matching to eliminate contribution of beam momentum spread in spectral resolution

$$\begin{pmatrix} x_{F5} \\ \theta_{F5} \\ \delta p_{F5} \end{pmatrix} = \begin{pmatrix} S_{11} & S_{12} & S_{16} \\ S_{21} & S_{22} & s_{26} \\ 0 & 0 & 1 \end{pmatrix} \begin{pmatrix} 1 & 0 & 0 \\ 0 & 1 & 0 \\ 0 & 0 & C \end{pmatrix} \begin{pmatrix} A_{11} & A_{12} & A_{16} \\ A_{21} & A_{22} & A_{26} \\ 0 & 0 & 1 \end{pmatrix} \begin{pmatrix} x_0 \\ \theta_0 \\ \delta p_0 \end{pmatrix}$$

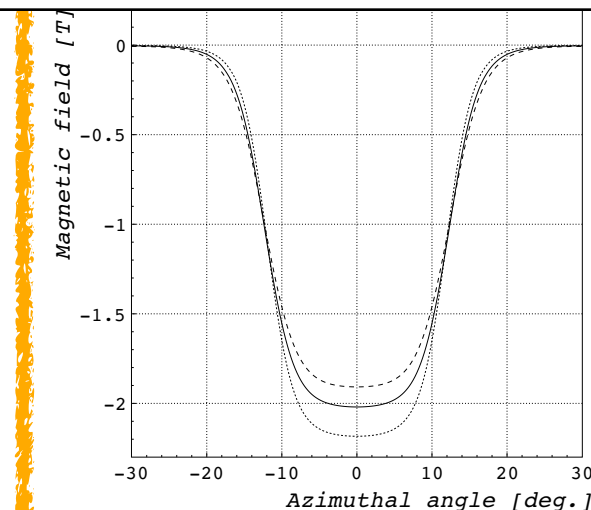
*C: kinematical factor = 1.31

$$x_{F5} = \dots + \underbrace{(S_{11}A_{16} + CS_{16})\delta p_0}_{\text{--- --- ---}}$$

Dispersion matching of primary beam



magnetic field in the magnet

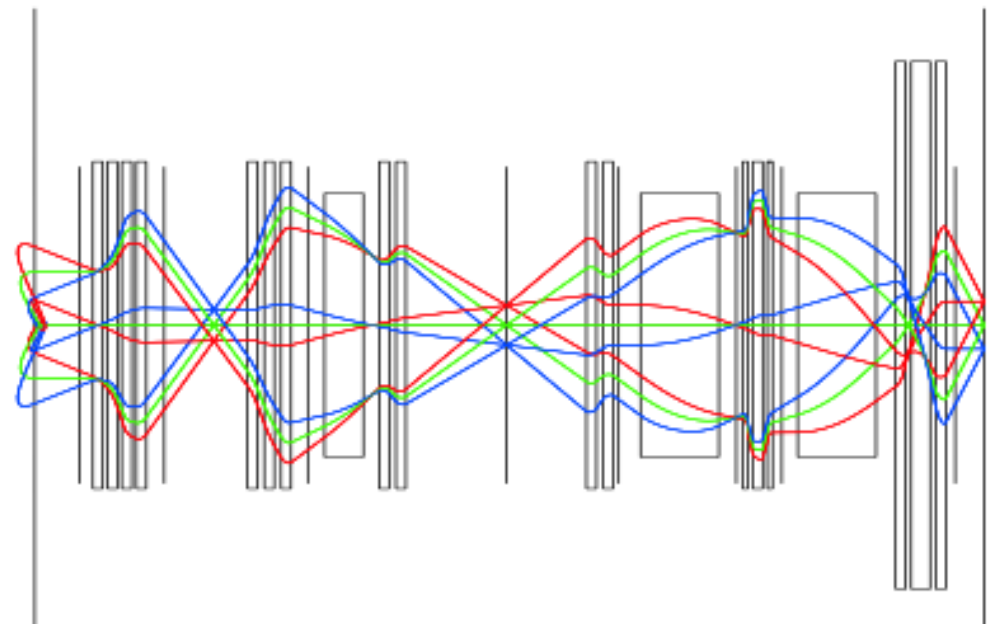


calculate the transfer matrix
using Runge-Kutta method

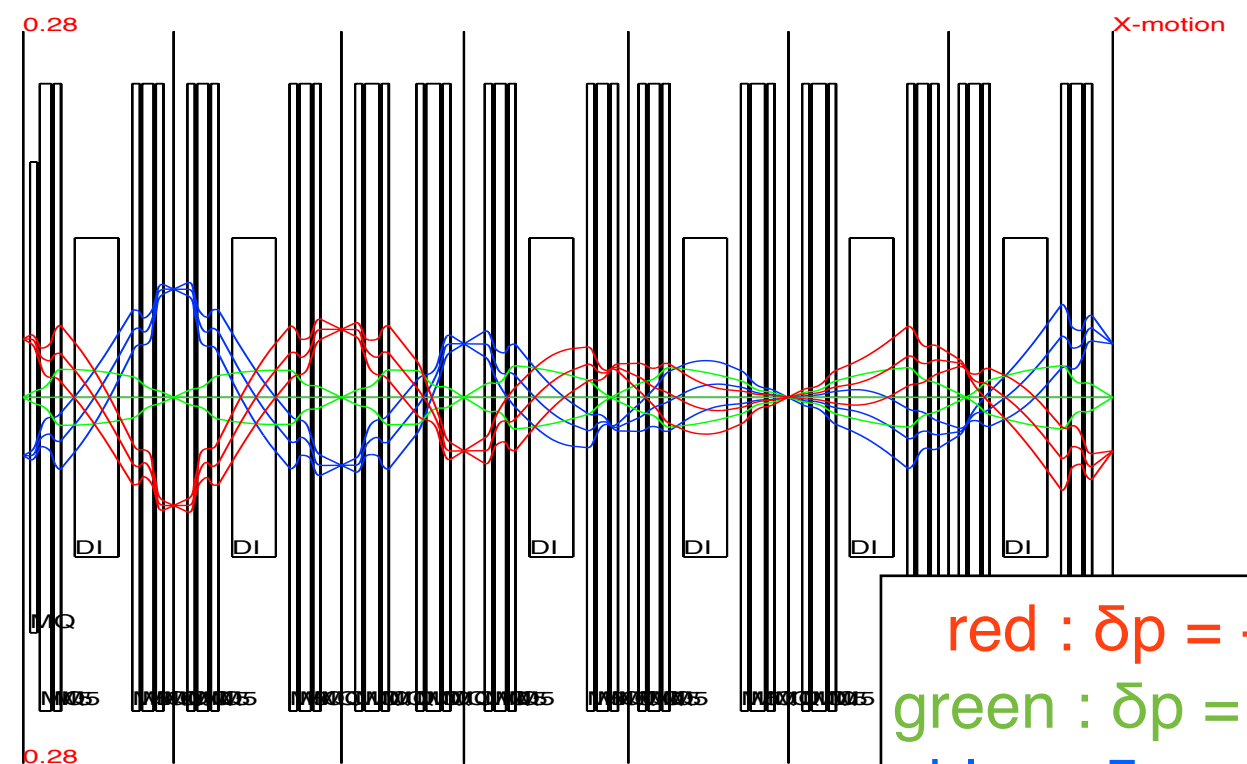
$$\begin{pmatrix} (x|x) & (x|a) & (x|y) & (x|b) & (x|\delta) \\ (a|x) & (a|a) & (a|y) & (a|b) & (a|\delta) \\ (y|x) & (y|a) & (y|y) & (y|b) & (y|\delta) \\ (b|x) & (b|a) & (b|y) & (b|b) & (b|\delta) \end{pmatrix}_{\text{EDC} \rightarrow \text{EBM}} = \begin{pmatrix} -1.00 & -3.35 & 0.0 & 0.0 & 76.9 \\ 0.30 & -0.01 & 0.0 & 0.0 & -25.4 \\ 0.0 & 0.0 & -1.03 & -1.75 & 0.0 \\ 0.0 & 0.0 & -0.09 & -1.12 & 0.0 \end{pmatrix}$$

Dispersion matching of primary beam

EBM



F0



F3

F5

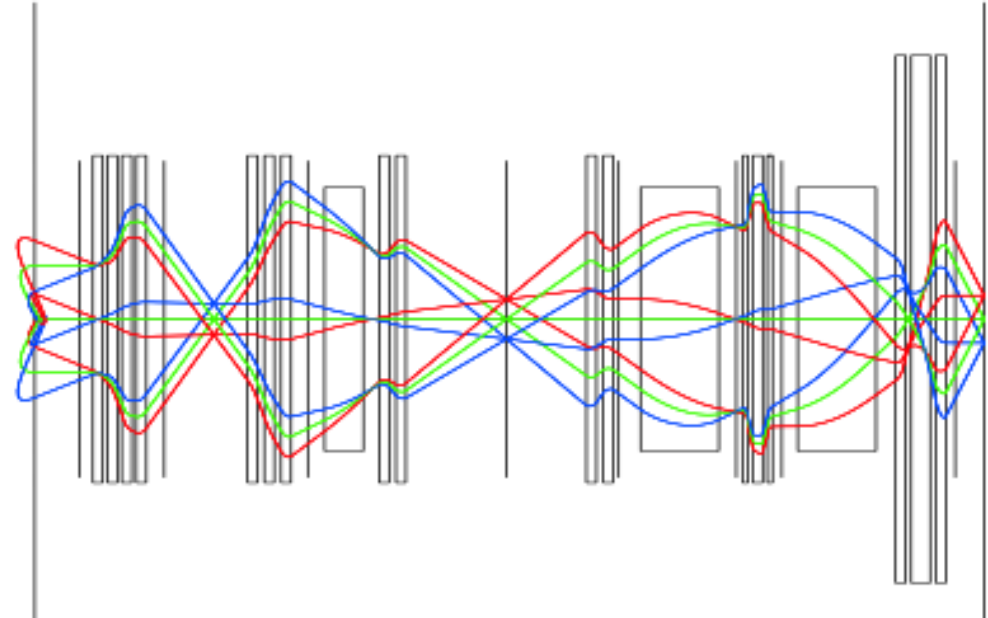
F7

red : $\delta p = +0.5\%$
green : $\delta p = 0\%$
blue : $\delta p = -0.5\%$

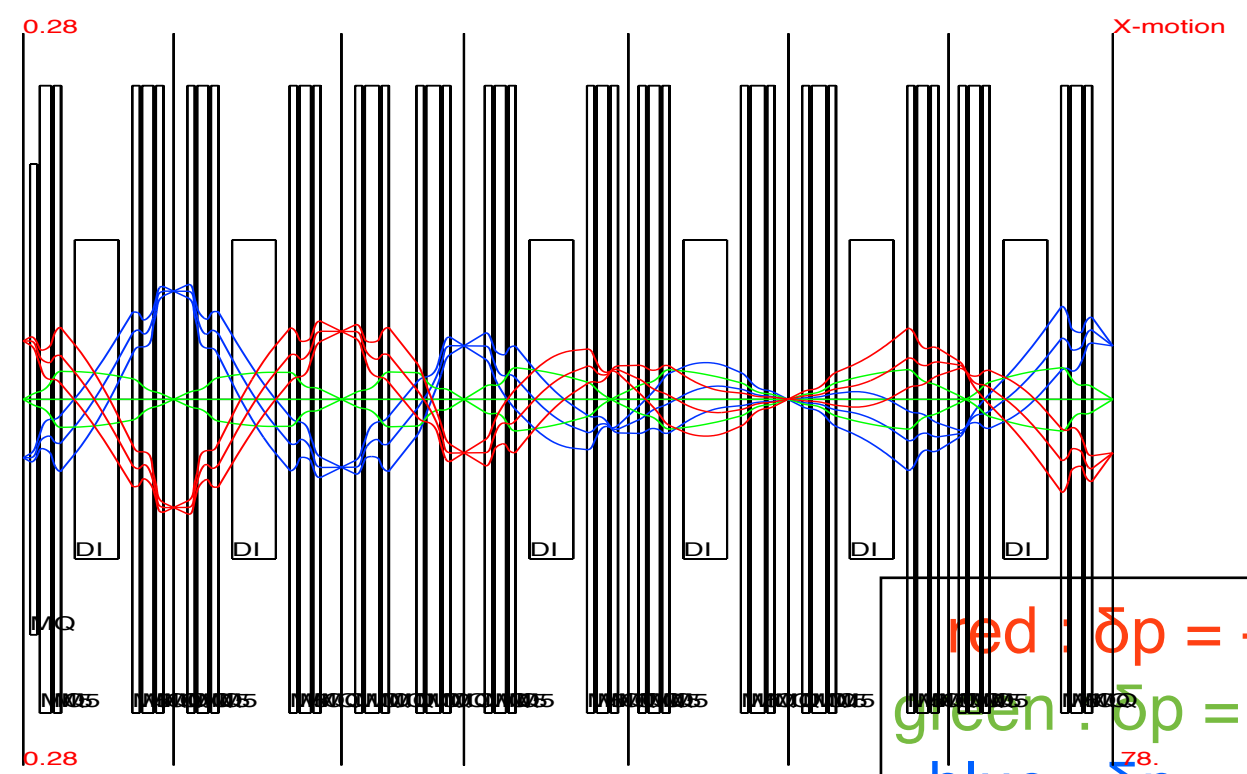
$$x_{F5} = \dots + \underbrace{(S_{11}A_{16} + CS_{16})}_{\text{red}} \delta p_0$$

Dispersion matching of primary beam

EBM



F0



F3

F5

F7

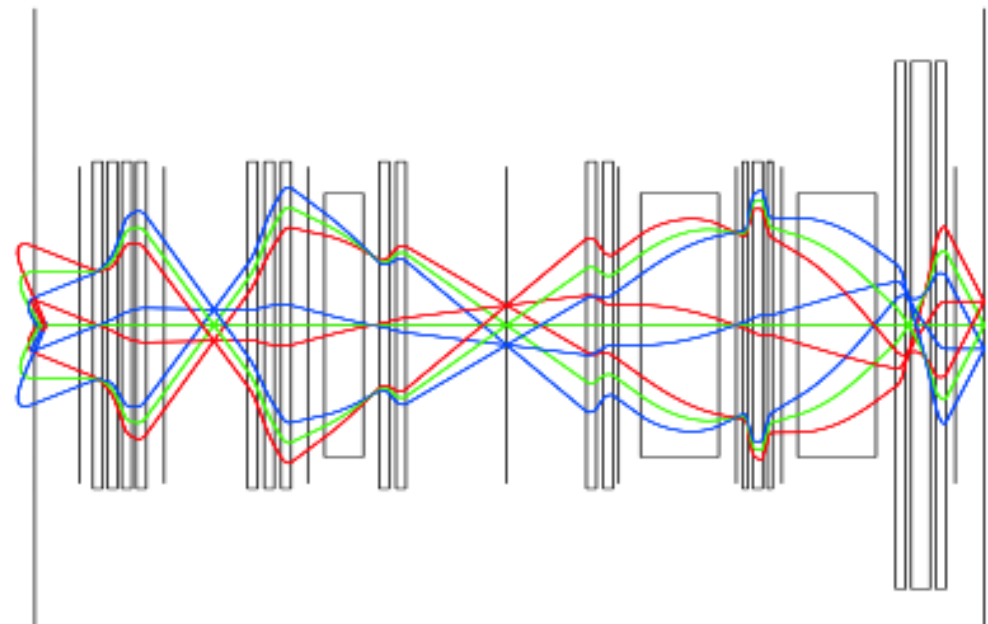
$$x_{F5} = \dots + \underbrace{(S_{11}A_{16} + CS_{16})\delta p_0}_{\text{magnification of BigRIPS}}$$

magnification of
BigRIPS

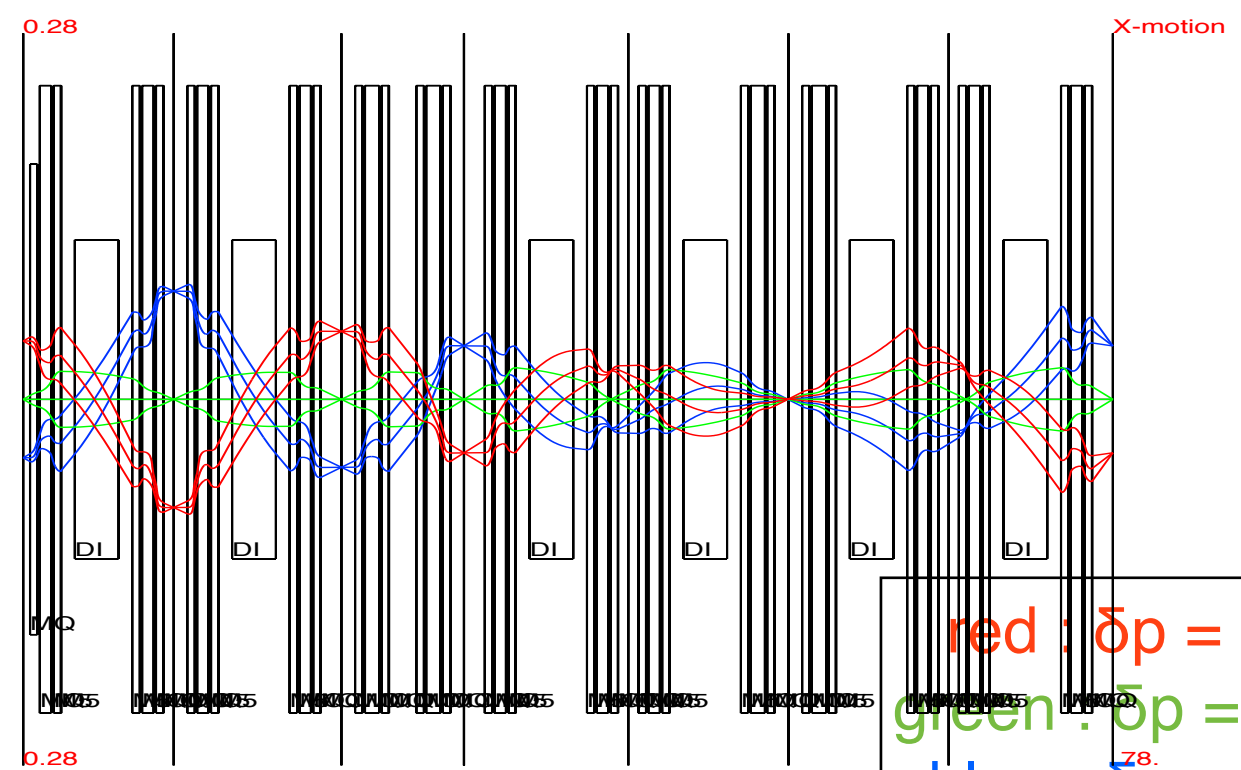
position at F0

Dispersion matching of primary beam

EBM



F0



F3

F5

F7

red : $\delta p = +0.5\%$
green : $\delta p = 0\%$
blue : $\delta p = -0.5\%$

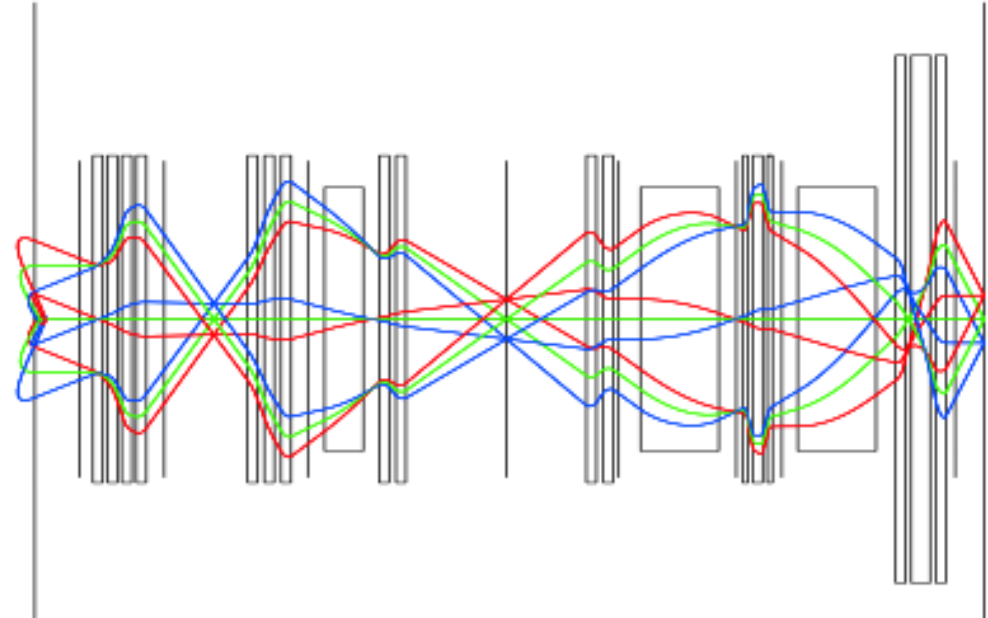
$$x_{F5} = \dots + \underbrace{(S_{11}A_{16} + CS_{16})}_{\text{Red}} \underbrace{\delta p_0}_{\text{Blue}} \quad \text{Cancel out}$$

design values: $S_{11} = -1.8$

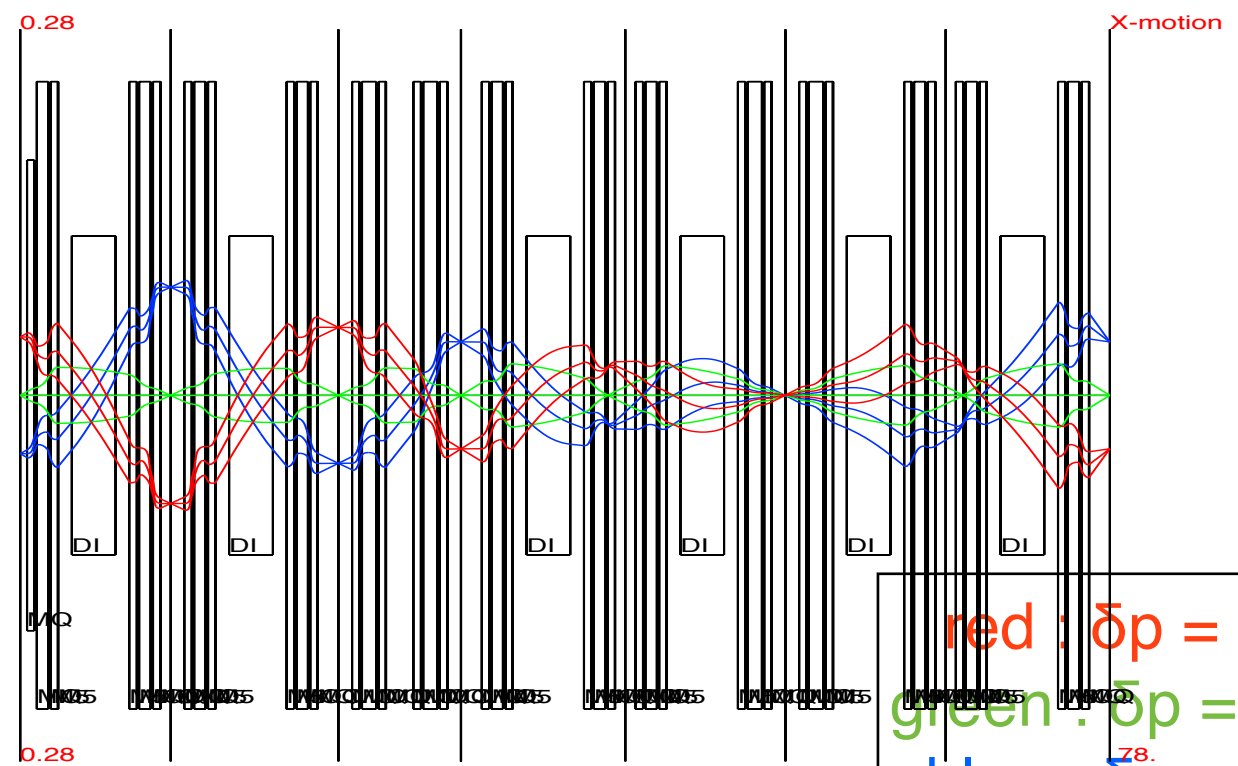
$C = 1.31$ $S_{16} = 62$ mm/%

Dispersion matching of primary beam

EBM



F0



F3

F5

F7

red : $\delta p = +0.5\%$
 green : $\delta p = 0\%$
 blue : $\delta p = -0.5\%$

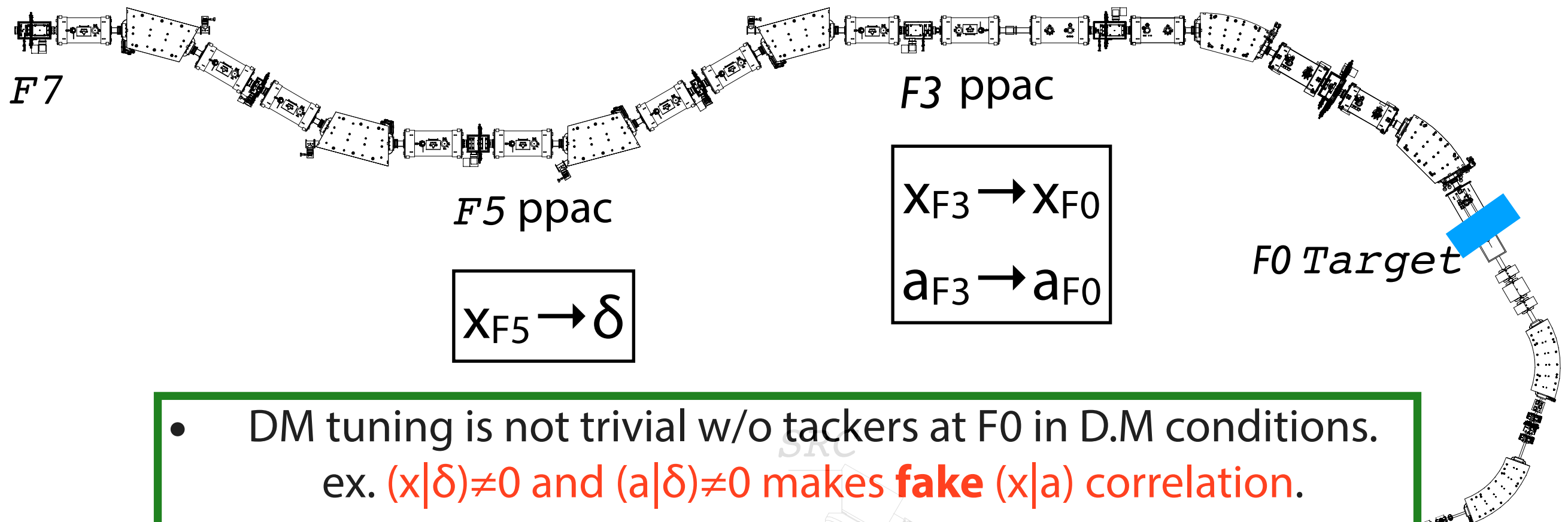
$$x_{F5} = \dots + \underbrace{(S_{11}A_{16} + CS_{16})}_{\text{Red}} \underbrace{\delta p_0}_{\text{Blue}} \quad \text{Cancel out}$$

design values: $S_{11} = -1.8$ $A_{16} = 44.6 \text{ mm}/\%$
 $C = 1.31$ $S_{16} = 62 \text{ mm}/\%$

New Method for Dispersion Matching Tuning

Track back to F0 using F3 and F5 trackers

RIKEN-BigRIPS



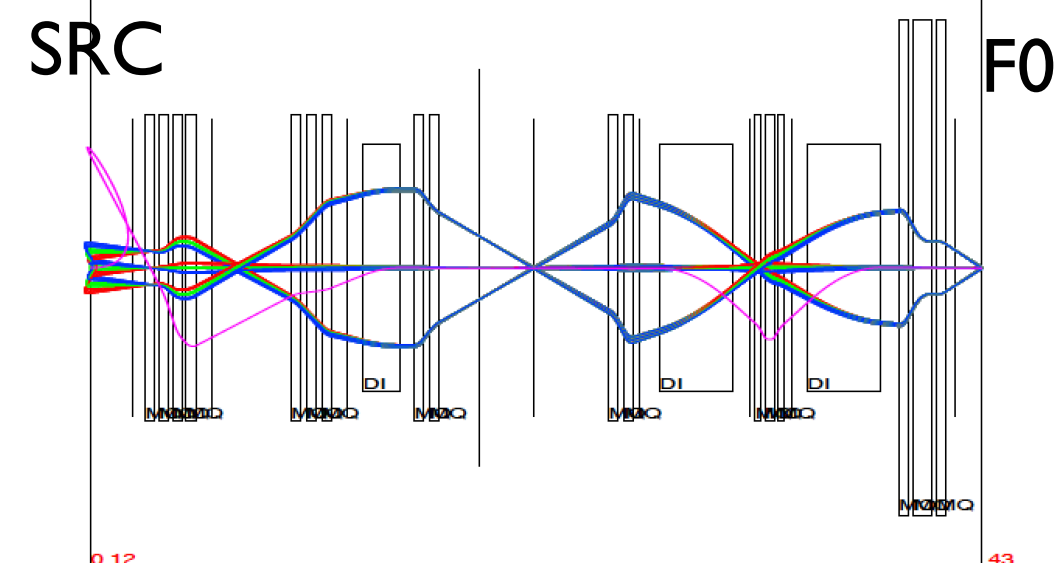
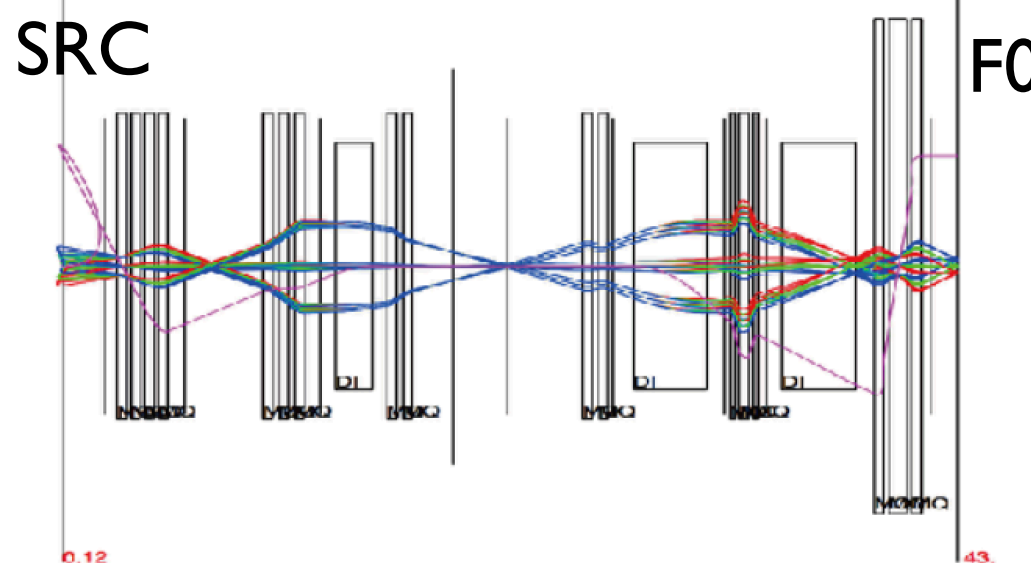
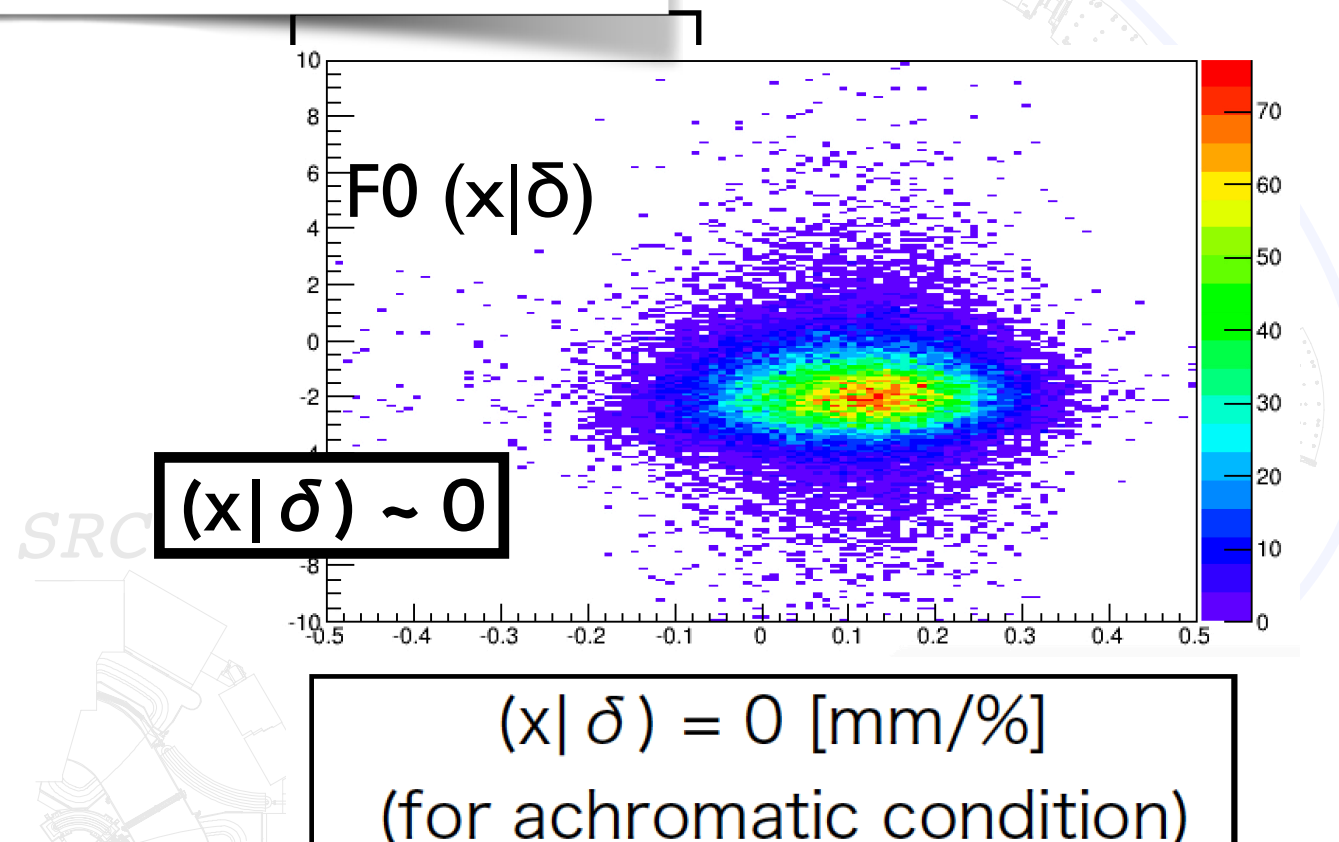
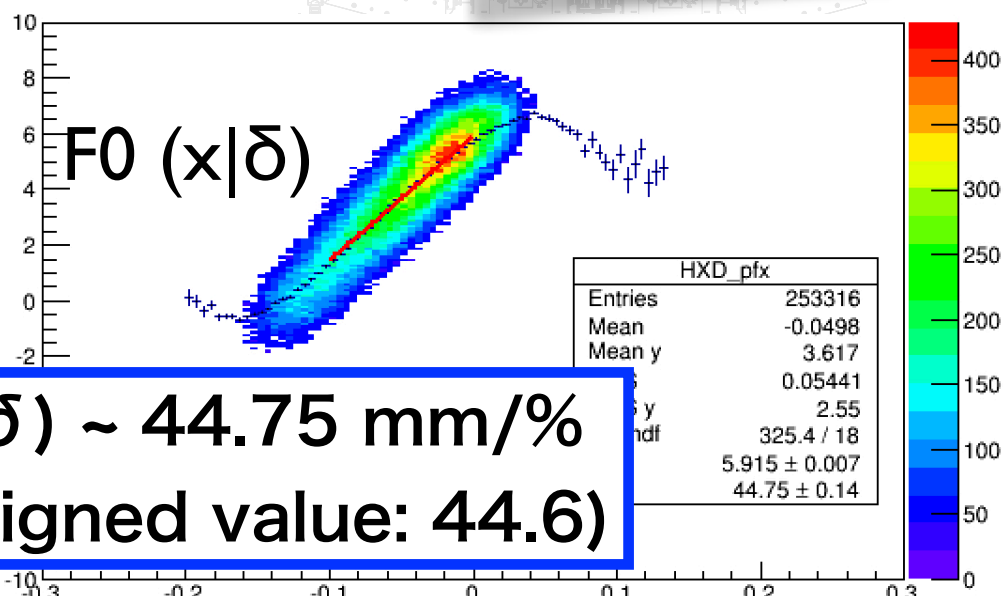
- DM tuning is not trivial w/o tackers at F0 in D.M conditions.
ex. $(x|\delta) \neq 0$ and $(a|\delta) \neq 0$ makes **fake** $(x|a)$ correlation.
- We established a new method “Trace-back method” by taking point-to-point image at F3 and dispersion measurement at F5

New Method for Dispersion Matching Tuning

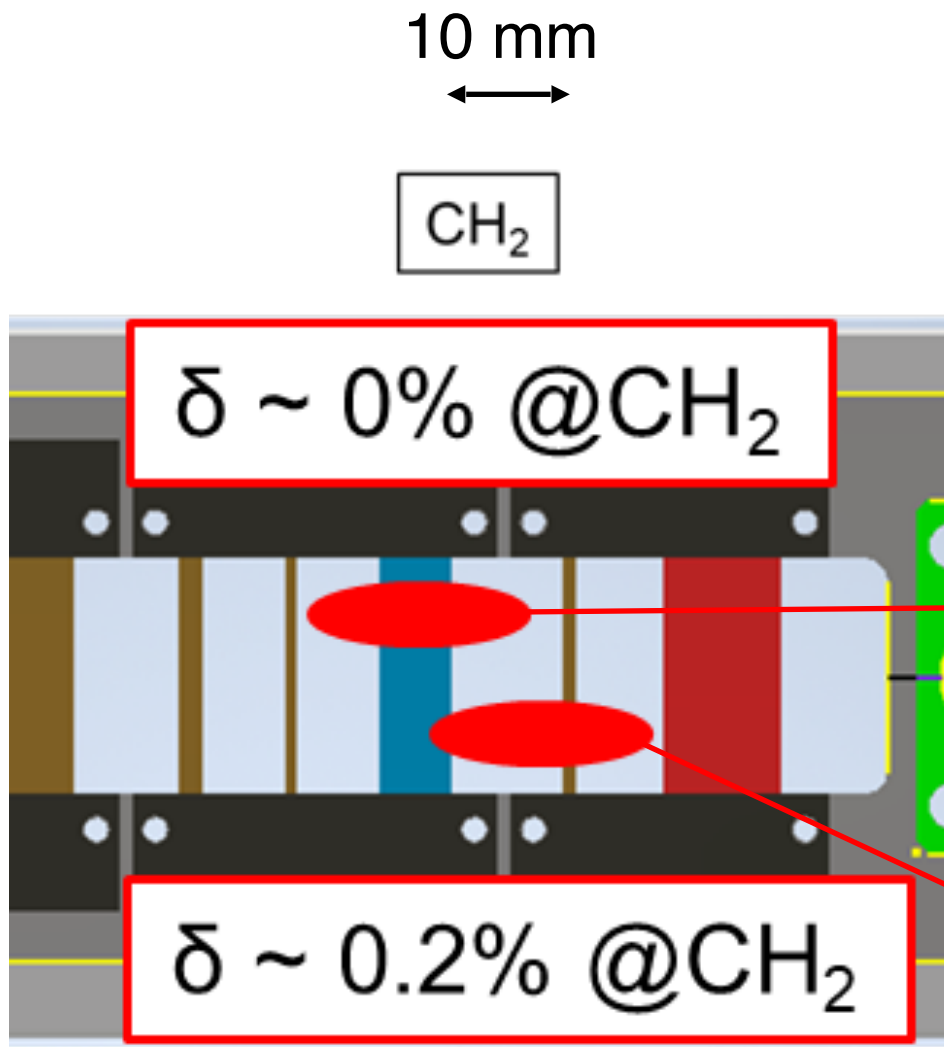
RIKEN-BigRIPS

Track back to T11 using F3 and F5 trackers

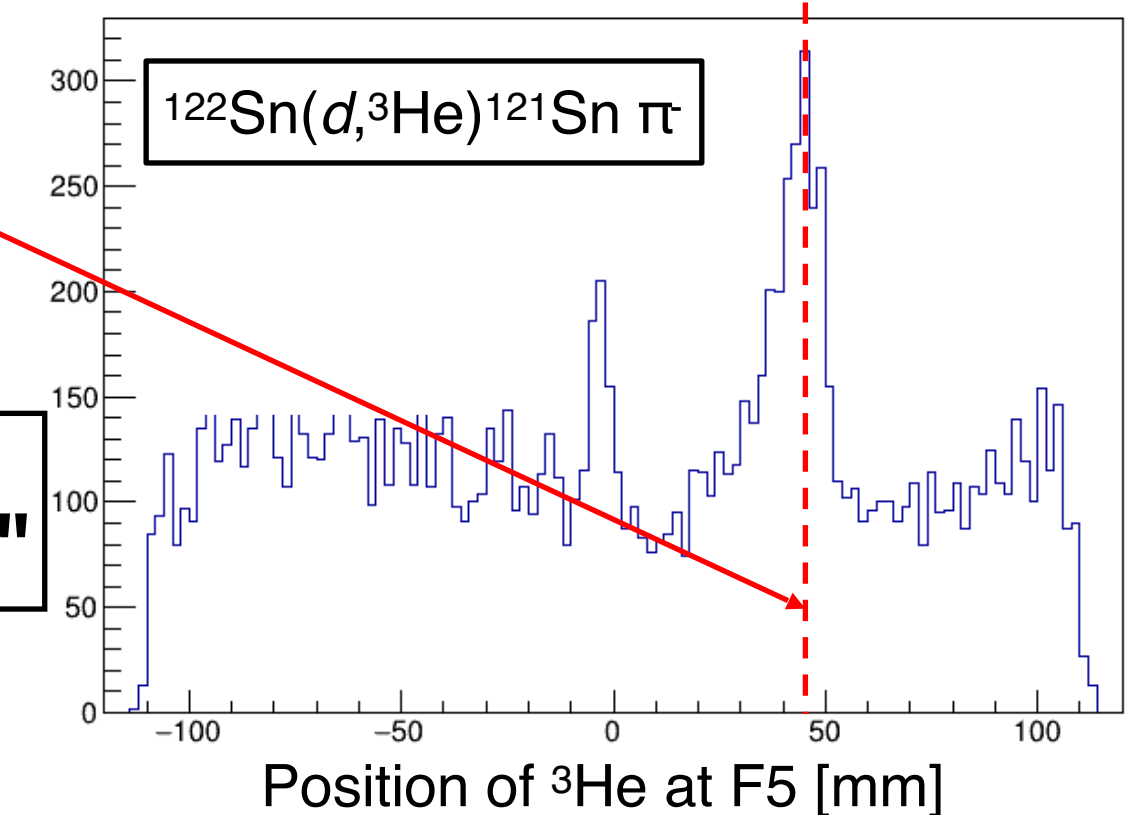
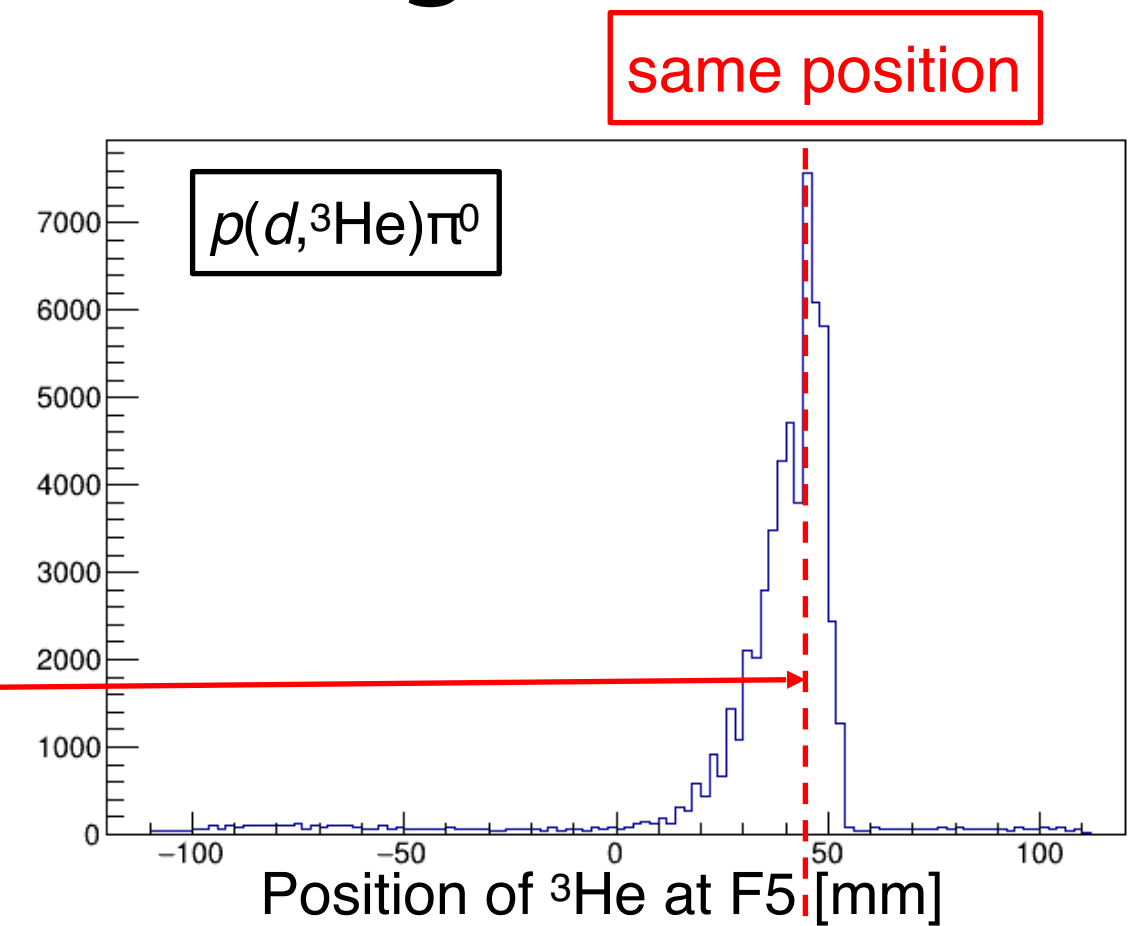
We have in our hands capability of freely tuning optical conditions at F0



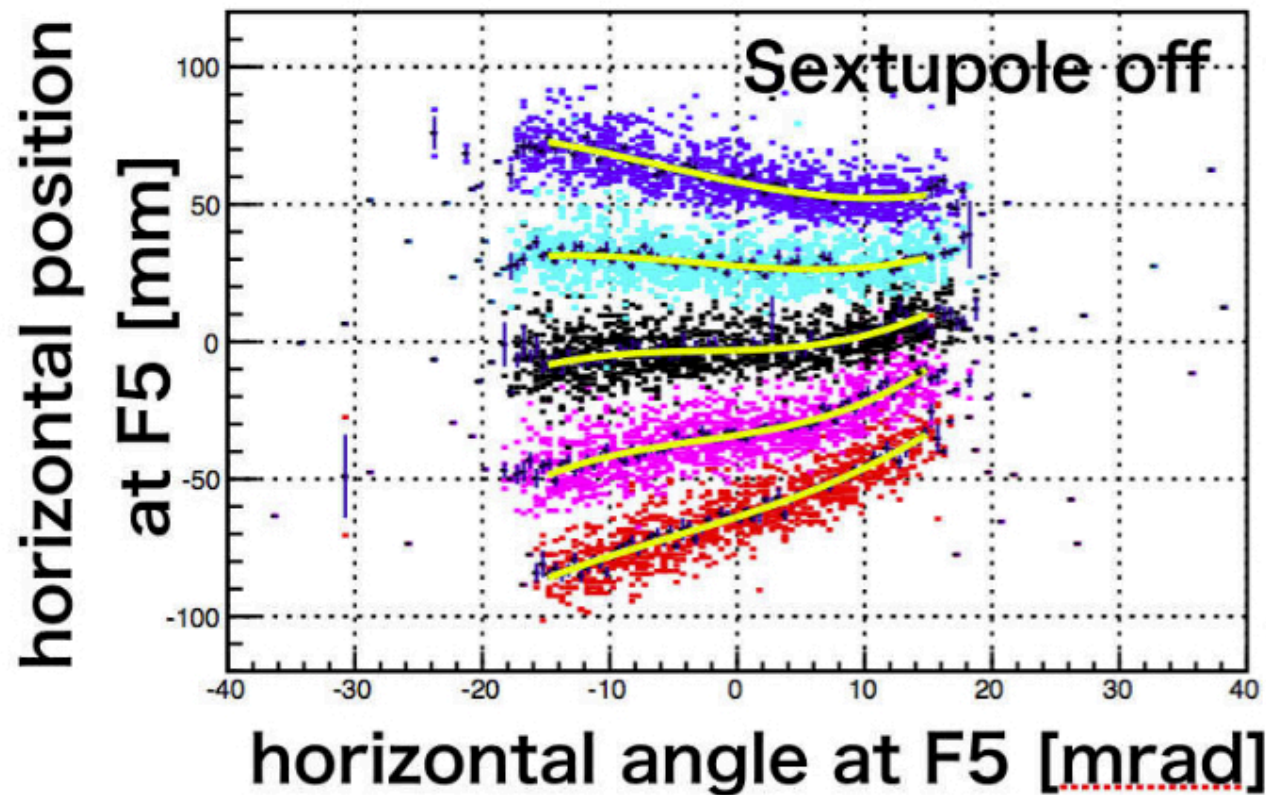
Improved dispersion matching in 2021



**Even with 20mm displacement at TA,
same position at F5 for same "physics"**

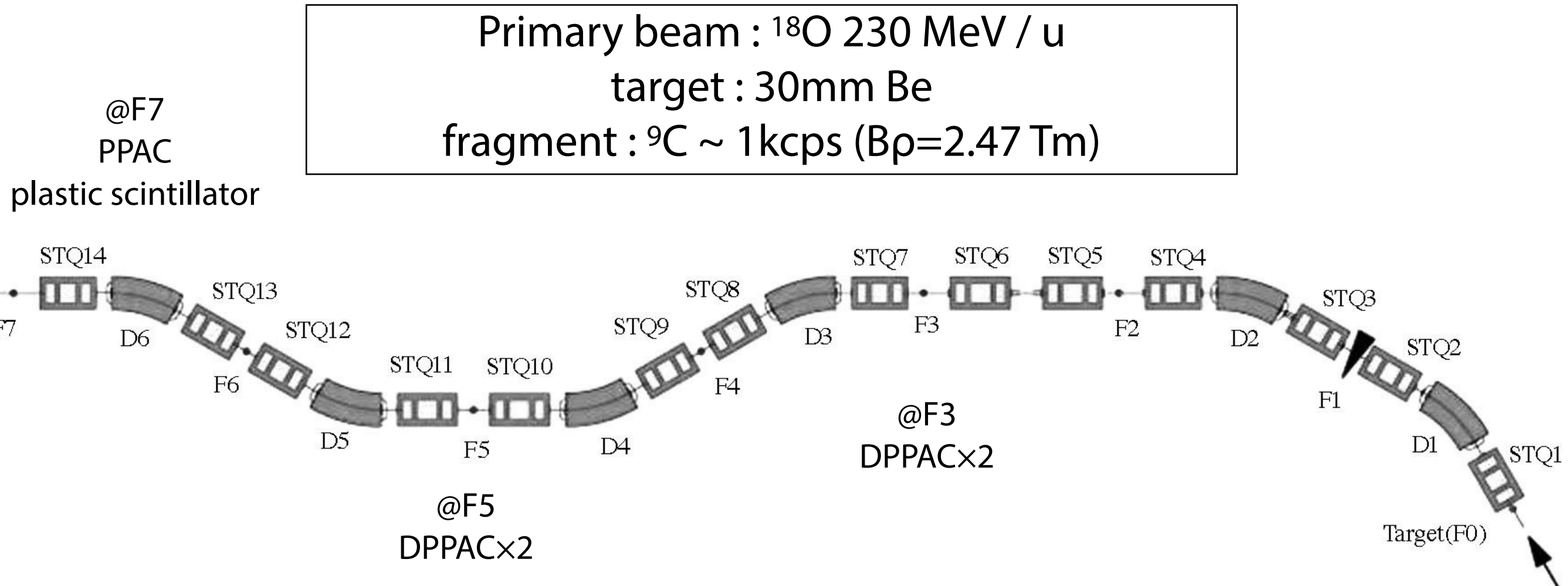


Higher-order aberration corrections of BigRIPS as a spectrometer



2nd ($x|ad$) and 3rd ($x|aaa$) order aberrations correction is required.

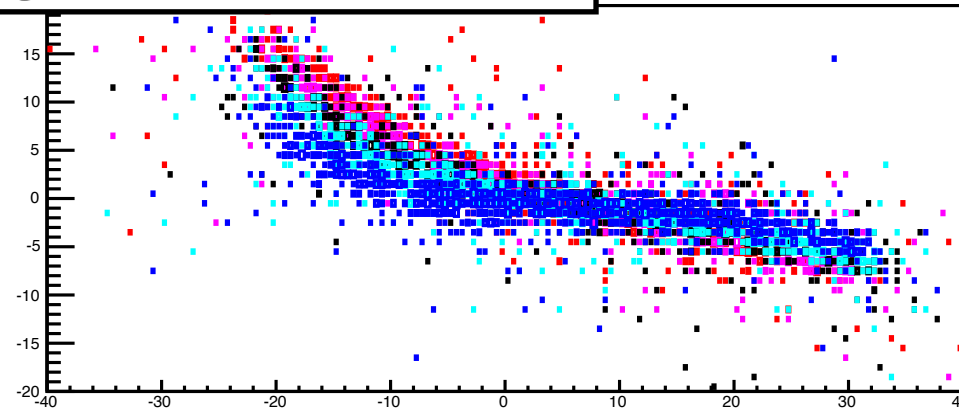
Higher-order aberration corrections



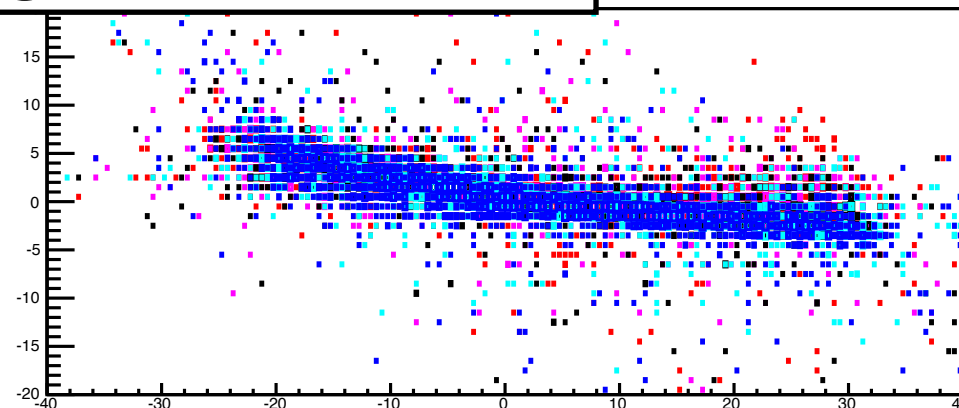
- ToF(F3-F7) : dE @F7 for PI
- Measure aberration at F3/F5 by selecting δ by ToF (RF-F7)
- Change SX settings respecting symmetry

Higher-order aberration measurement

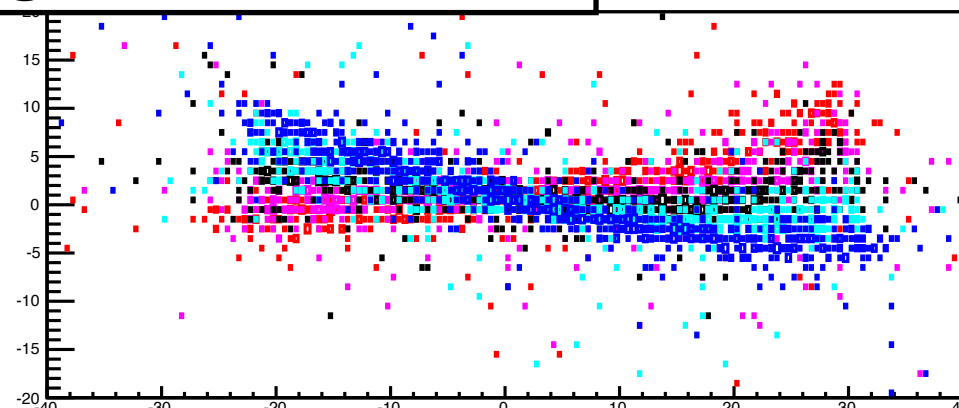
designed value $\times 2.0$



designed value $\times 1.0$



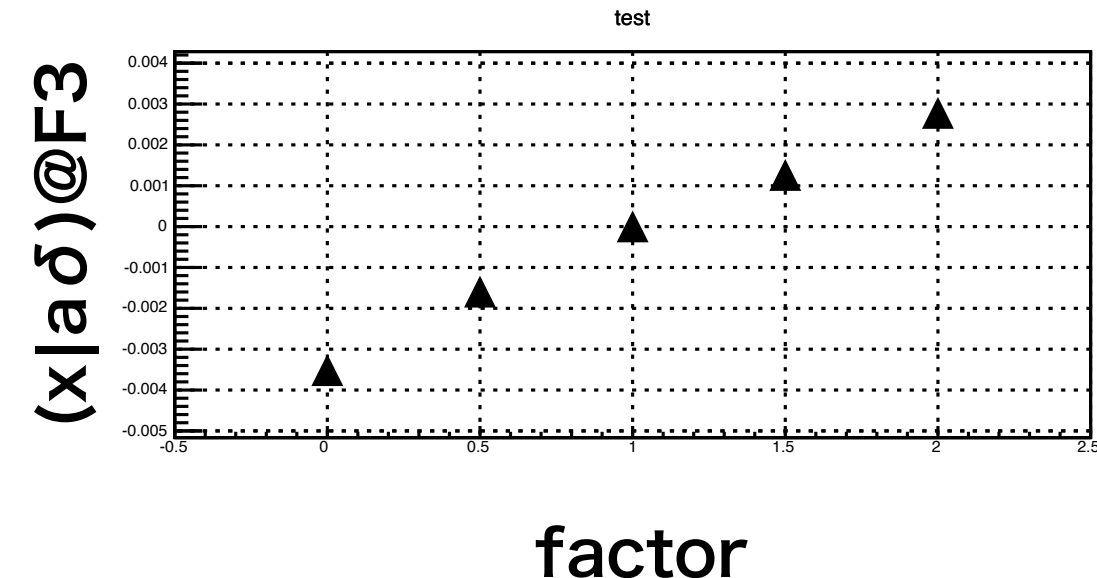
designed value $\times 0.0$



horizontal angle @ F3 [mrad]

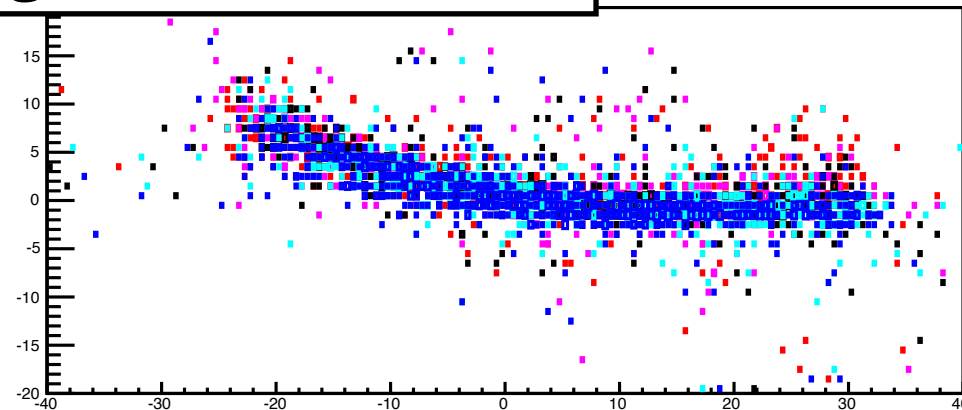
Chromatic aberration

$(x|a\delta)@F3$
 $(SX 2, 3)$

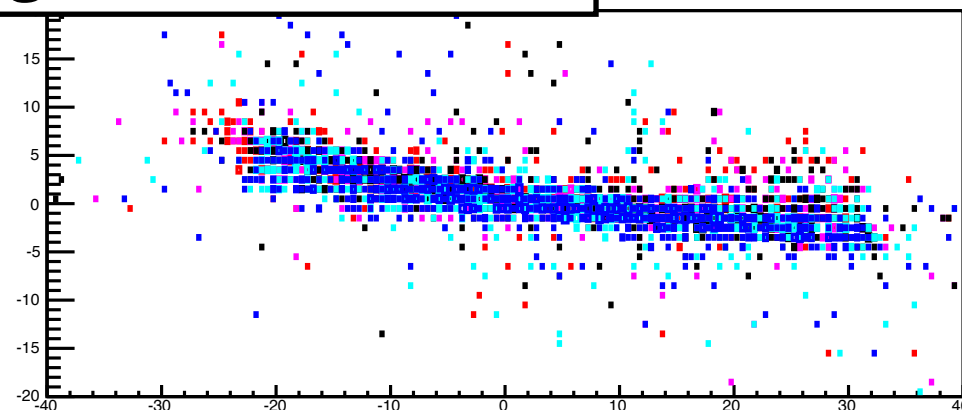


Higher-order aberration measurement

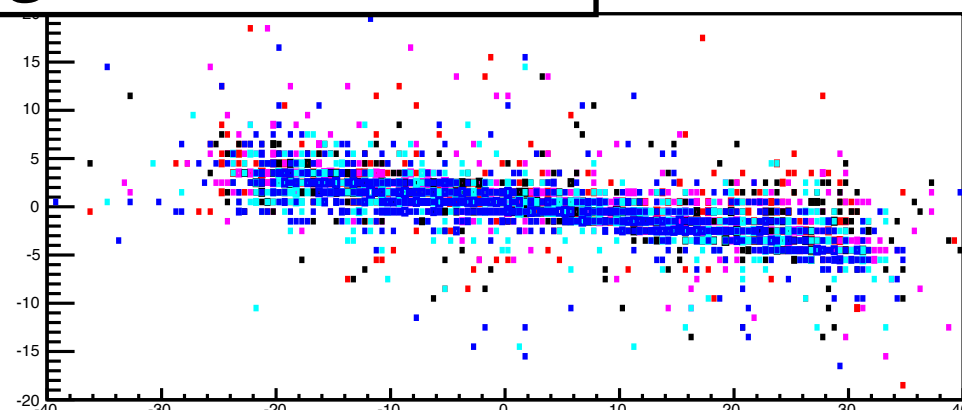
designed value $\times 2.0$



designed value $\times 1.0$



designed value $\times 0.0$

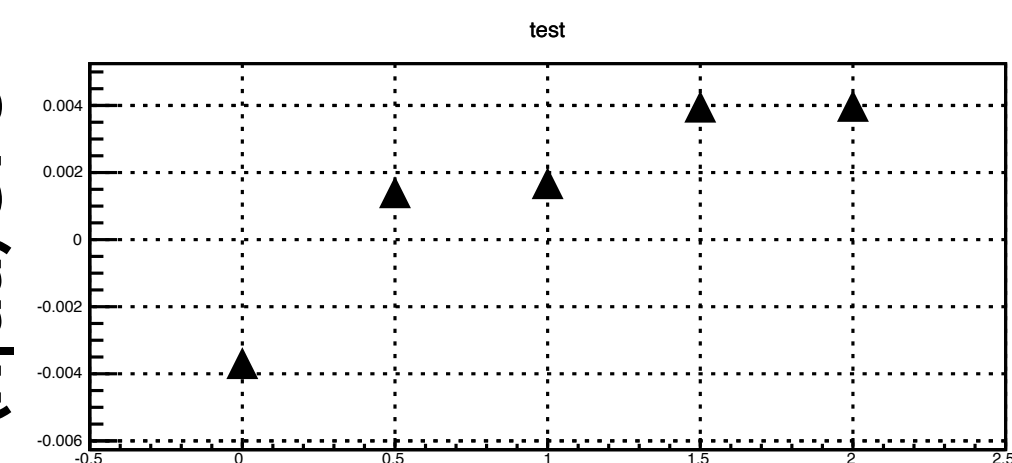


horizontal angle @ F3 [mrad]

Field curvature

$(x|aa)@F3$
 $(SX 1, 4)$

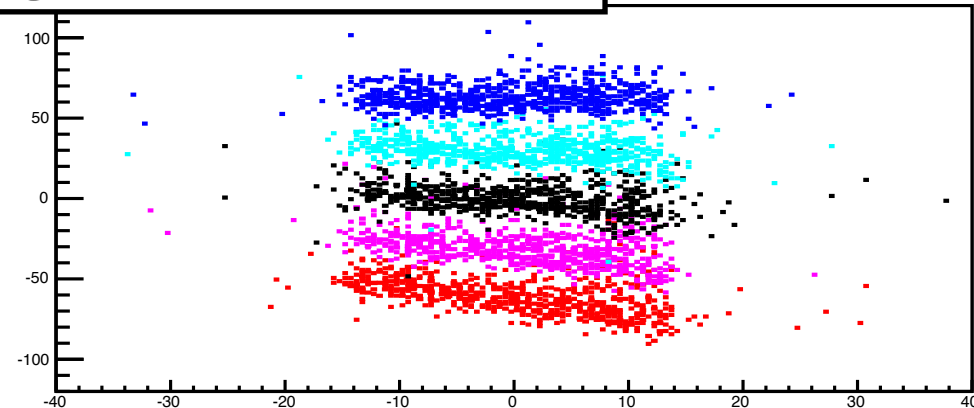
$(x|aa)@F3$



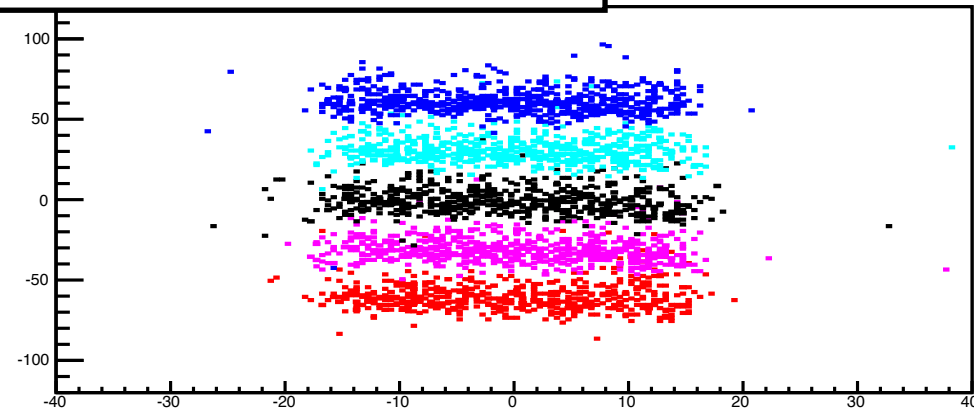
factor

Higher-order aberration measurement

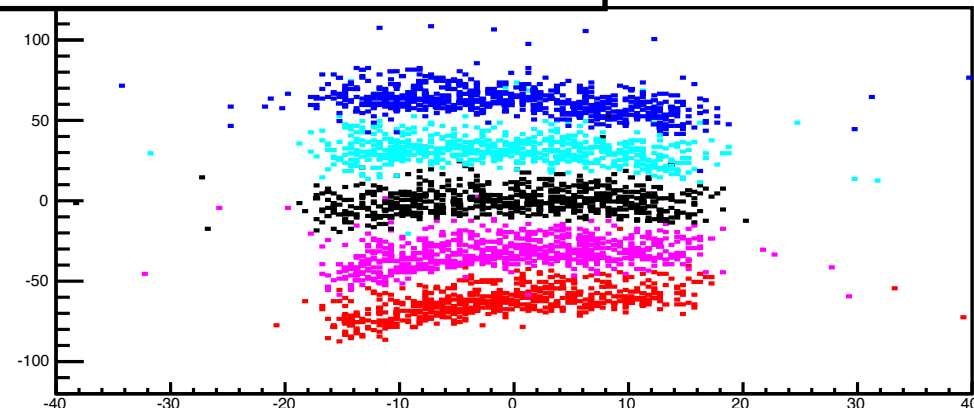
designed value $\times 2.0$



designed value $\times 1.0$



designed value $\times 0.0$

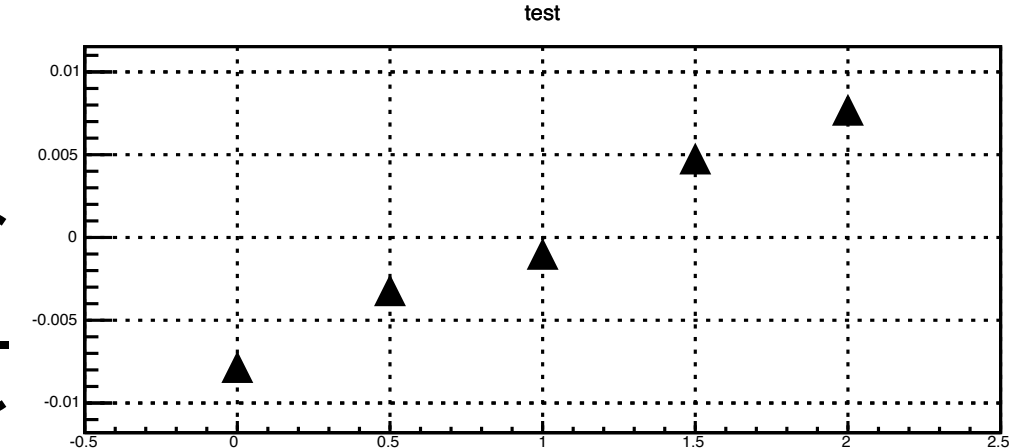


horizontal angle @ F5 [mrad]

Chromatic aberration

$(x|a\delta)@F5$
 $(SX 7, 14)$

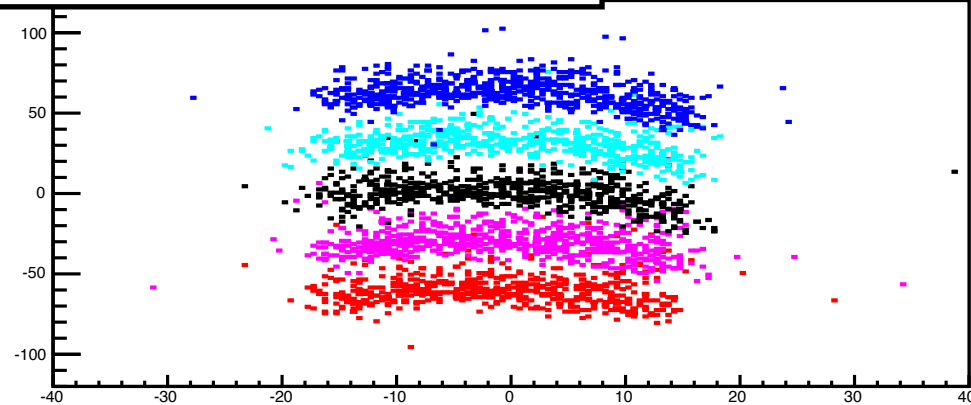
$(x|a\delta)@F5$



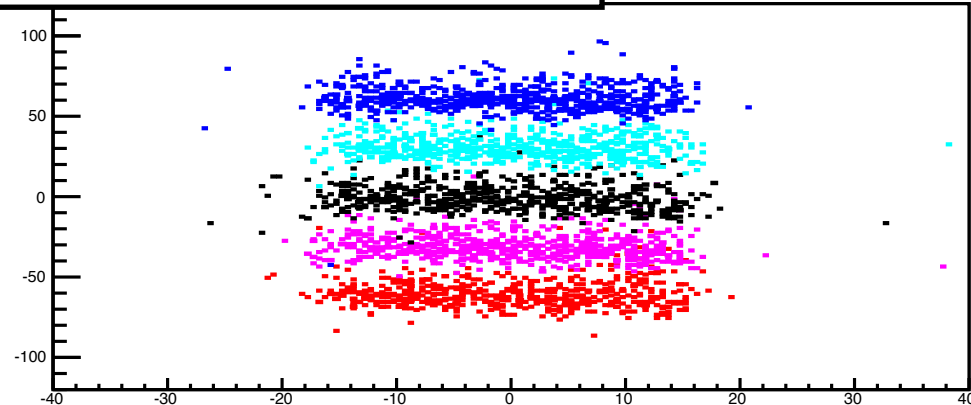
factor

Higher-order aberration measurement

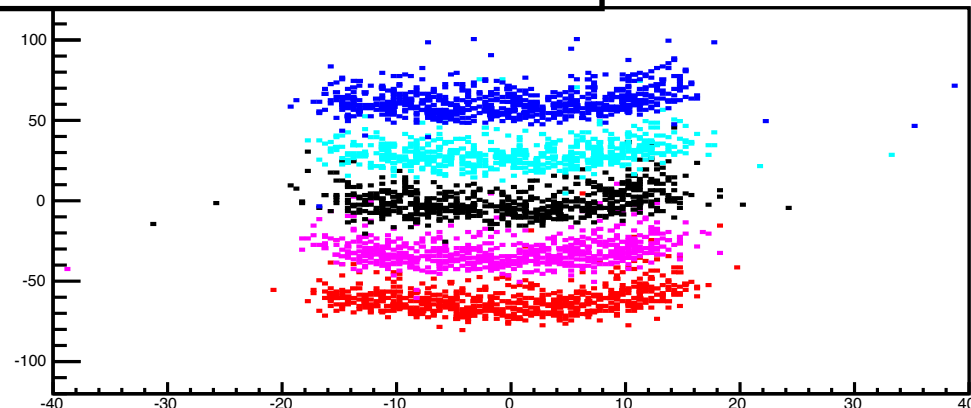
designed value $\times 2.0$



designed value $\times 1.0$



designed value $\times 0.0$

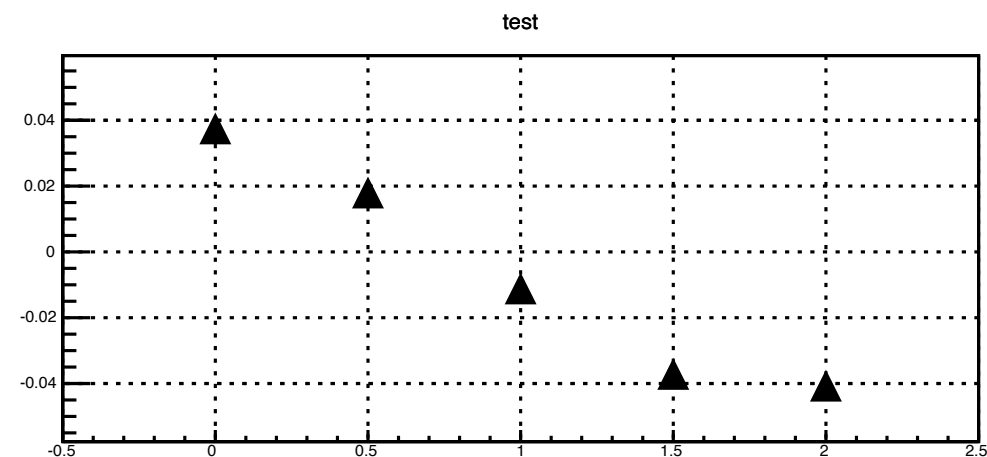


horizontal angle @ F5 [mrad]

Field curvature

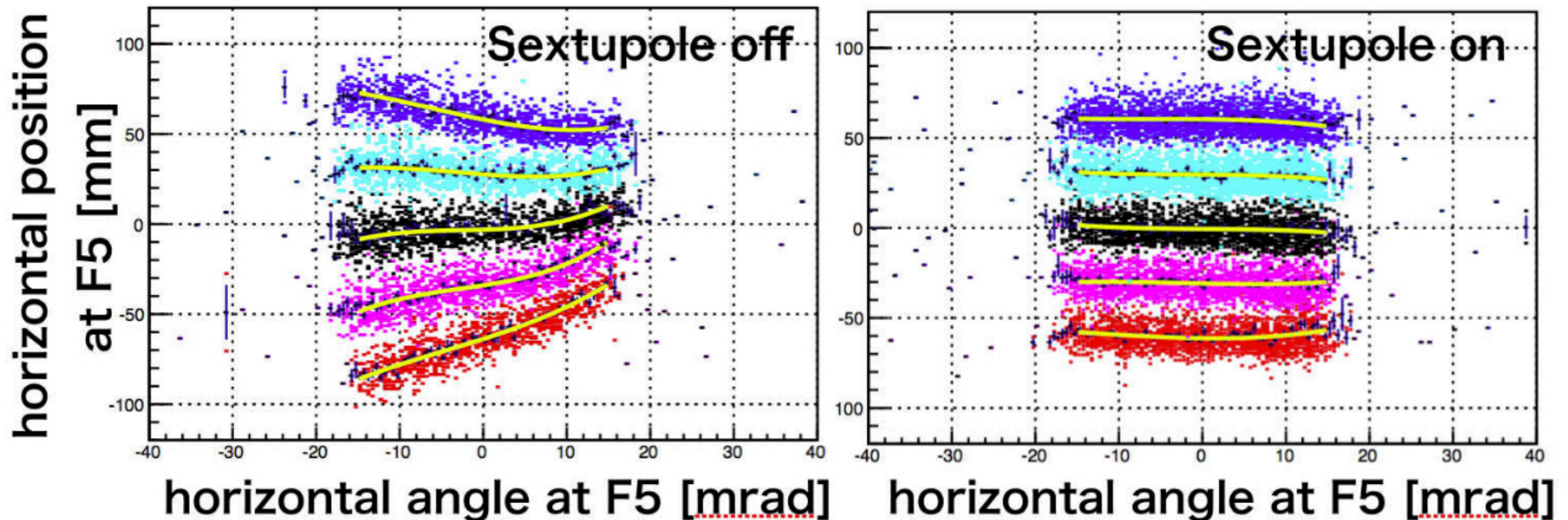
$(x|aa)@F5$
 $(SX 8, 9, 12, 13)$

$(x|aa)@F5$



factor

Higher-order aberration corrections



We achieved reduction of 2nd ($x|ad$) and 3rd ($x|aaa$) order aberrations.

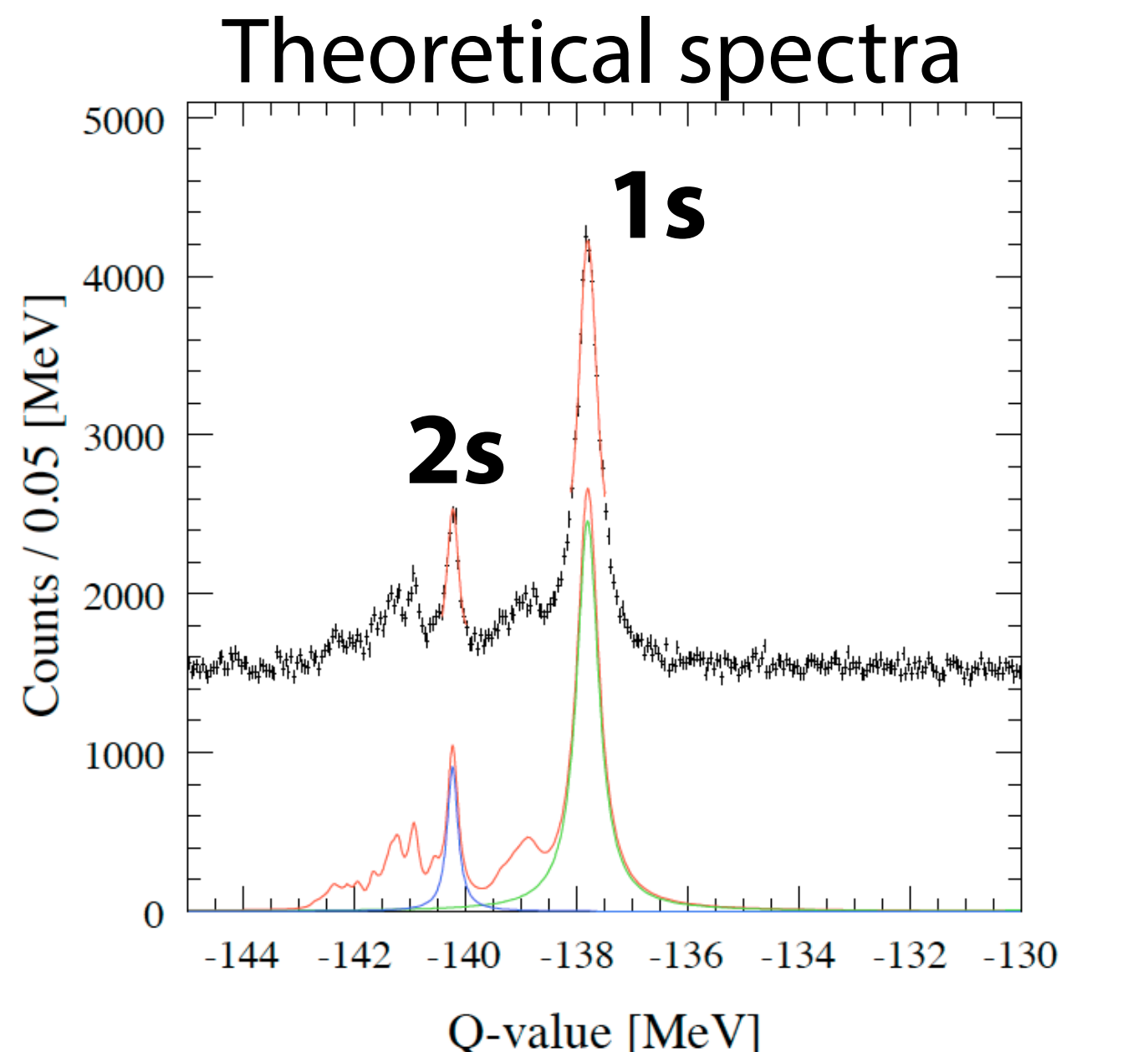
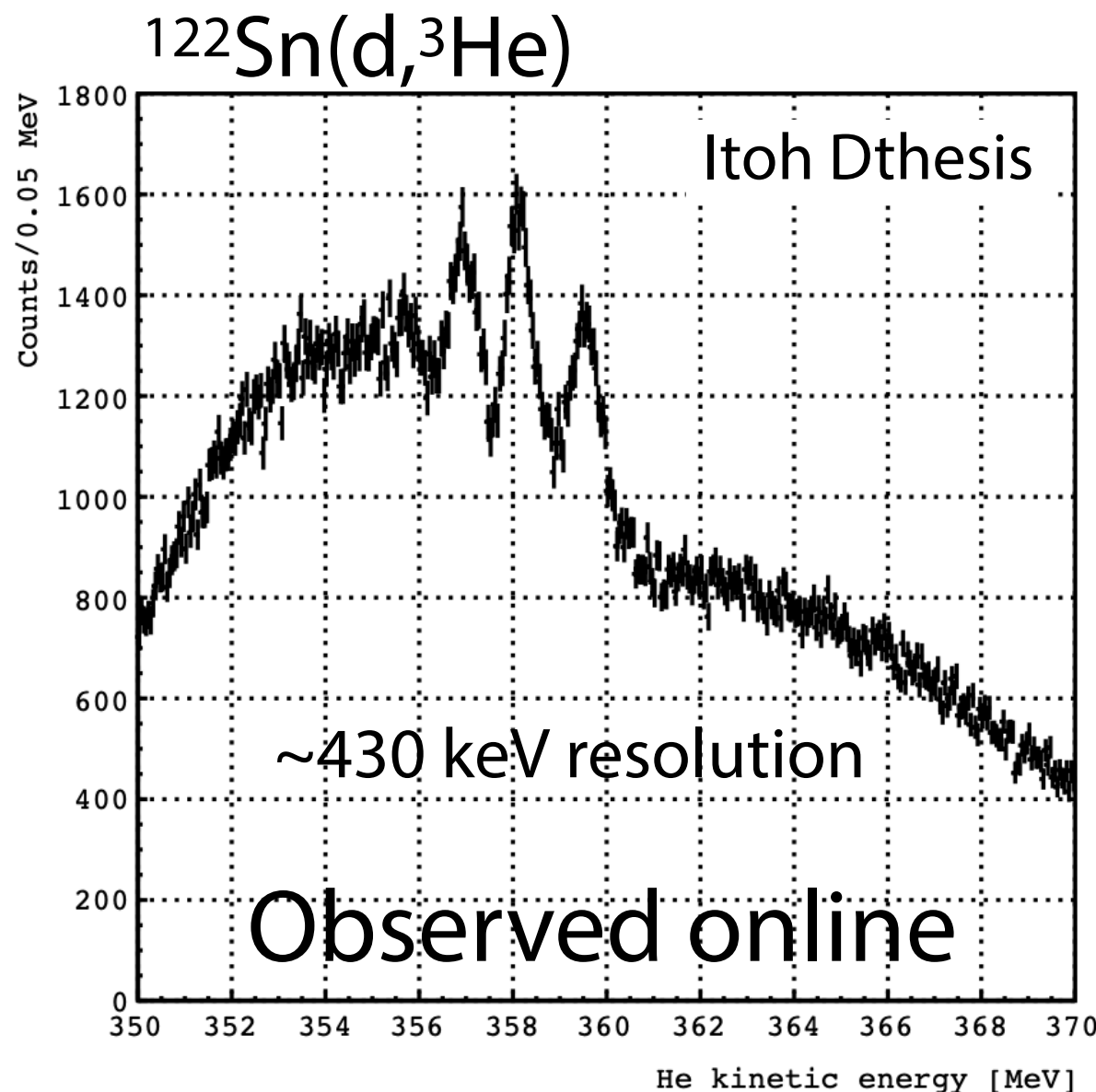
Ready for high resolution spectroscopy!!

Measured spectra, pion-nucleus interaction, and deduction of chiral condensate

Pionic ^{121}Sn atom

Pilot run of $^{122}\text{Sn}(\text{d},^3\text{He})$

15 hours DAQ in 2010

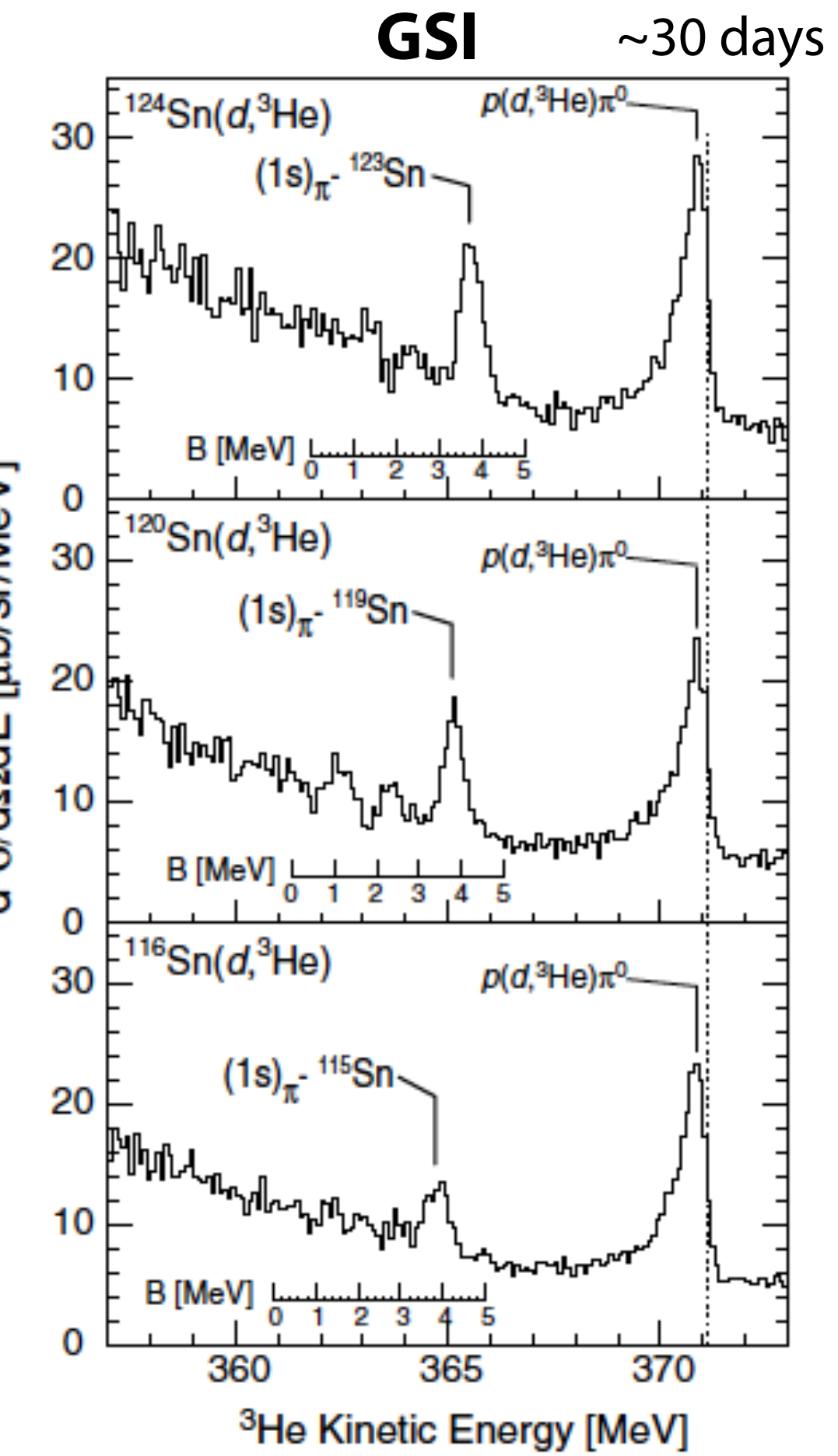
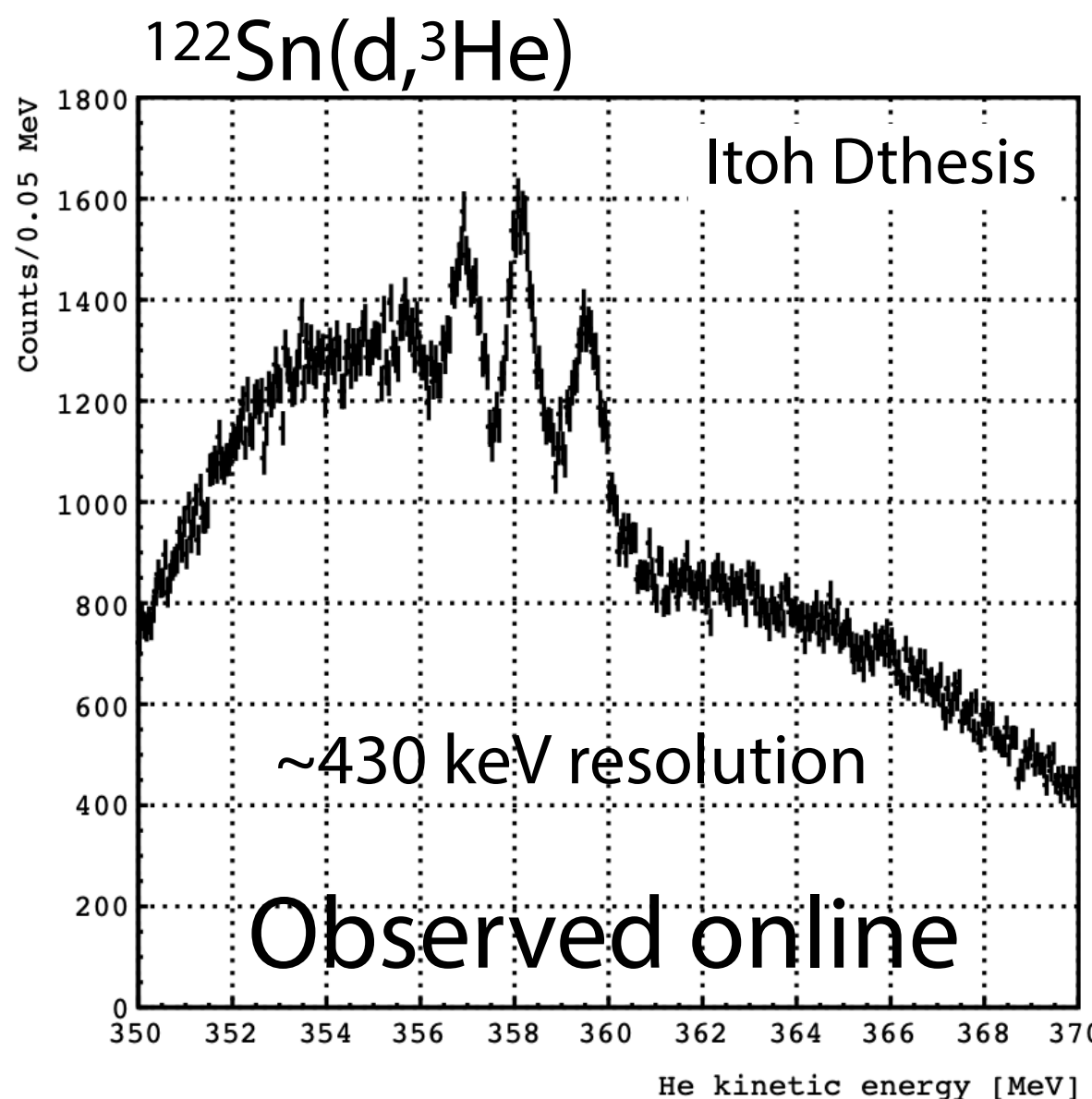


Ikeno, Hirenzaki

Pionic ^{121}Sn atom

Pilot run of $^{122}\text{Sn}(d,^3\text{He})$

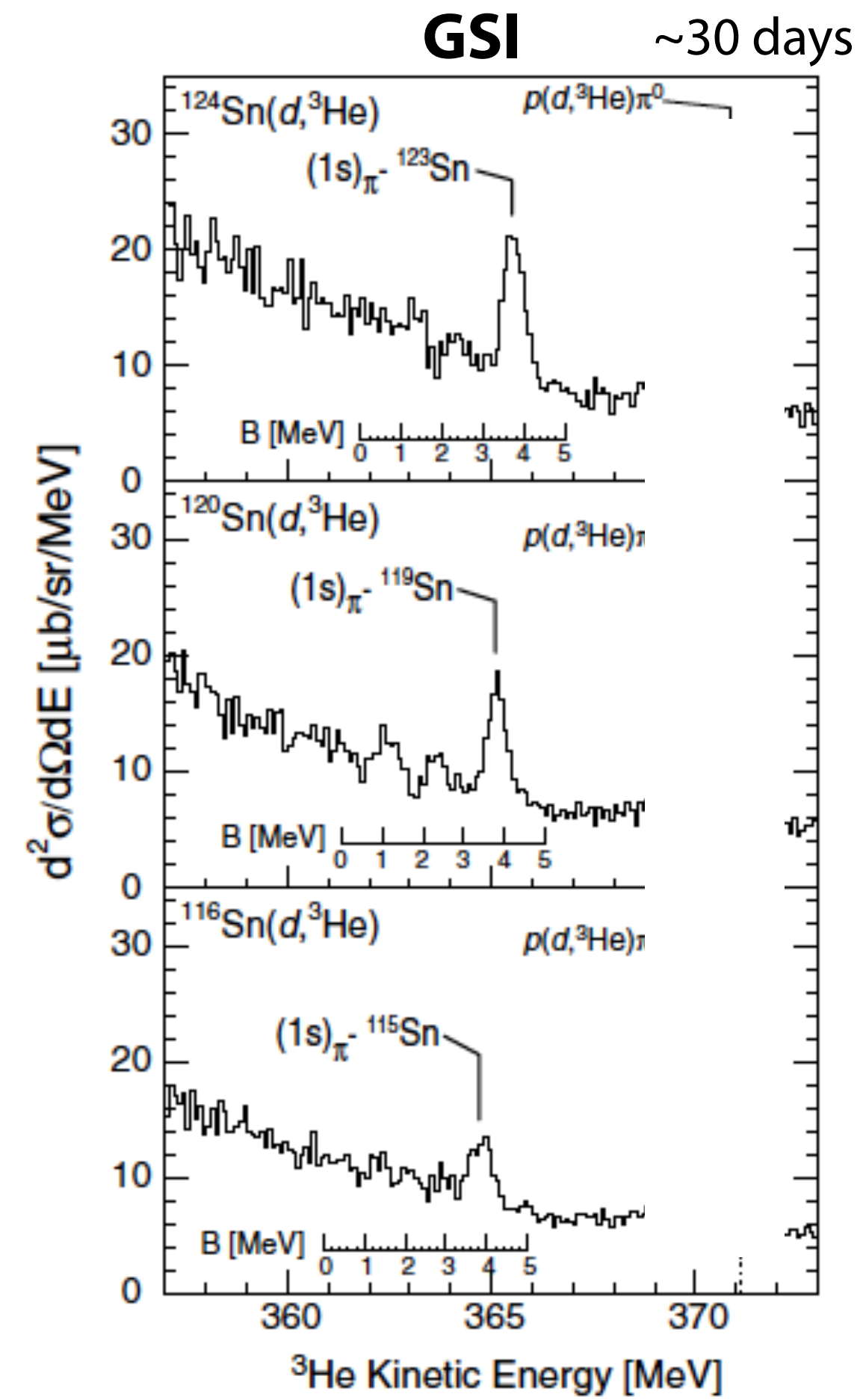
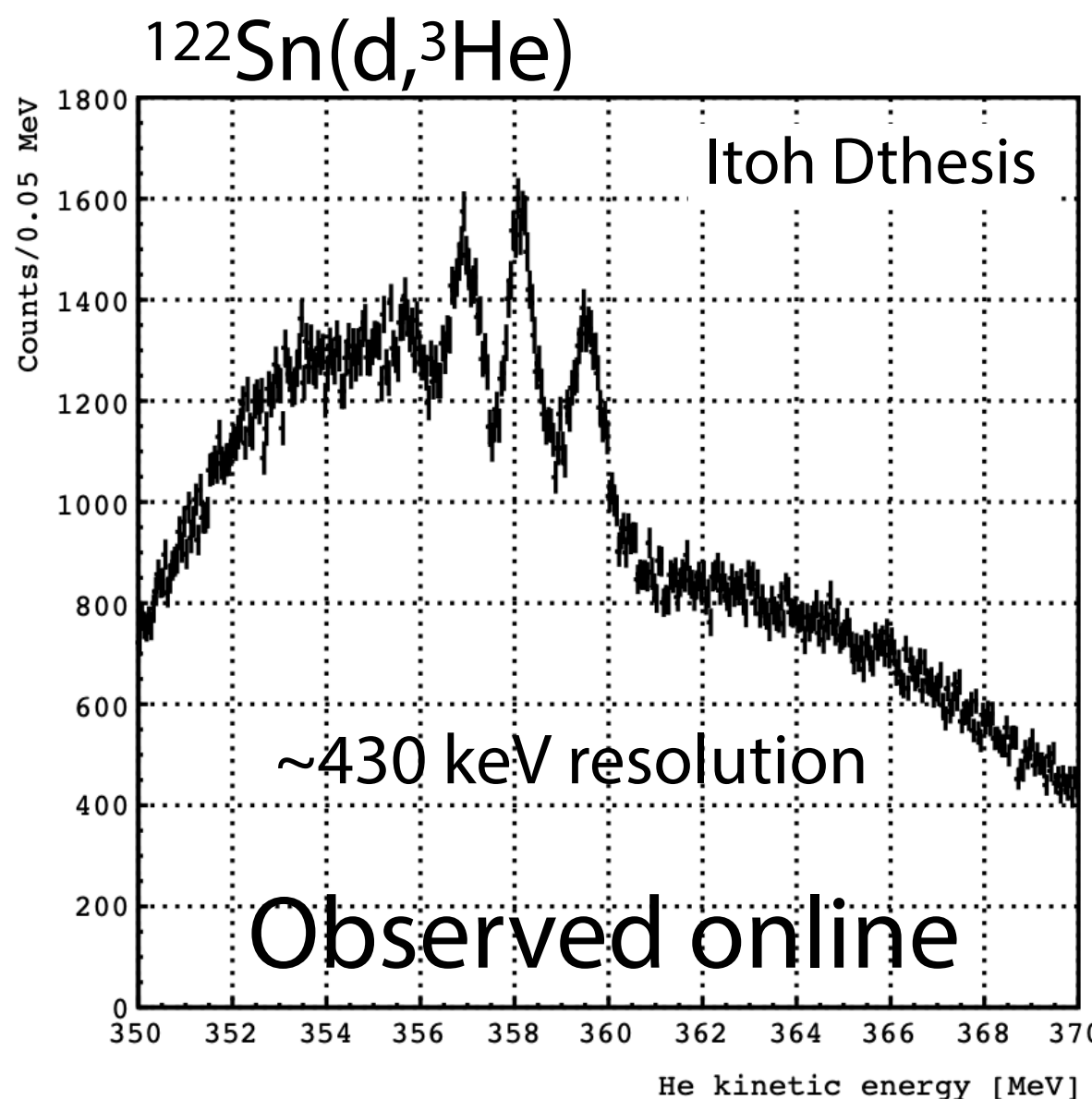
15 hours DAQ in 2010



Pionic ^{121}Sn atom

Pilot run of $^{122}\text{Sn}(d,^3\text{He})$

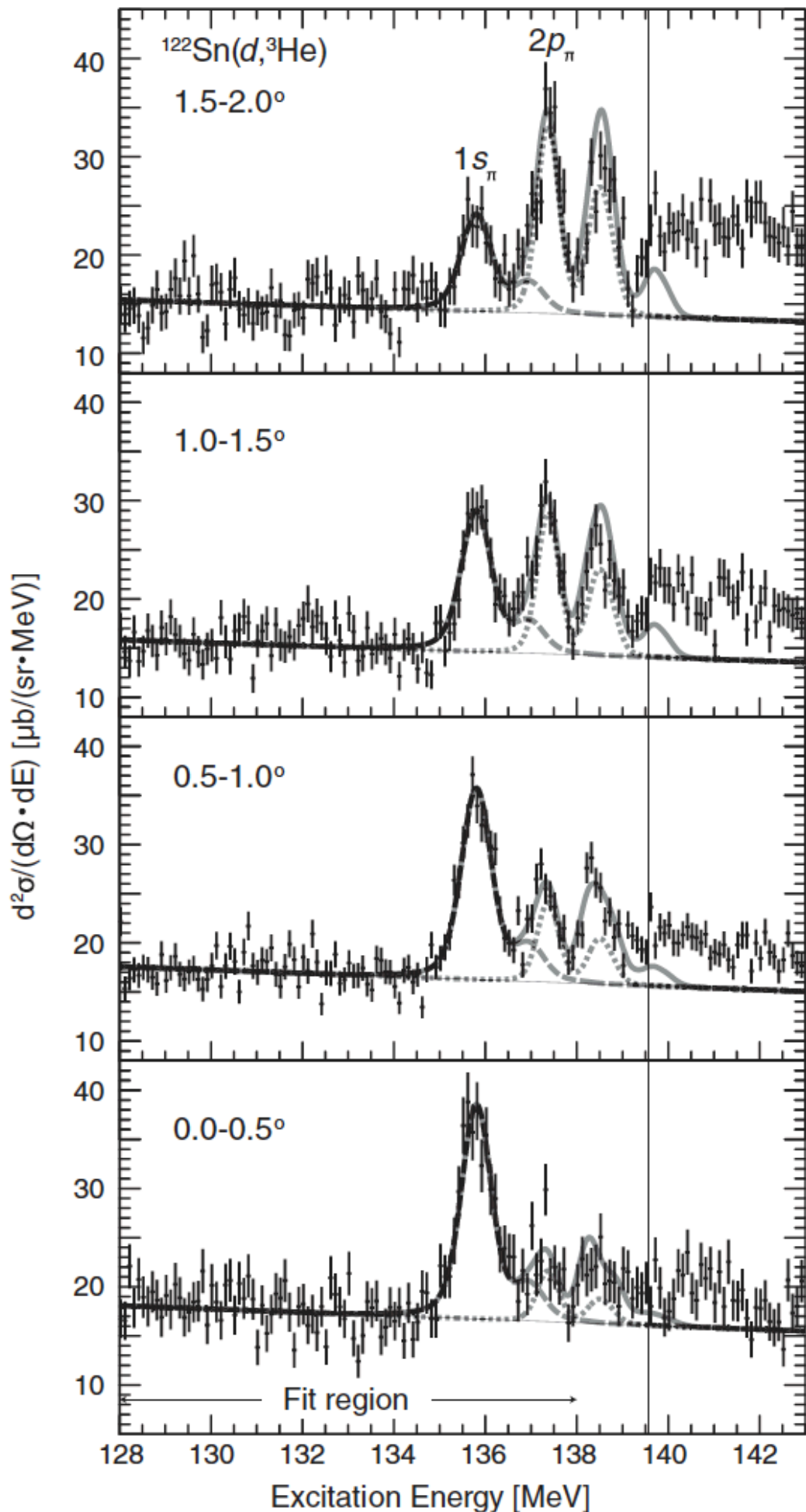
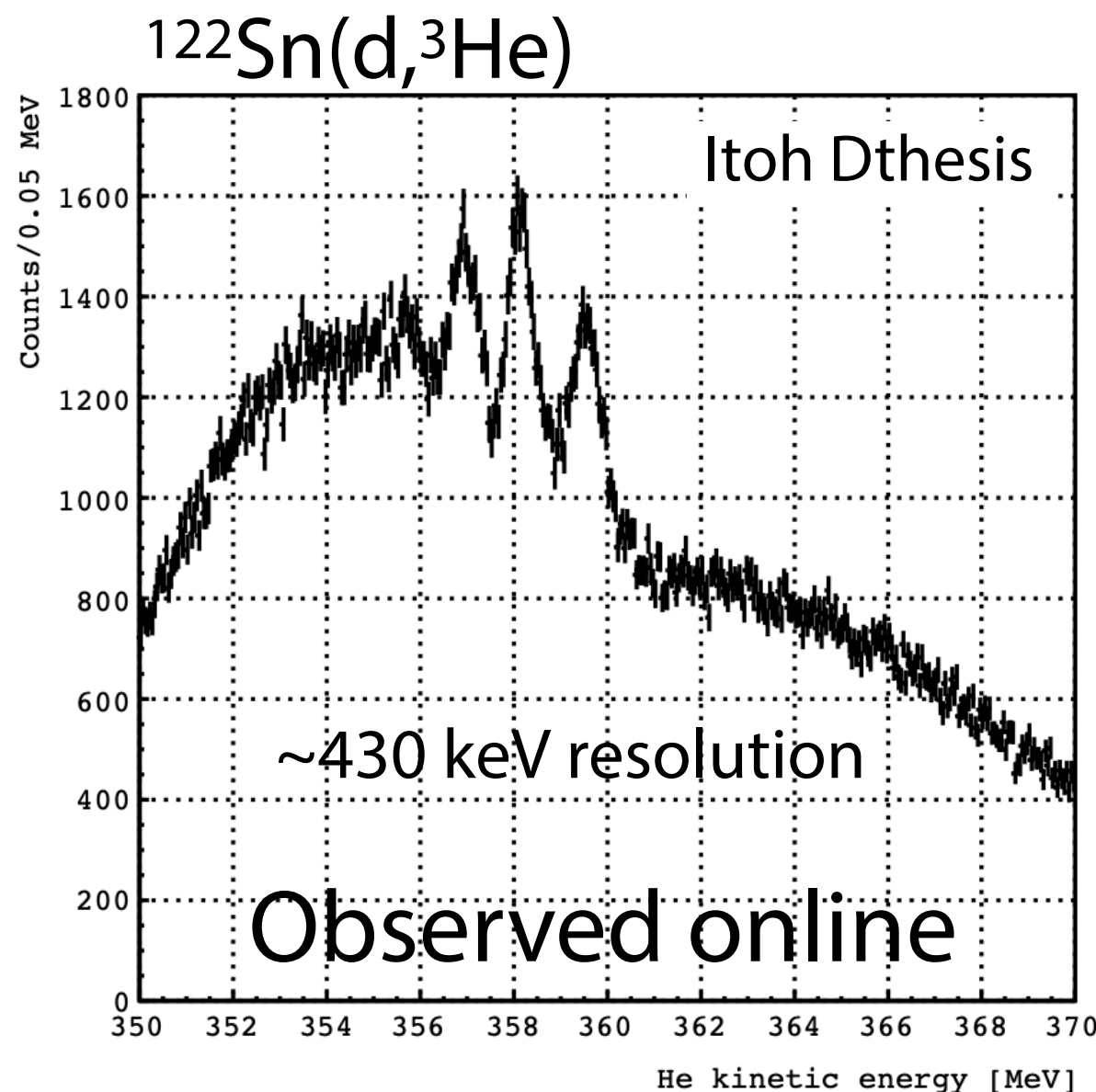
15 hours DAQ in 2010



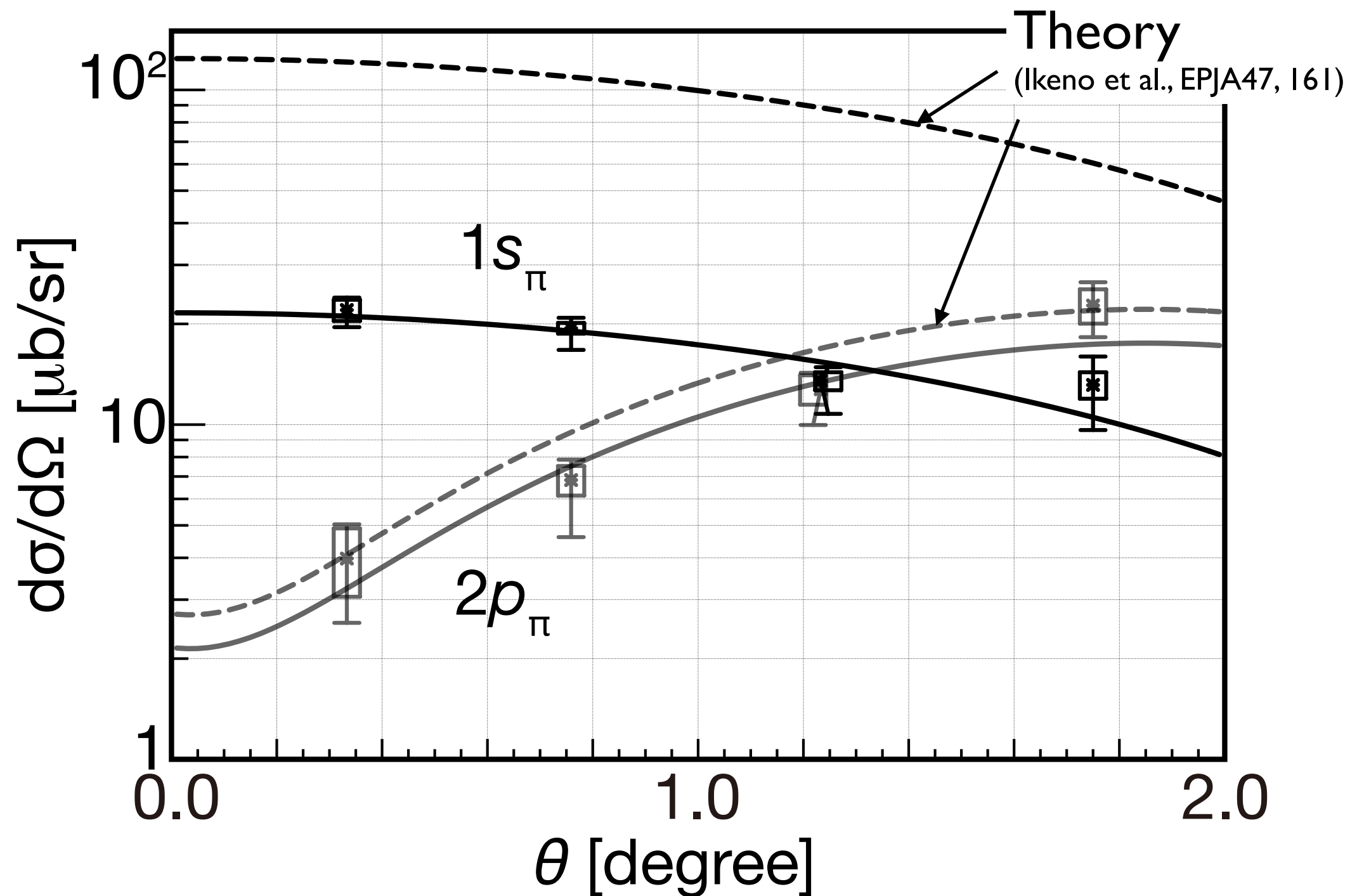
Pionic ^{121}Sn atom

Pilot run of $^{122}\text{Sn}(d,^3\text{He})$
15 hours DAQ in 2010

First observation of
 θ dependence of
 π atom cross section



1s and 2p pionic atom cross sections in ($d, {}^3He$)



θ dependence is well reproduced.
Theory calculates 5x larger cross section for 1s

Pionic ^{121}Sn atom

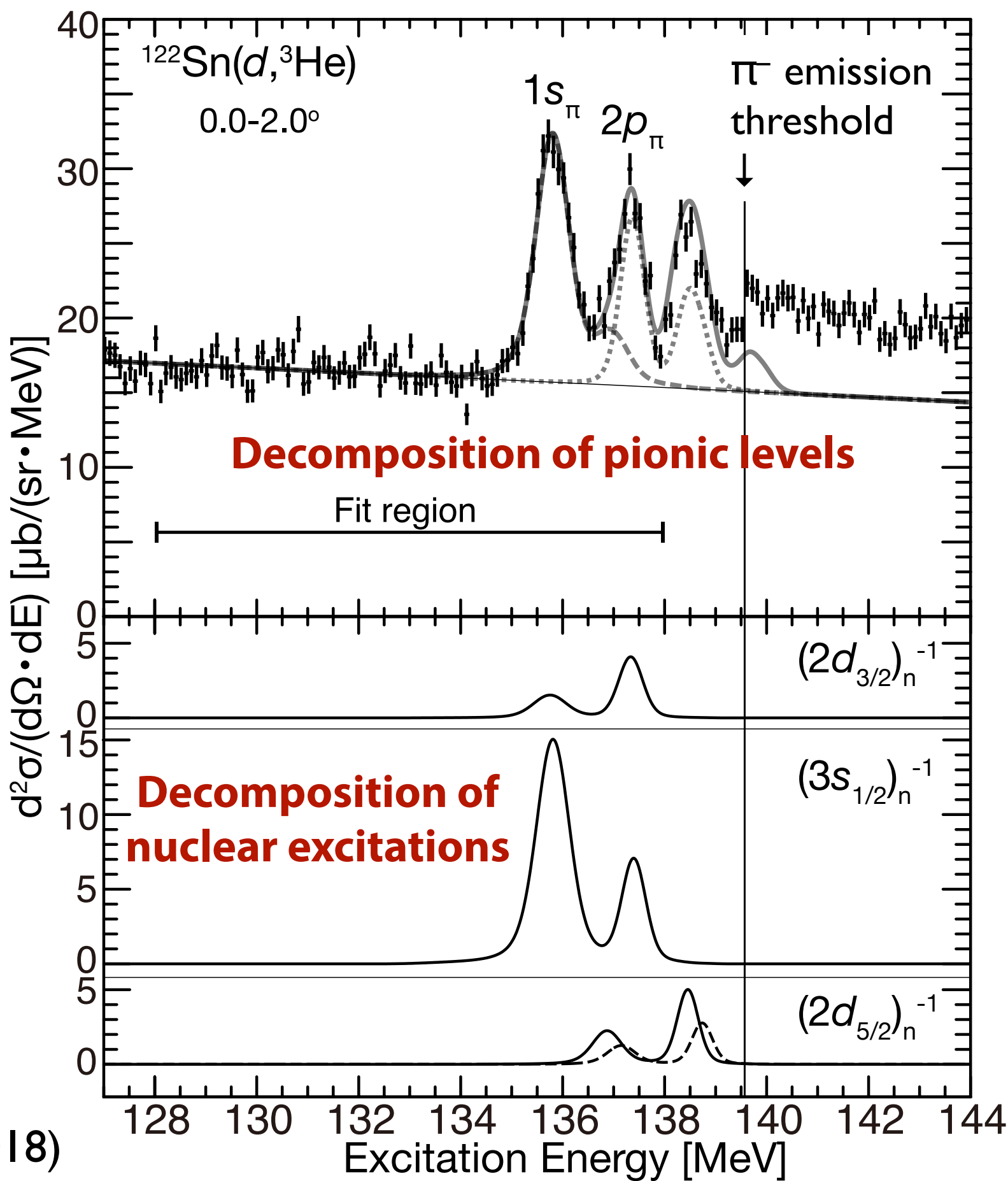
Pilot run
15 hours DAQ in 2010

First simultaneous 1s and 2p observation

$B_{1s} = 3.828 \pm 0.013(\text{stat})^{+0.036}_{-0.033}(\text{syst}) \text{ MeV}$
$\Gamma_{1s} = 0.252 \pm 0.054(\text{stat})^{+0.053}_{-0.070}(\text{syst}) \text{ MeV}$
$B_{2p} = 2.238 \pm 0.015(\text{stat})^{+0.046}_{-0.043}(\text{syst}) \text{ MeV}$

Resolution 394 keV (FWHM)

Theories
 $B_{1s} = 3.787\text{--}3.850 \text{ MeV}$
 $\Gamma_{1s} = 0.306\text{--}0.324 \text{ MeV}$
 $B_{2p} = 2.257\text{--}2.276 \text{ MeV}$



Pionic ^{121}Sn atom

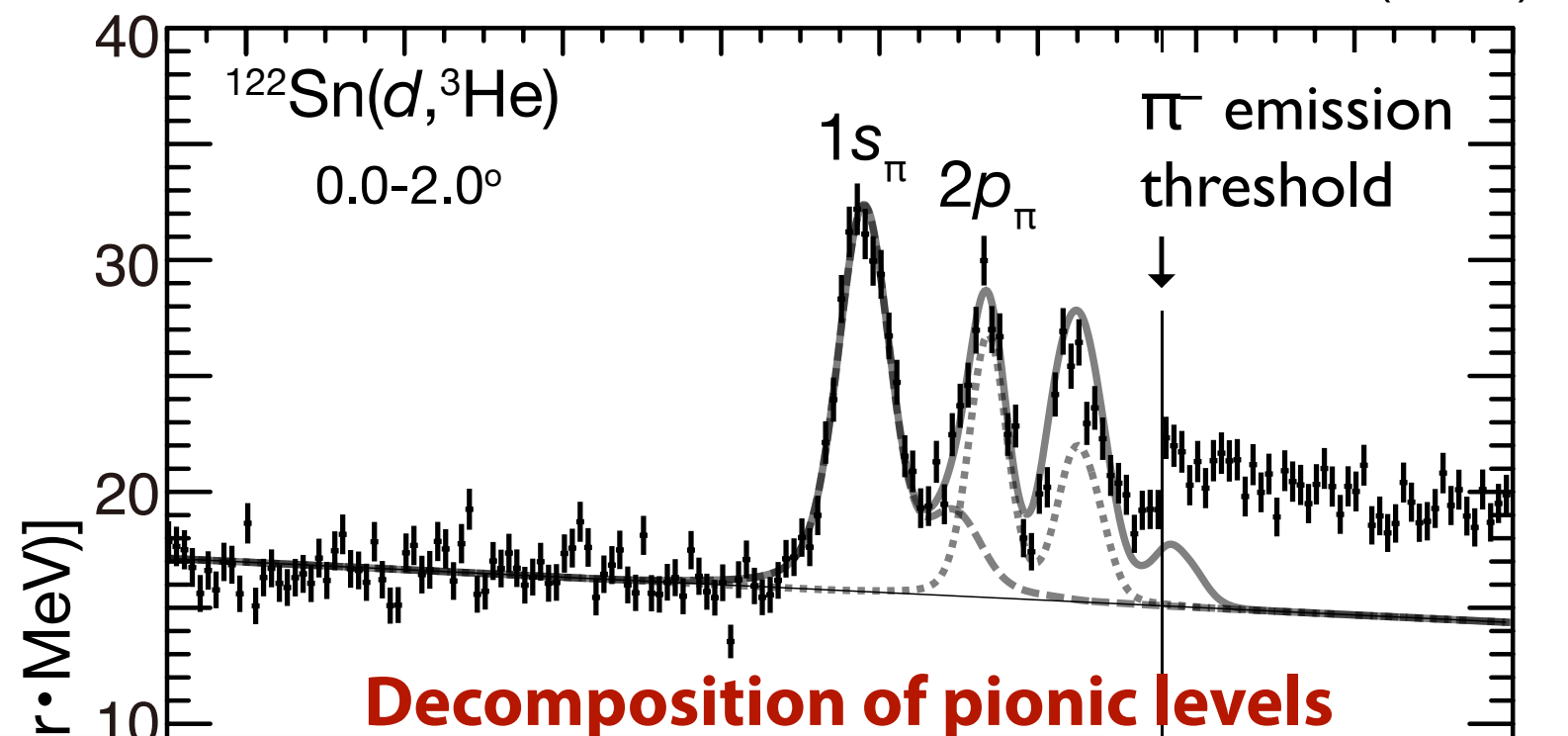
Pilot run
15 hours DAQ in 2010

First simultaneous 1s and 2p observation

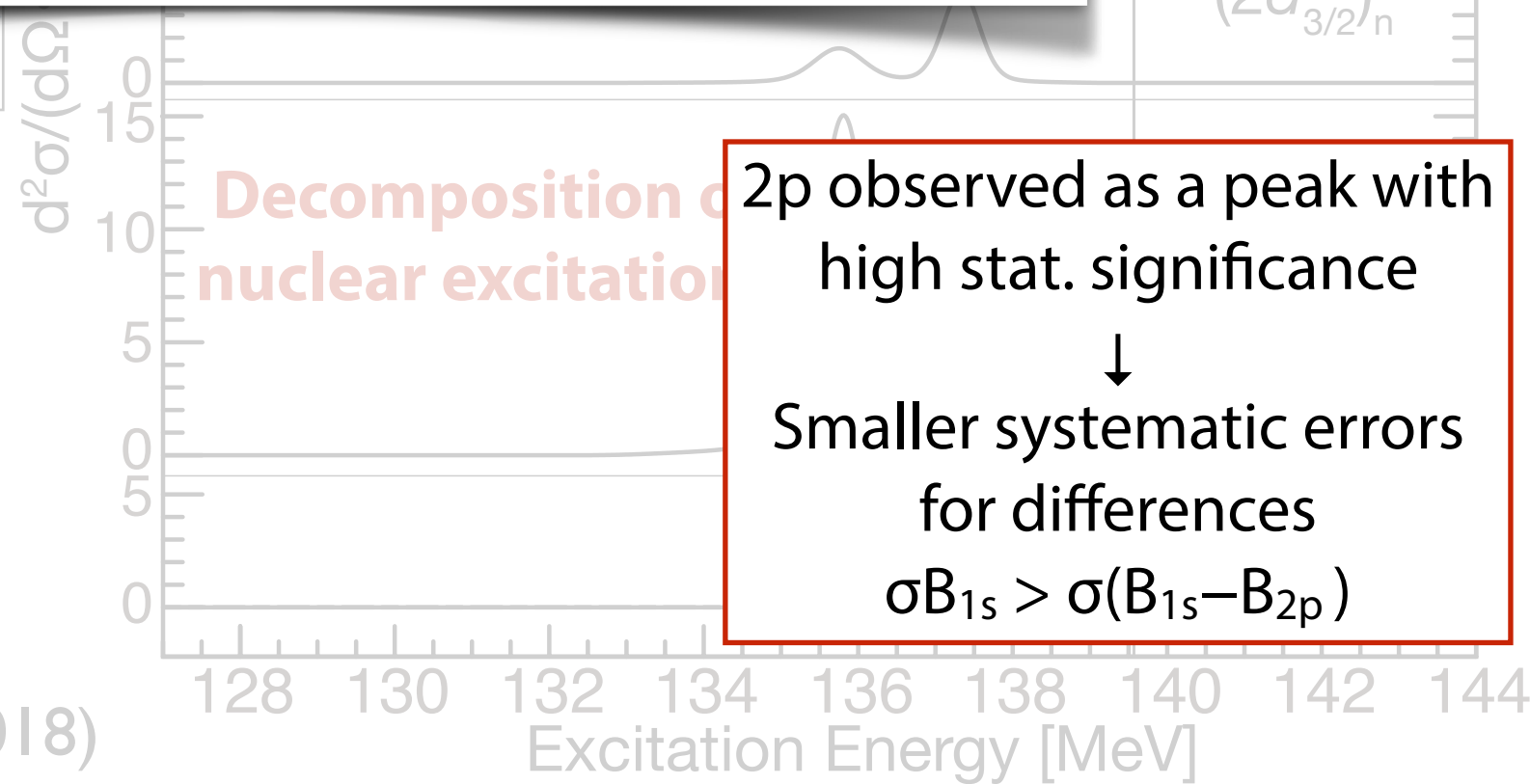
$B_{1s} = 3.828 \pm 0.0$
$\Gamma_{1s} = 0.252 \pm 0.0$
$B_{2p} = 2.238 \pm 0.015(\text{stat})^{+0.046}_{-0.043}(\text{syst}) \text{ MeV}$

Resolution 394 keV (FWHM)

Theories
 $B_{1s} = 3.787\text{--}3.850 \text{ MeV}$
 $\Gamma_{1s} = 0.306\text{--}0.324 \text{ MeV}$
 $B_{2p} = 2.257\text{--}2.276 \text{ MeV}$



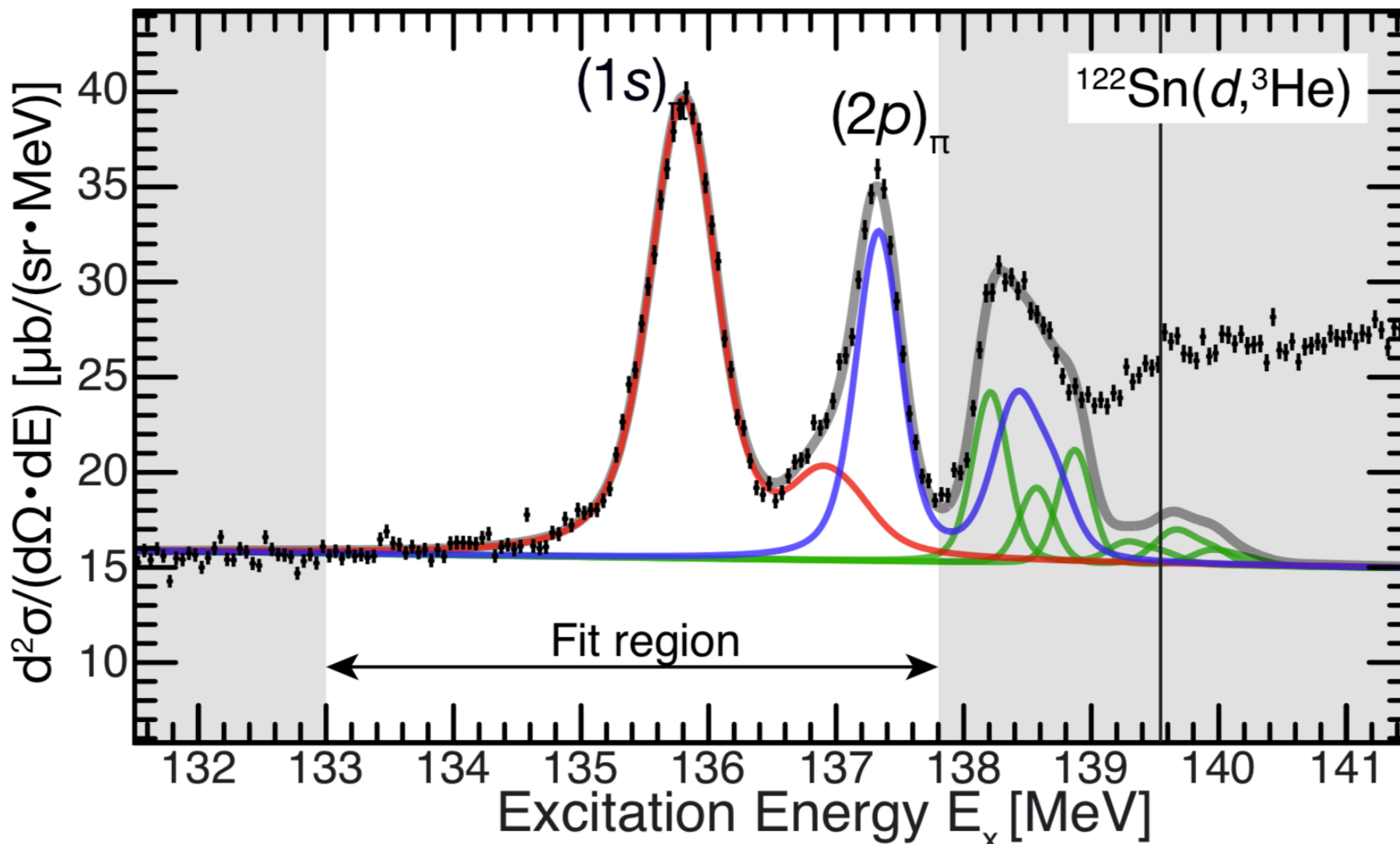
**However, precision was not enough...
DM tuning is needed!!**



High Precision Spectrum of $^{122}\text{Sn}(d,^3\text{He})$ in 2014 run

Pionic atom unveils hidden structure of QCD vacuum

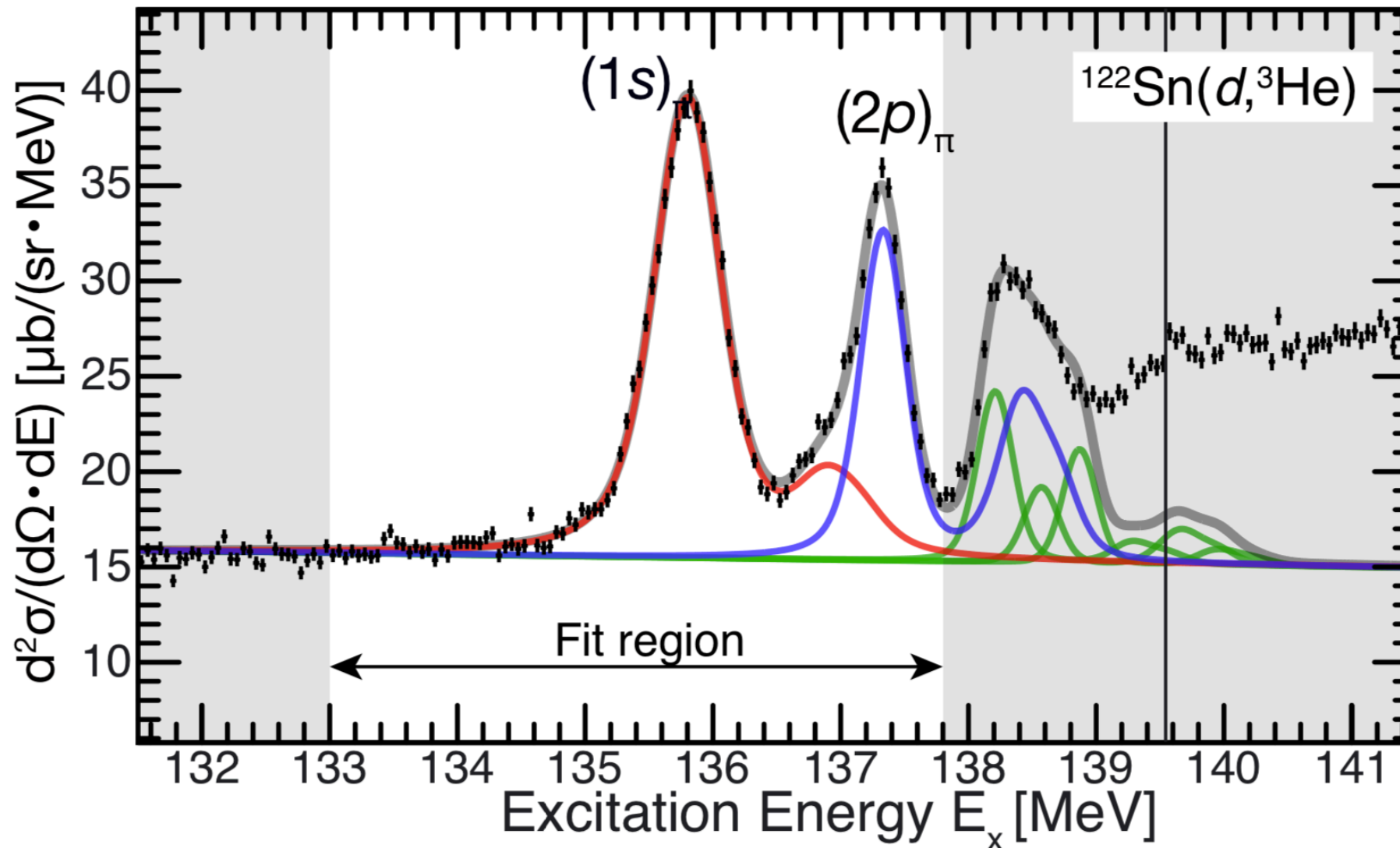
Takahiro Nishi¹, Kenta Itahashi^{1,*}, DeukSoon Ahn^{1,2}, Georg P.A. Berg³, Masanori Dozono¹, Daijiro Etoh⁴, Hiroyuki Fujioka⁵, Naoki Fukuda¹, Nobuhisa Fukunishi¹, Hans Geissel⁶, Emma Haettner⁶, Tadashi Hashimoto¹, Ryugo S. Hayano⁷, Satoru Hirenzaki⁸, Hiroshi Horii⁷, Natsumi Ikeno⁹, Naoto Inabe¹, Masahiko Iwasaki¹, Daisuke Kameda¹, Keichi Kisamori¹⁰, Yu Kiyokawa¹⁰, Toshiyuki Kubo¹, Kensuke Kusaka¹, Masafumi Matsushita¹⁰, Shin'ichiro Michimasa¹⁰, Go Mishima⁷, Hiroyuki Miya¹, Daichi Murai¹, Hideko Nagahiro⁸, Megumi Niikura⁷, Naoko Nose-Togawa¹¹, Shinsuke Ota¹⁰, Naruhiko Sakamoto¹, Kimiko Sekiguchi⁴, Yuta Shiokawa⁴, Hiroshi Suzuki¹, Ken Suzuki¹², Motonobu Takaki¹⁰, Hiroyuki Takeda¹, Yoshiki K. Tanaka¹, Tomohiro Uesaka¹, Yasumori Wada⁴, Atamu Watanabe⁴, Yun N. Watanabe⁷, Helmut Weick⁶, Hiroki Yamakami⁵, Yoshiyuki Yanagisawa¹, and Koichi Yoshida¹



Optimized DM

2p observed as a peak with
high stat. significance
↓
Smaller systematic errors
for differences
 $\sigma B_{1s} > \sigma(B_{1s} - B_{2p})$

High Precision Spectrum of $^{122}\text{Sn}(d,^3\text{He})$ in 2014 run



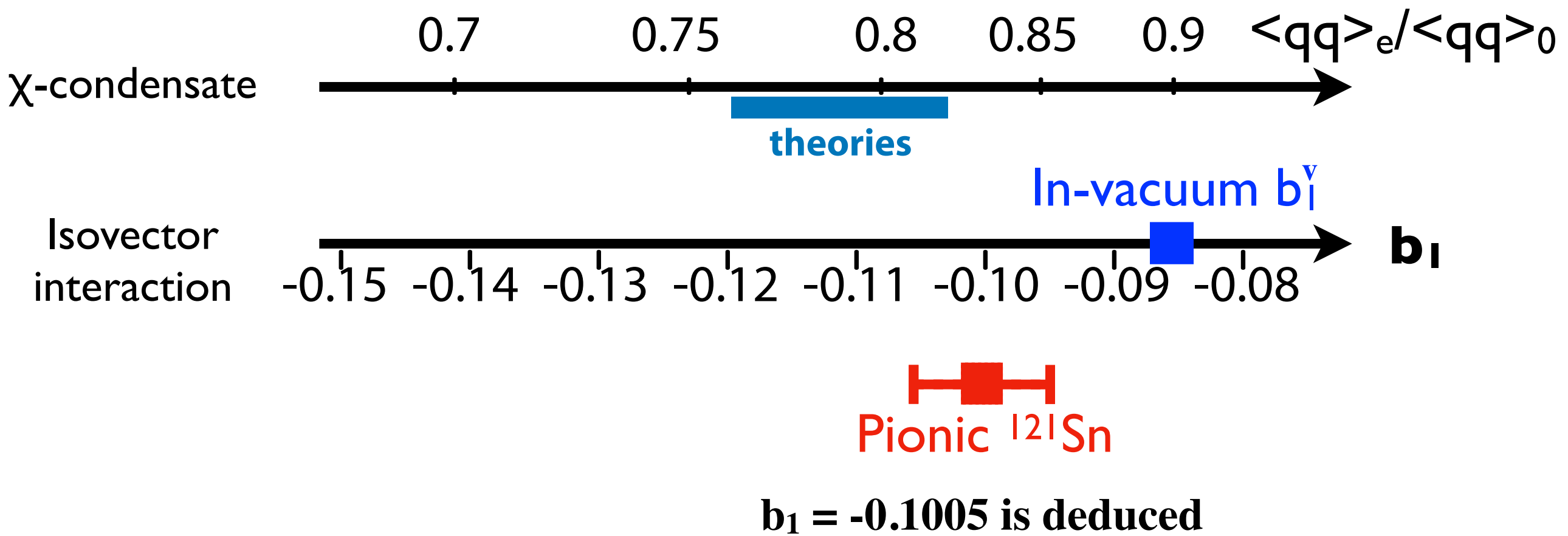
	[keV]	Statistical	Systematic
$B_\pi(1s)$	3831	±3	+78 – 76
$B_\pi(2p)$	2276	±3	+84 – 83
$B_\pi(1s) - B_\pi(2p)$	1555	±4	±12
$\Gamma_\pi(1s)$	316	±12	+36 – 39
$\Gamma_\pi(2p)$	164	±17	+41 – 32
$\Gamma_\pi(1s) - \Gamma_\pi(2p)$	152	±20	+28 – 36

Best resolution 287 keV (FWHM)

52

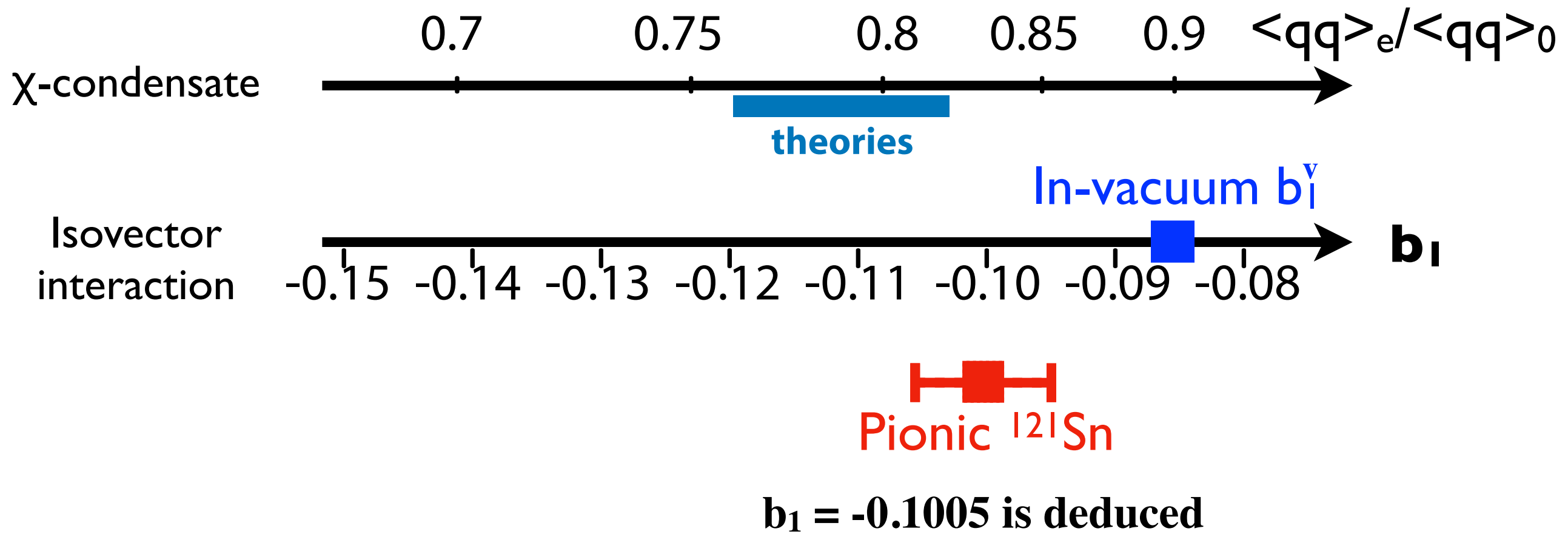
2p observed as a peak with
high stat. significance
↓
Smaller systematic errors
for differences
 $\sigma B_{1s} > \sigma(B_{1s} - B_{2p})$

Deduced b_1 from pionic Sn spectrum



	[keV]	Statistical	Systematic
$B_\pi(1s)$	3831	± 3	$+78 - 76$
$B_\pi(2p)$	2276	± 3	$+84 - 83$
$B_\pi(1s) - B_\pi(2p)$	1555	± 4	± 12
$\Gamma_\pi(1s)$	316	± 12	$+36 - 39$
$\Gamma_\pi(2p)$	164	± 17	$+41 - 32$
$\Gamma_\pi(1s) - \Gamma_\pi(2p)$	152	± 20	$+28 - 36$

Deduced b_1 from pionic Sn spectrum



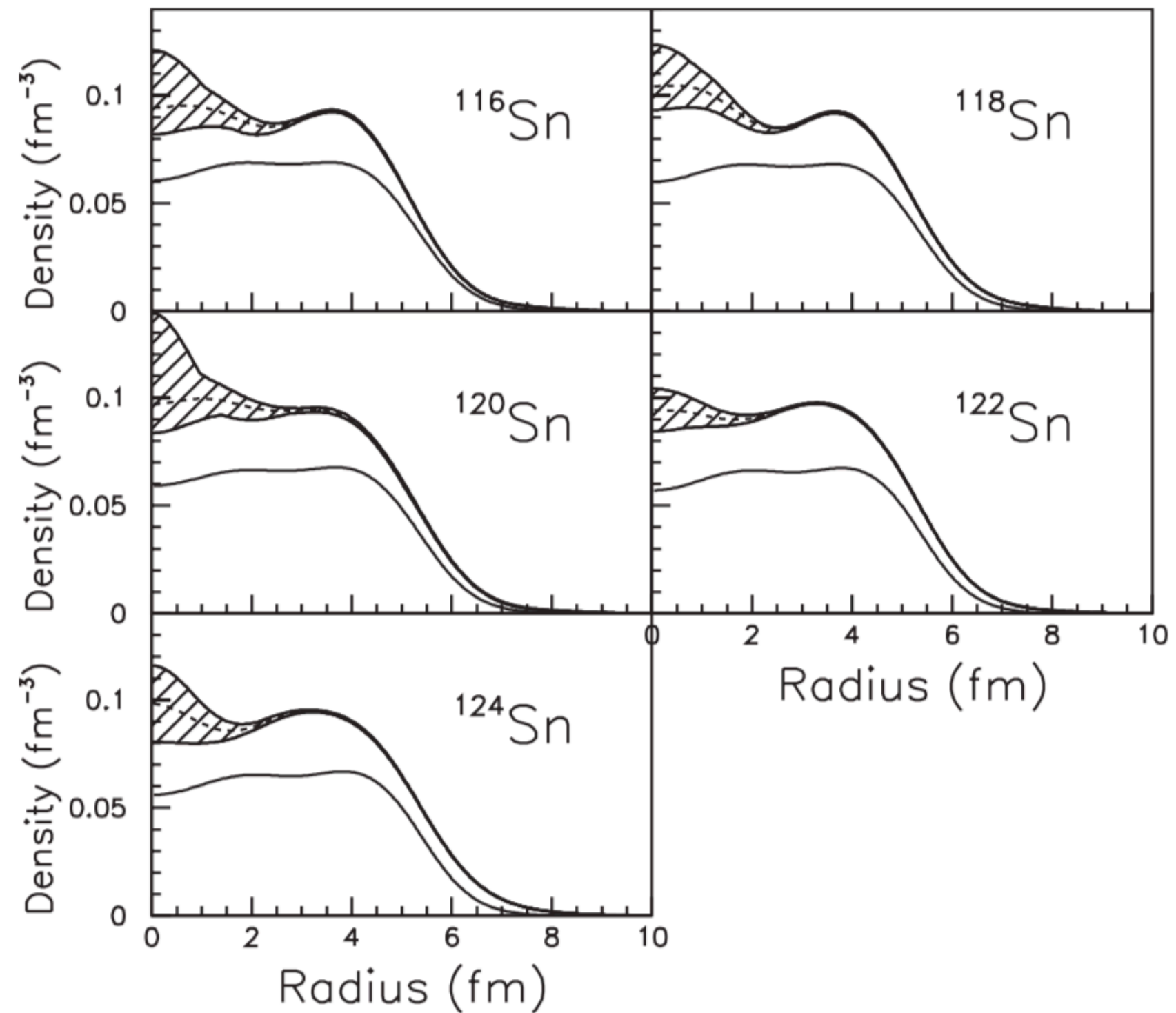
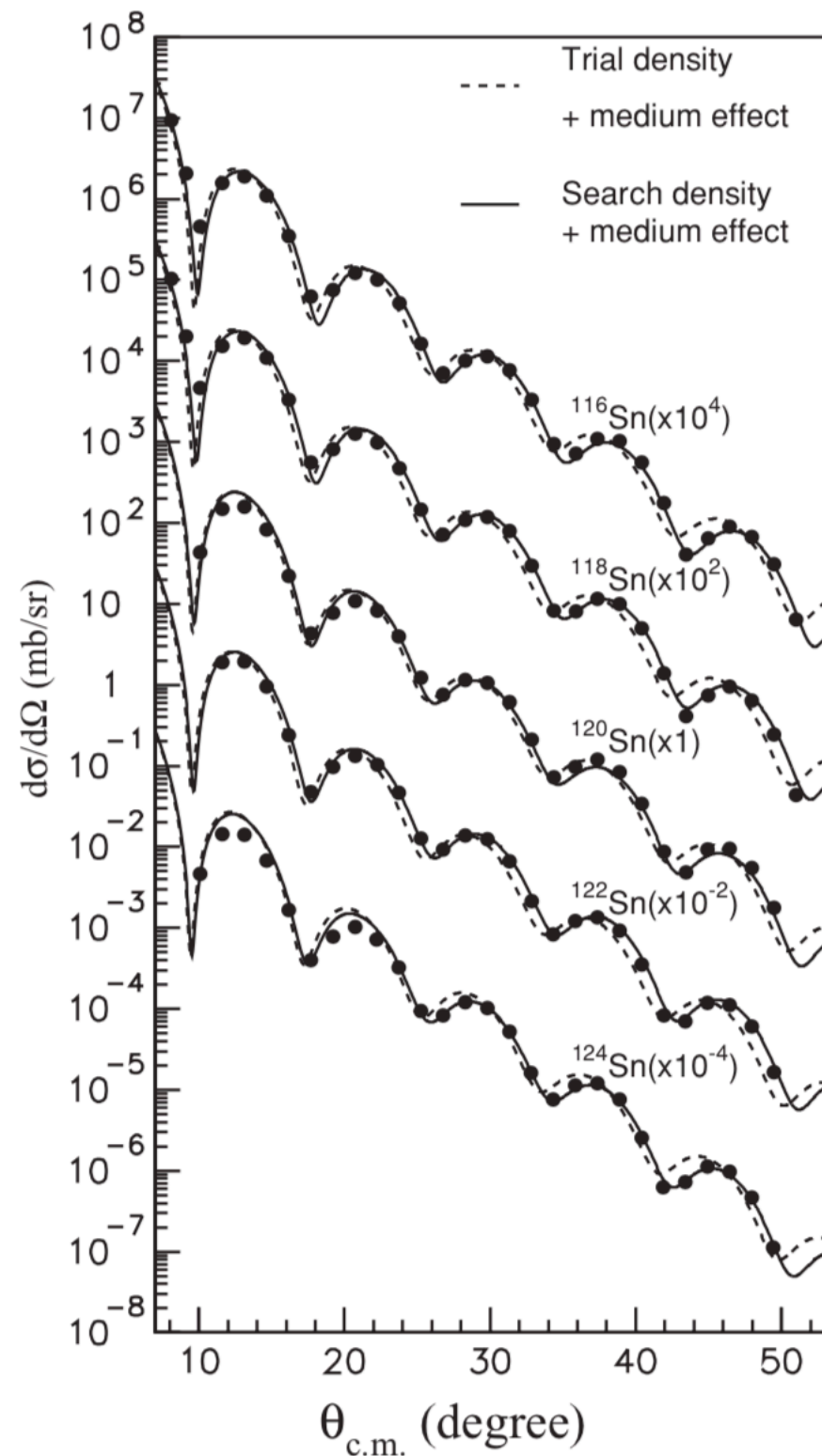
	[keV]	Statistical	Systematic
$B_\pi(1s)$	3831	± 3	$+78 - 76$
$B_\pi(2p)$	2276	± 3	$+84 - 83$
$B_\pi(1s) - B_\pi(2p)$	1555	± 4	± 12
$\Gamma_\pi(1s)$	316	± 12	$+36 - 39$
$\Gamma_\pi(2p)$	164	± 17	$+41 - 32$
$\Gamma_\pi(1s) - \Gamma_\pi(2p)$	152	± 20	$+28 - 36$

LLE : short-range correction
Sn p : neutron density distribution
Abs. : representation of absorption term
Green : cross section calculation method
Res. : Residual interaction
Spec. : neutron spectroscopic factors

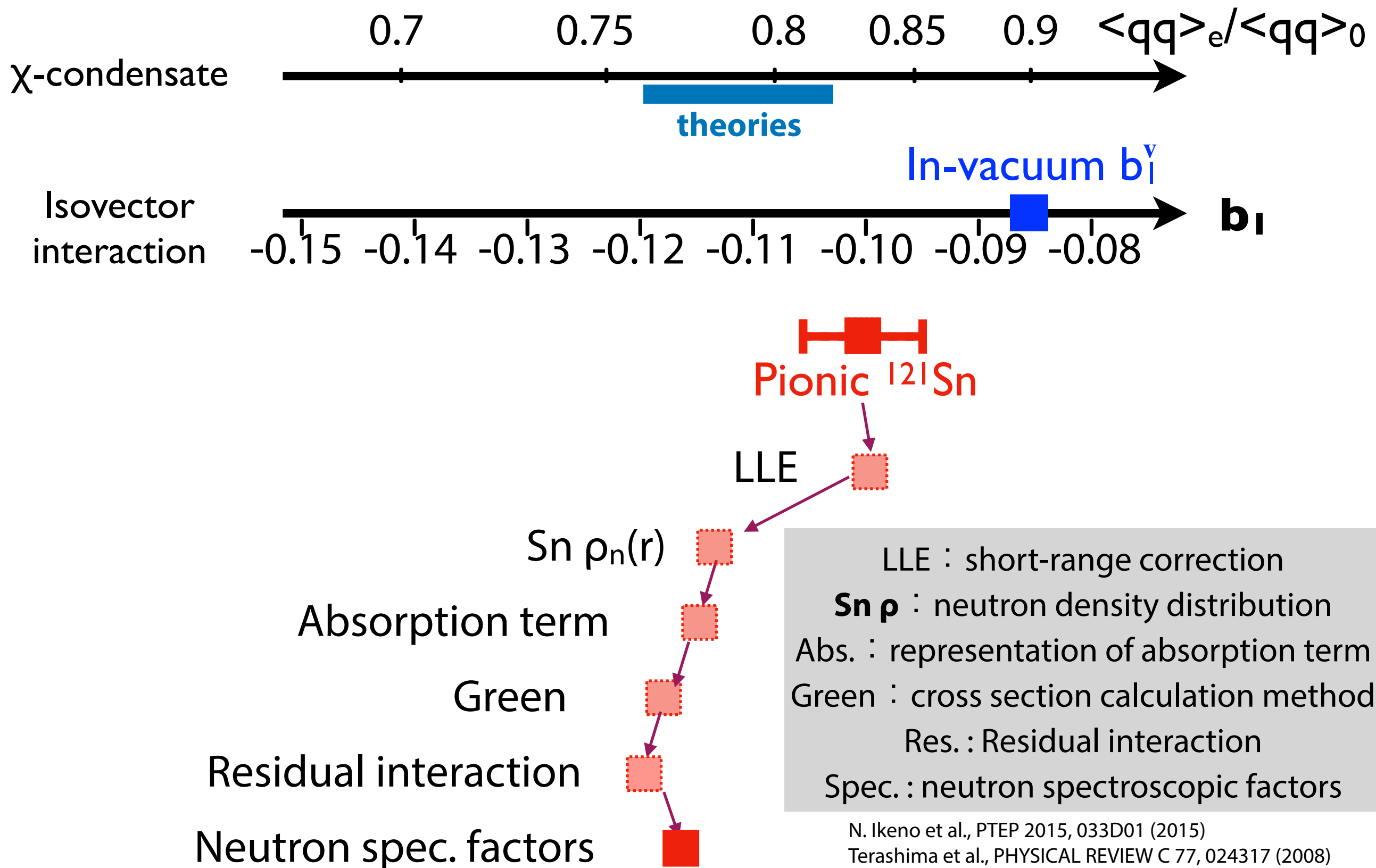
N. Ikeno et al., PTEP 2015, 033D01 (2015)
Terashima et al., PHYSICAL REVIEW C 77, 024317 (2008)
Nose-Togawa et al., PRC71, 061601(R) (2005)
Szwec et al., PRC104,054308 (2022)

Measured nuclear density distribution of Sn isotopes

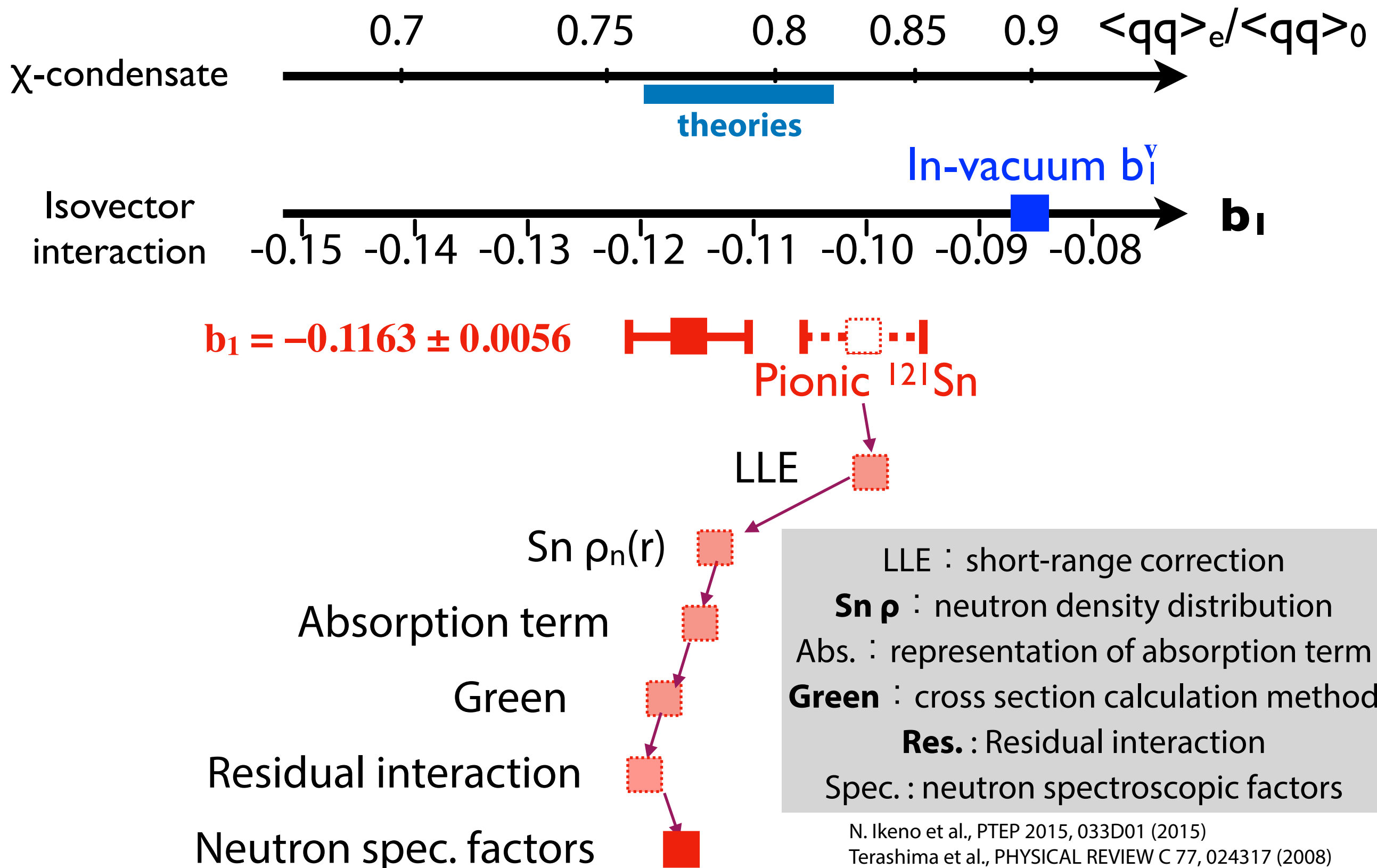
Sn(p,p') reaction at RCNP, Osaka



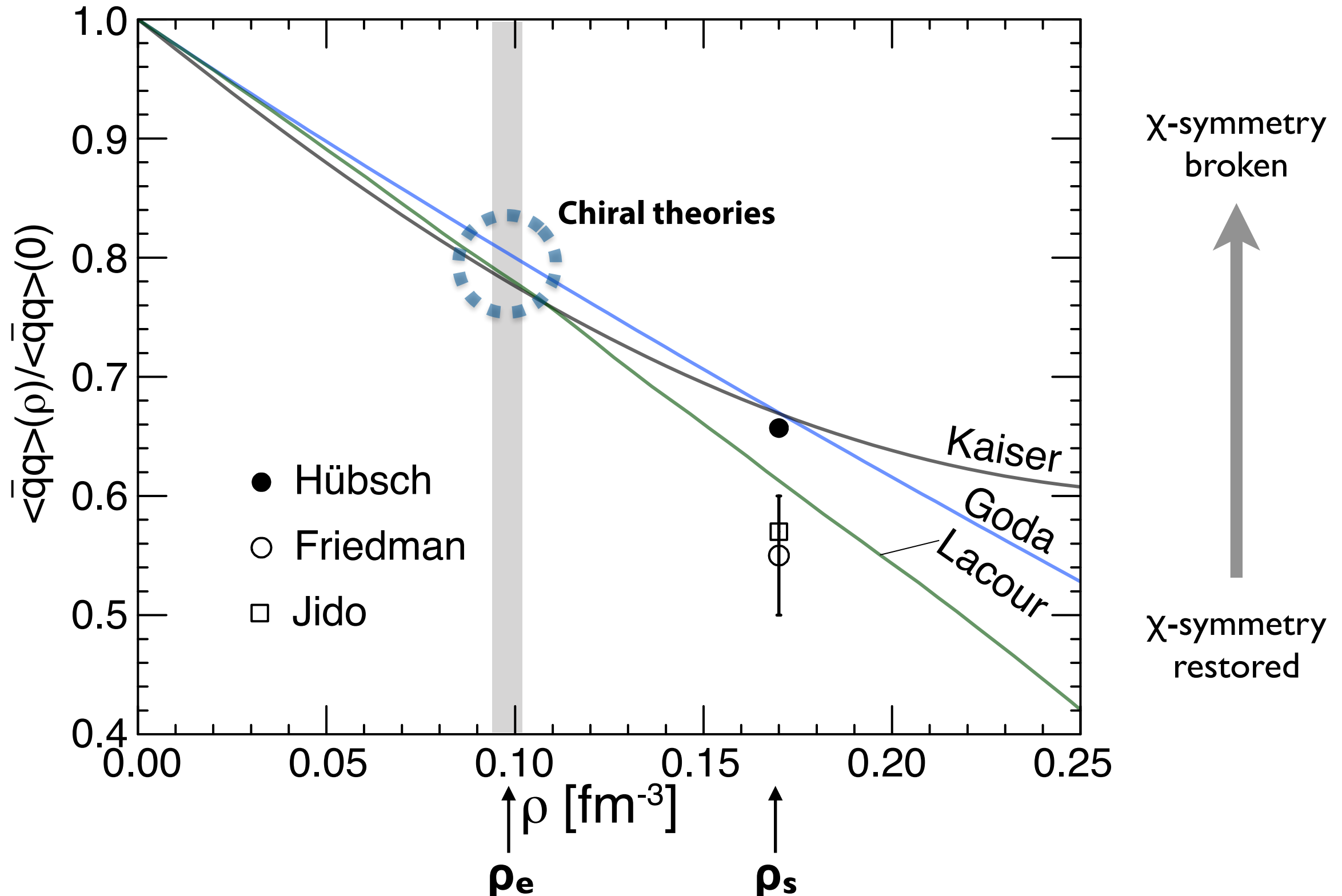
Deduced b_1 with corrections



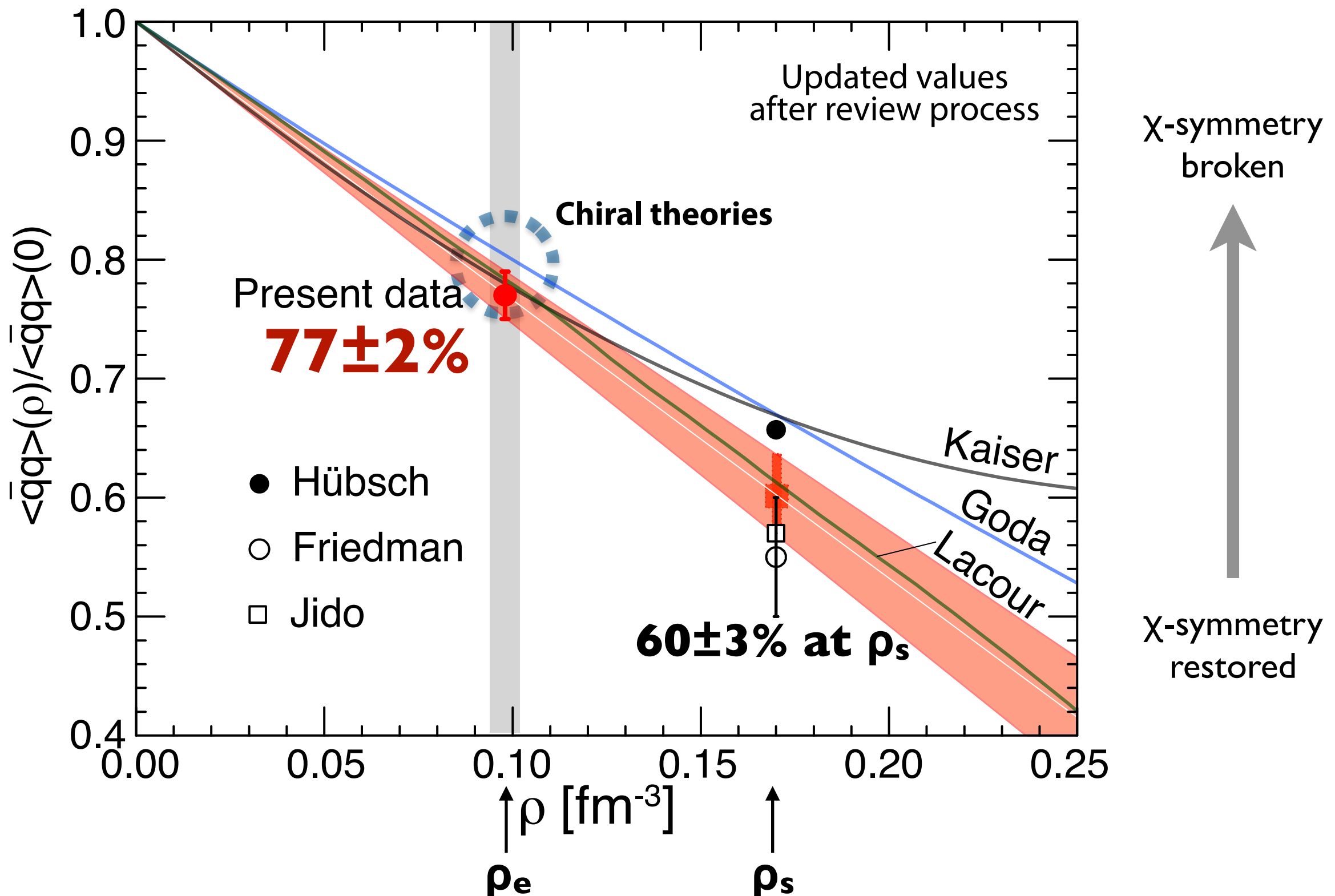
Deduced b_1 with corrections



Result: deduced chiral condensate



Result: deduced chiral condensate



Next Experiments and Future plans

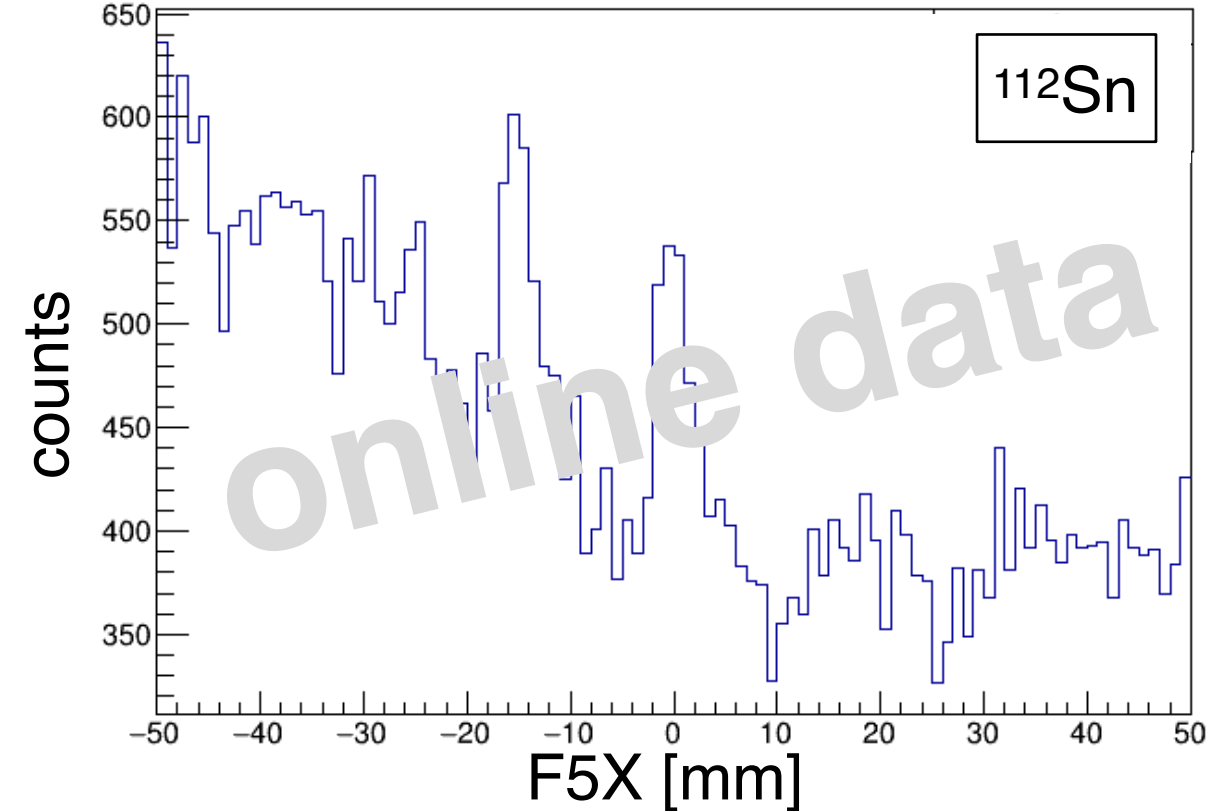
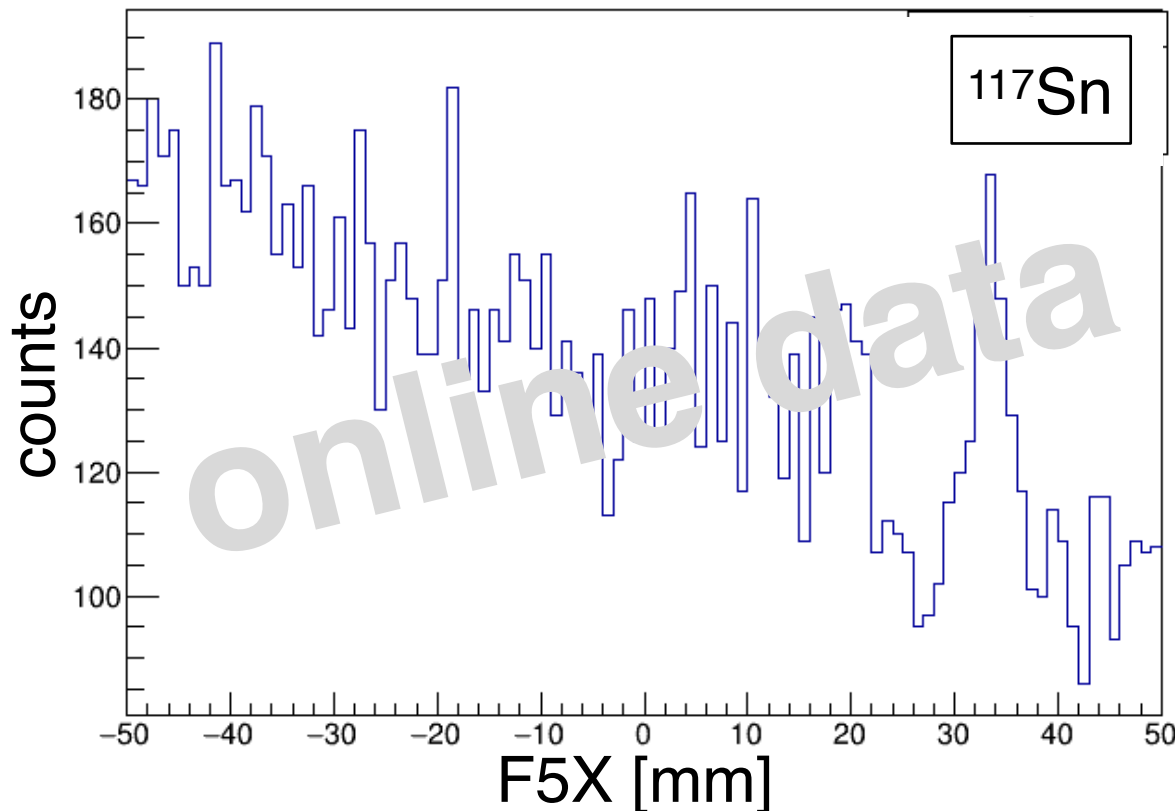
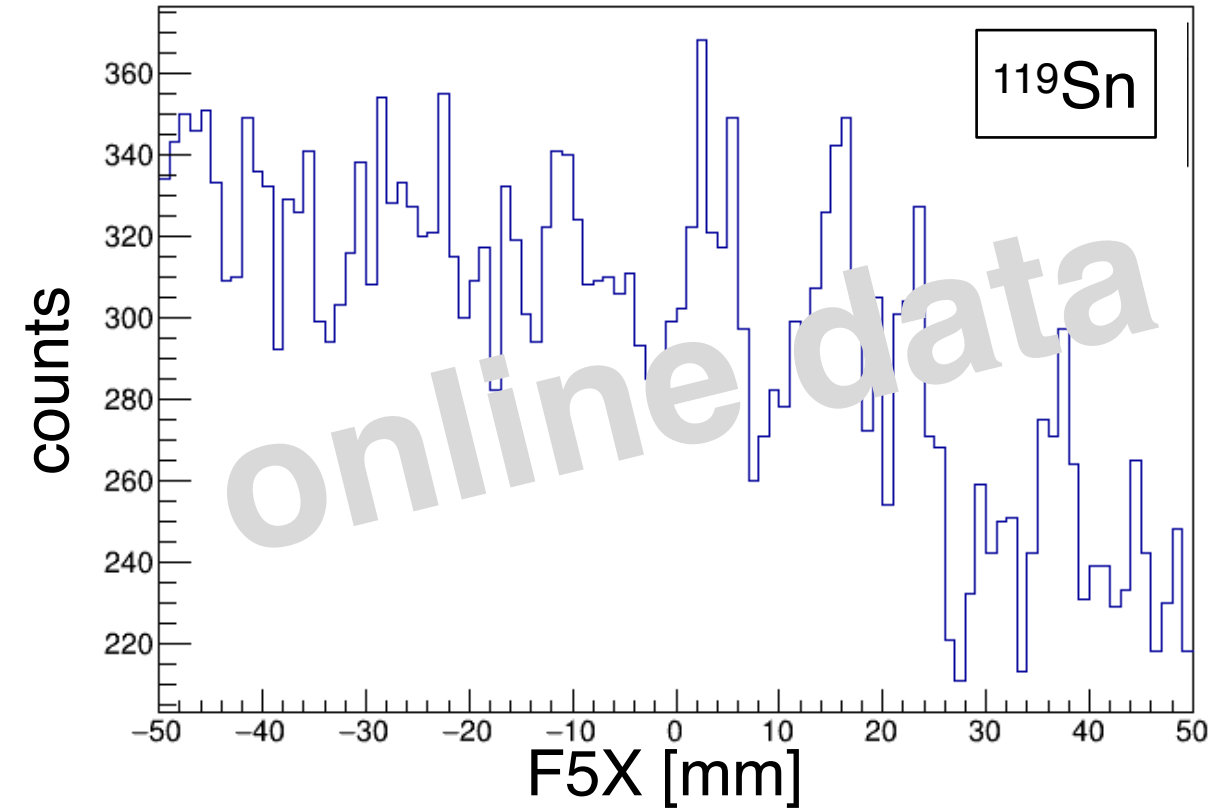
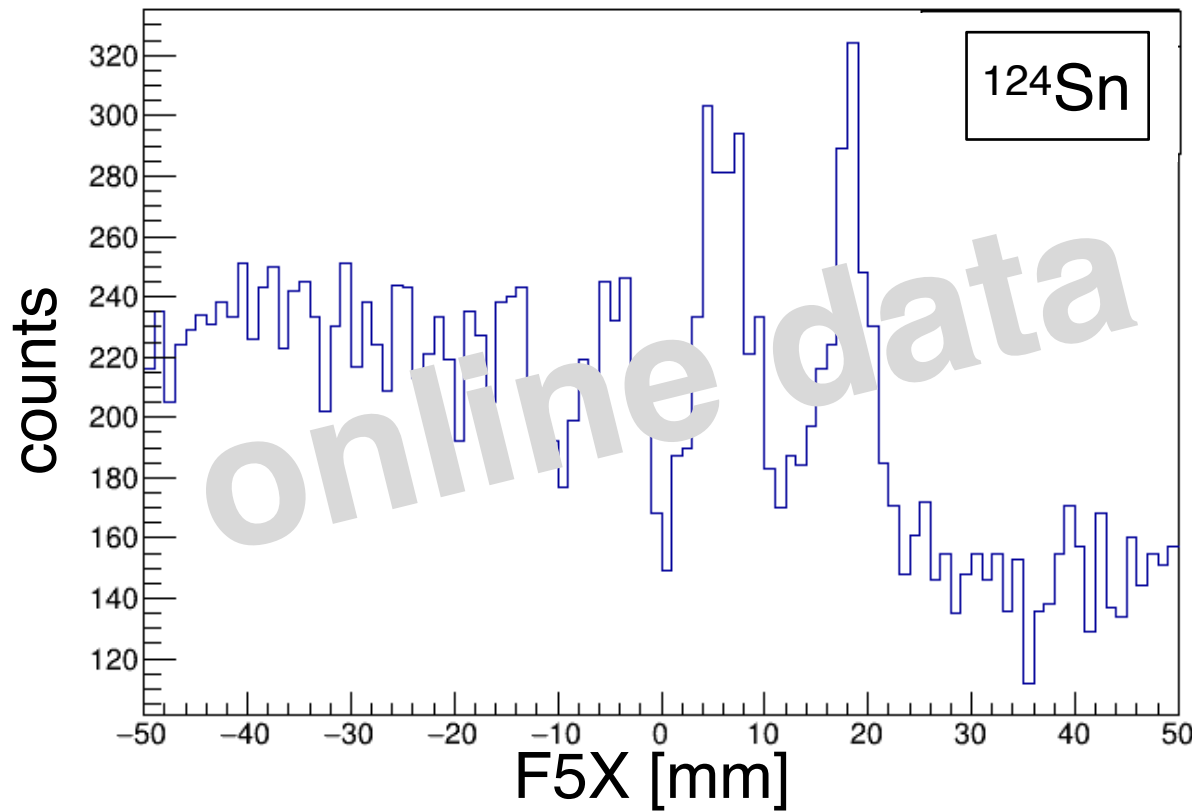
Systematic spectroscopy of pionic Sn isotopes

RIBF-135

113	114	115	116	117	118	119	120	121	122	123	124	125	126	127	128
I	I	I	I	I	I	I	I	I	I	I	I	I	I	I	I
112	113	114	115	116	117	118	119	120	121	122	123	124	125	126	127
Te															
111	112	113	114	115	116	117	118	119	120	121	122	123	124	125	126
Sb															
110	111	112	113	114	115	116	117	118	119	120	121	122	123	124	125
Sn															
109	110	111	112	113	114	115	116	117	118	119	120	121	122	123	124
In															
108	109	110	111	112	113	114	115	116	117	118	119	120	121	122	123
Cd															
107	108	109	110	111	112	113	114	115	116	117	118	119	120	121	122
Ag															

for better precision

Online spectra in RIBF-135 (2021)



Now, we are interested in $\sigma_{\pi N}$

$$\sigma_{\pi N} \equiv m_q / 2m_N \sum_{u,d} \langle N | \bar{q}q | N \rangle$$

quark contribution to nucleon mass

$$\frac{b_1^0}{b_1(\rho)} = \frac{\langle \bar{q}q \rangle(\rho)}{\langle \bar{q}q \rangle(0)} \simeq 1 - \frac{\rho \sigma_{\pi N}}{f_\pi^2 m_\pi^2} \left(1 - \frac{3k_F^2}{10M_N^2} + \frac{9k_F^4}{56M_N^4} \right) + O(\rho^2)$$

$$k_F = (3/2\pi^2\rho)^{1/3}$$

Kaiser et al., PRC77, 025204 (2008)
Gubler, Sato, PPNP106,1(2019)

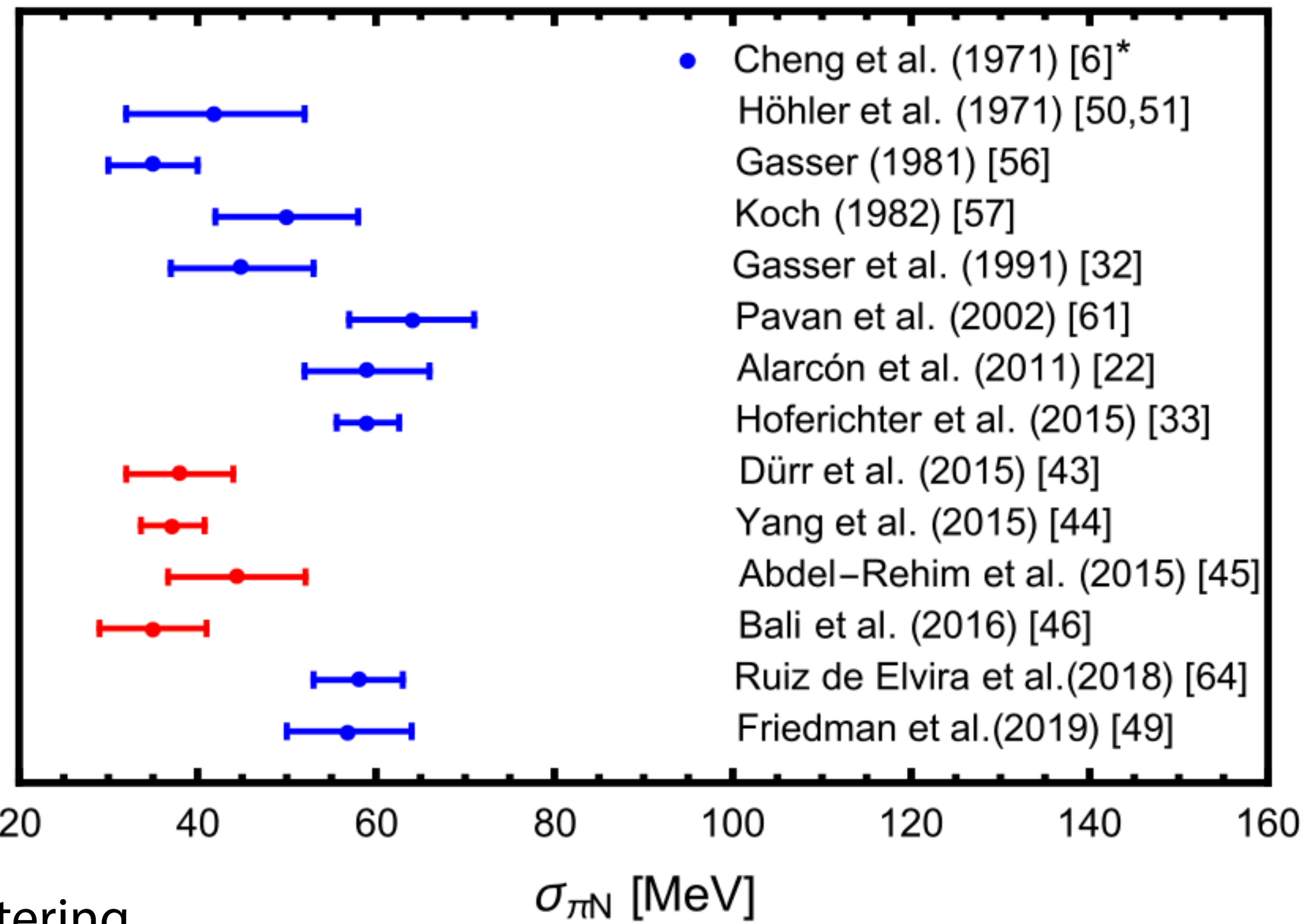
Two approaches:

1. derivation from $b_1(\rho)$

Ikeno et al., PTEP 2023, 033D03

2. determine $d\langle q\bar{q} \rangle/d\rho$ at ρ_e
and extrapolate to $\rho=0$

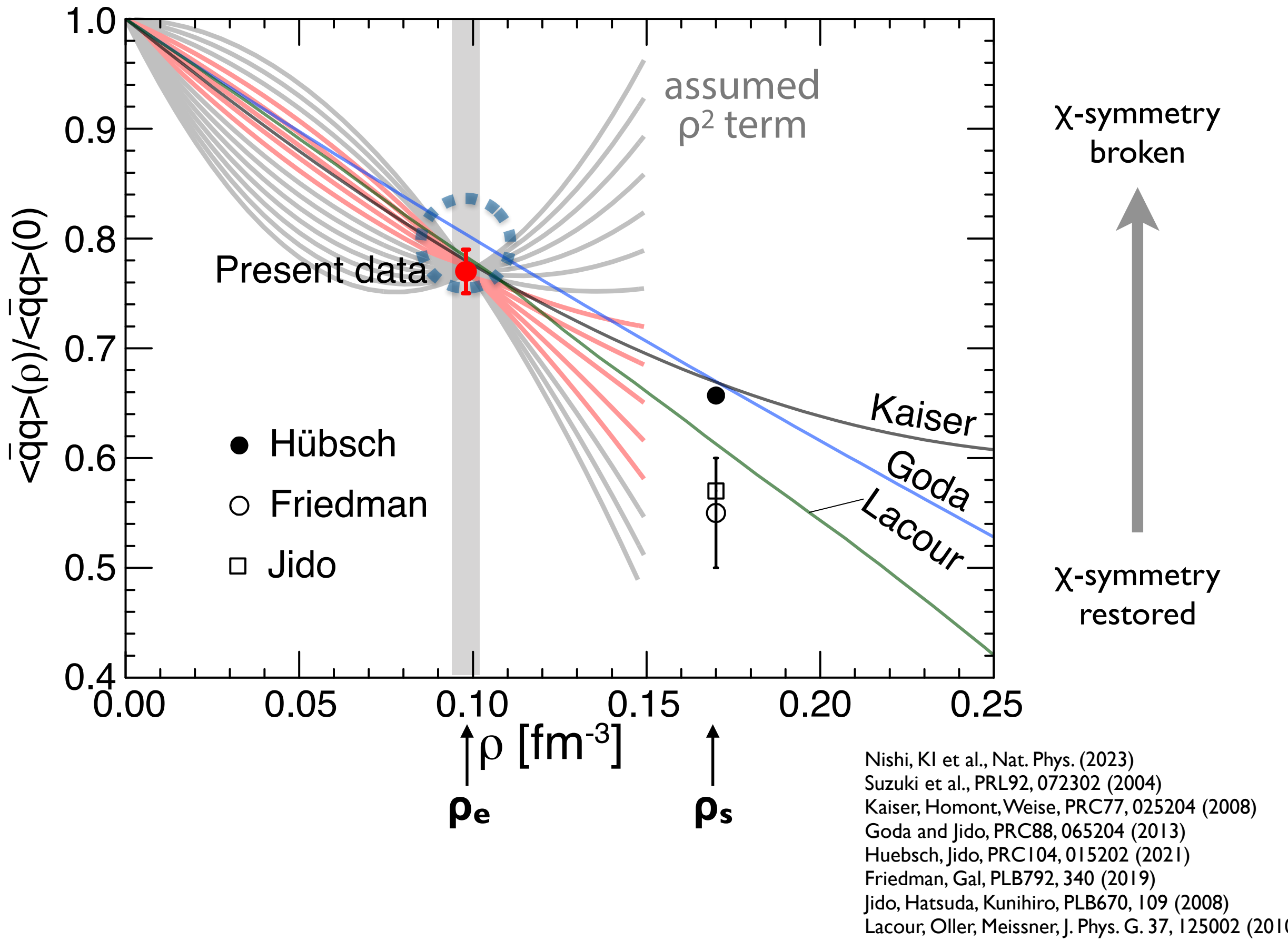
Now, we are interested in $\sigma_{\pi N}$



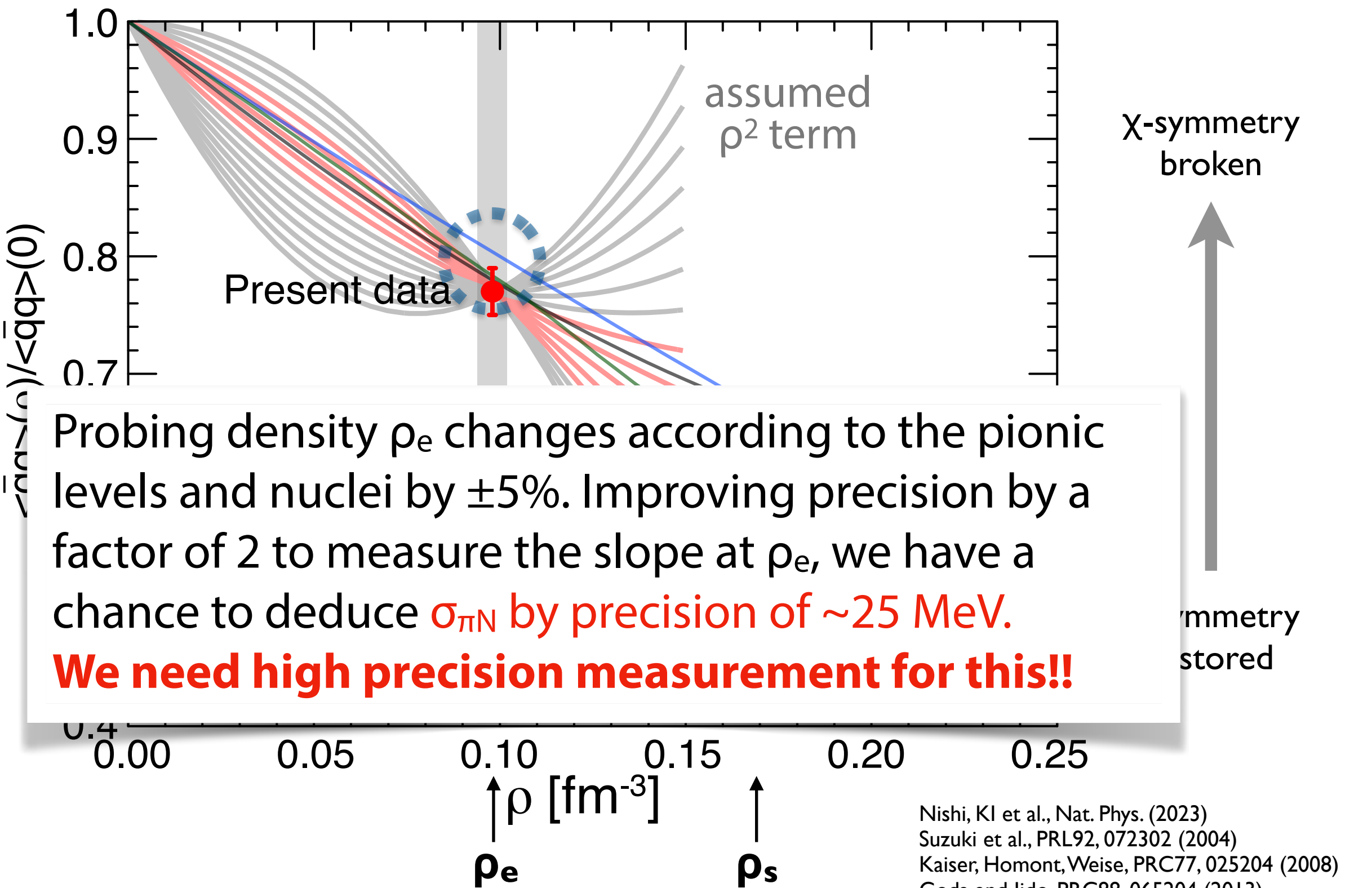
piN scattering
Lattice QCD
Chiral effective theory...

Alarcon, EPJ Spec. Top. (2021) 230:1609–1622
<https://doi.org/10.1140/epjs/s11734-021-00145-6>

New interest in $\sigma_{\pi N}$ term



New interest in $\sigma_{\pi N}$ term



↑
 ρ_e ↑
 ρ_s

- Nishi, KI et al., Nat. Phys. (2023)
Suzuki et al., PRL92, 072302 (2004)
Kaiser, Homont, Weise, PRC77, 025204 (2008)
Goda and Jido, PRC88, 065204 (2013)
Huebsch, Jido, PRC104, 015202 (2021)
Friedman, Gal, PLB792, 340 (2019)
Jido, Hatsuda, Kunihiro, PLB670, 109 (2008)
Lacour, Oller, Meissner, J. Phys. G. 37, 125002 (2010)

Next Experiment RIBF-214

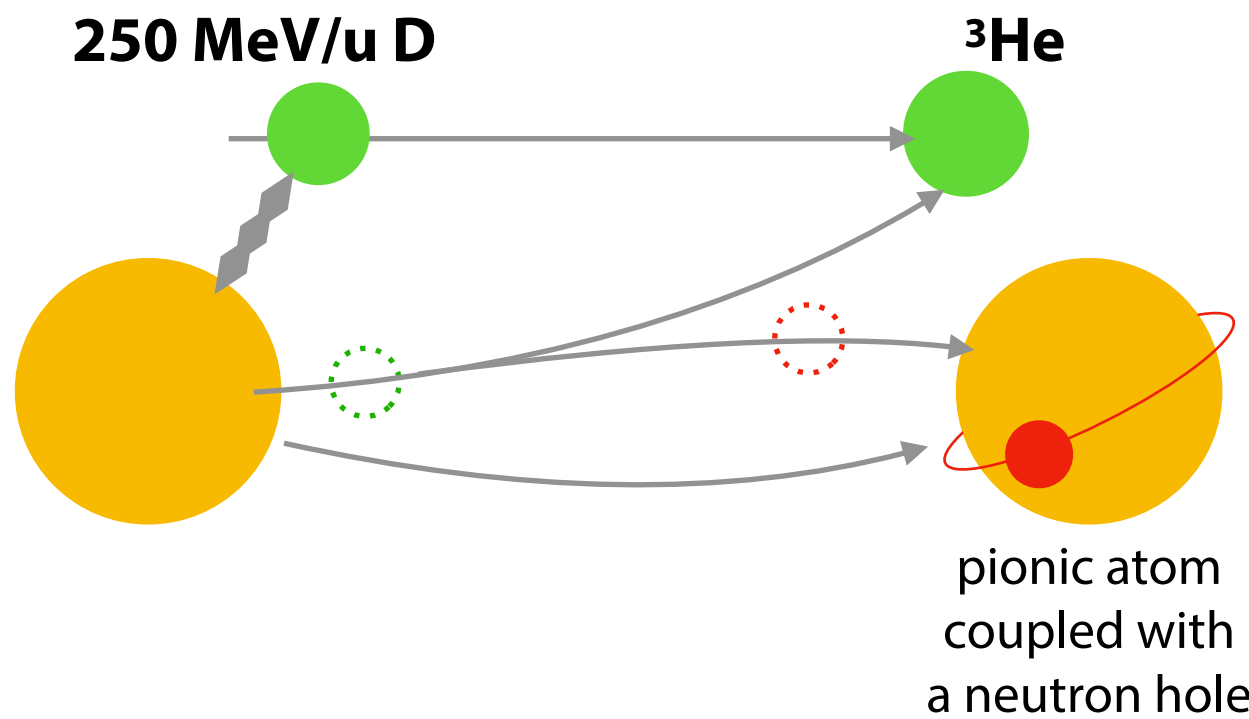
PAC approved with A

Proposing D(^{136}Xe , ^3He) reaction at T = 250 MeV/u at RIBF

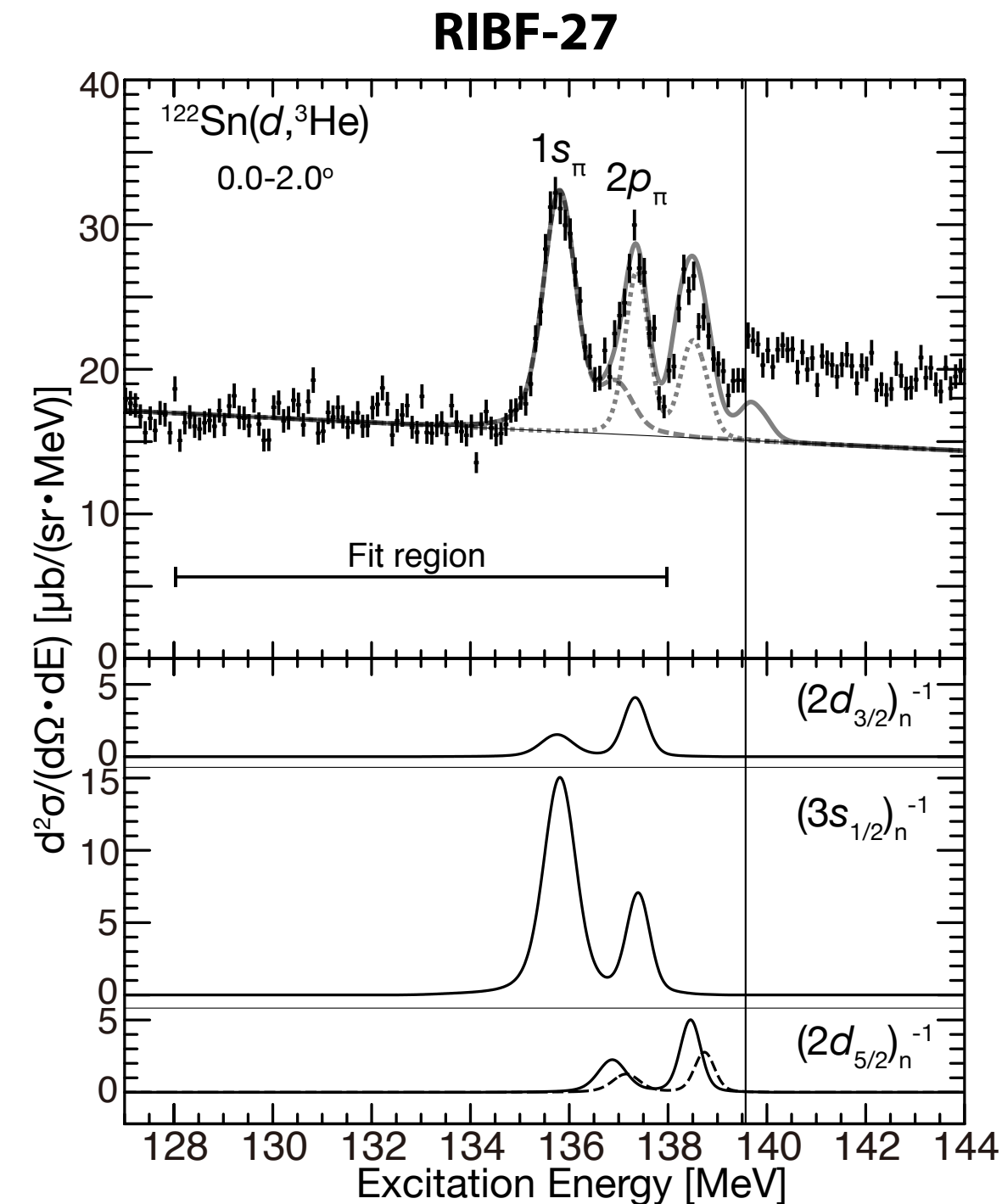
N=82

inverse kinematics reactions

Normal kinematics ($d, {}^3\text{He}$) reactions

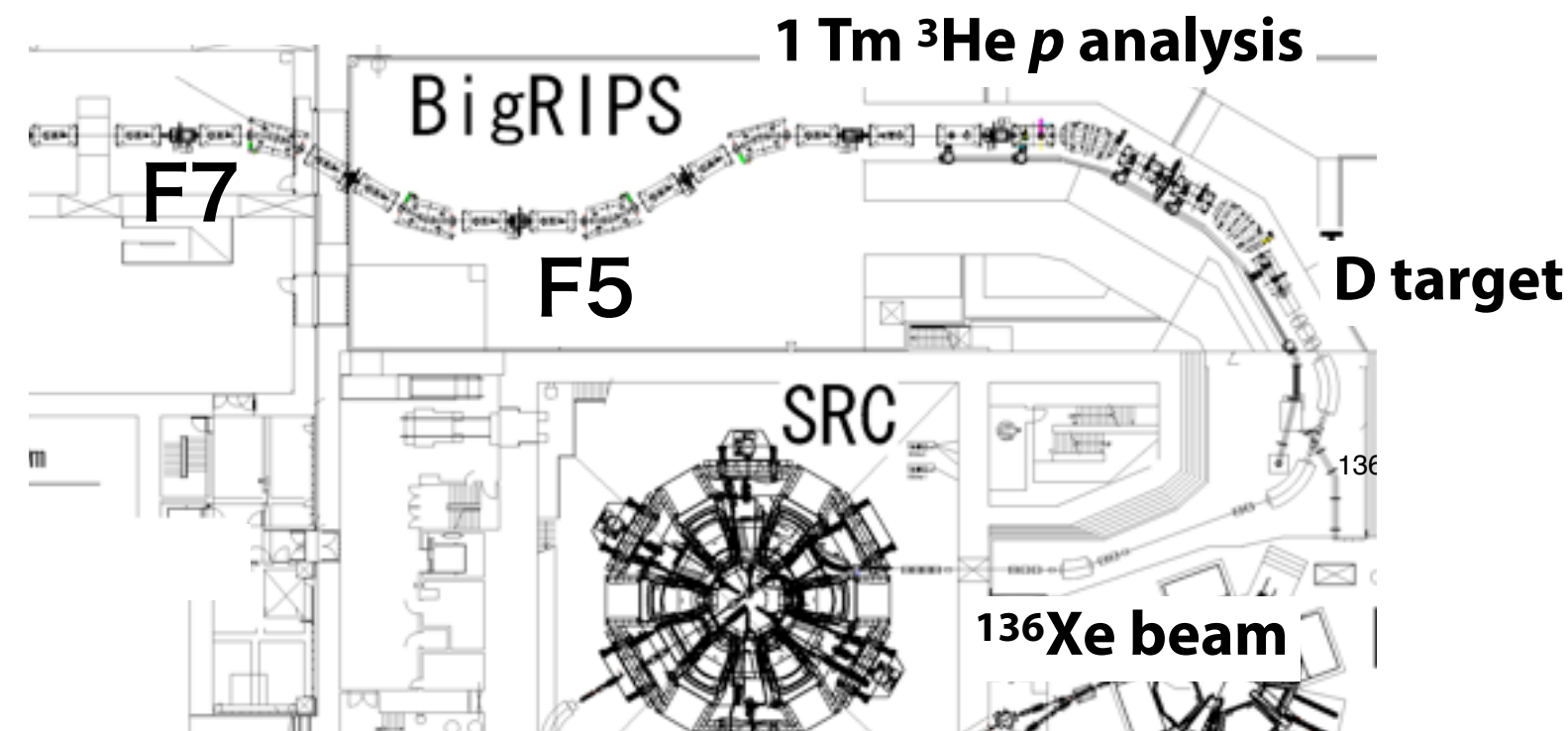
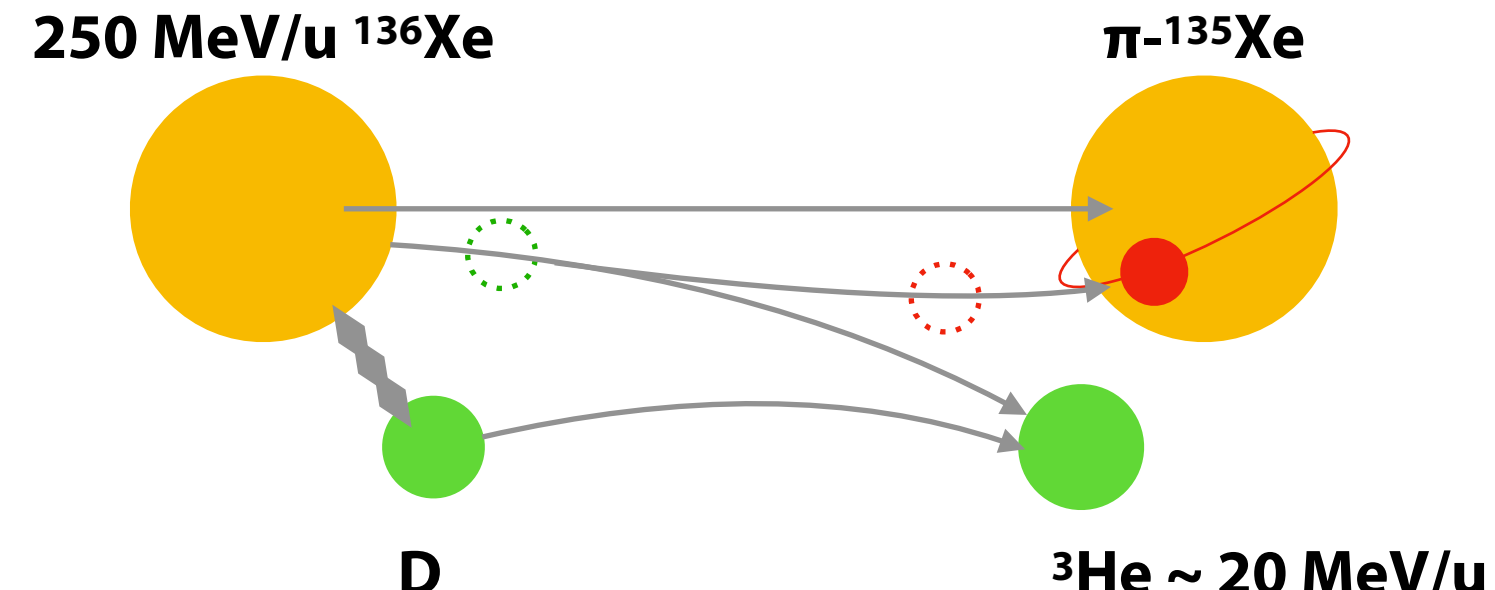


We measure ${}^3\text{He}$ energy for missing-mass and deduce mass of reaction product



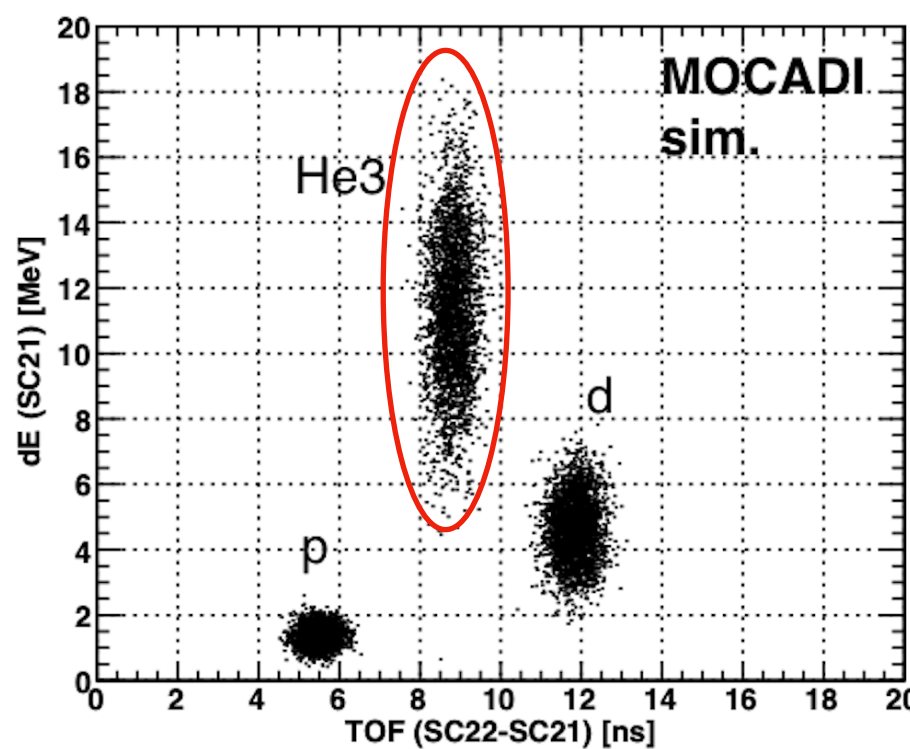
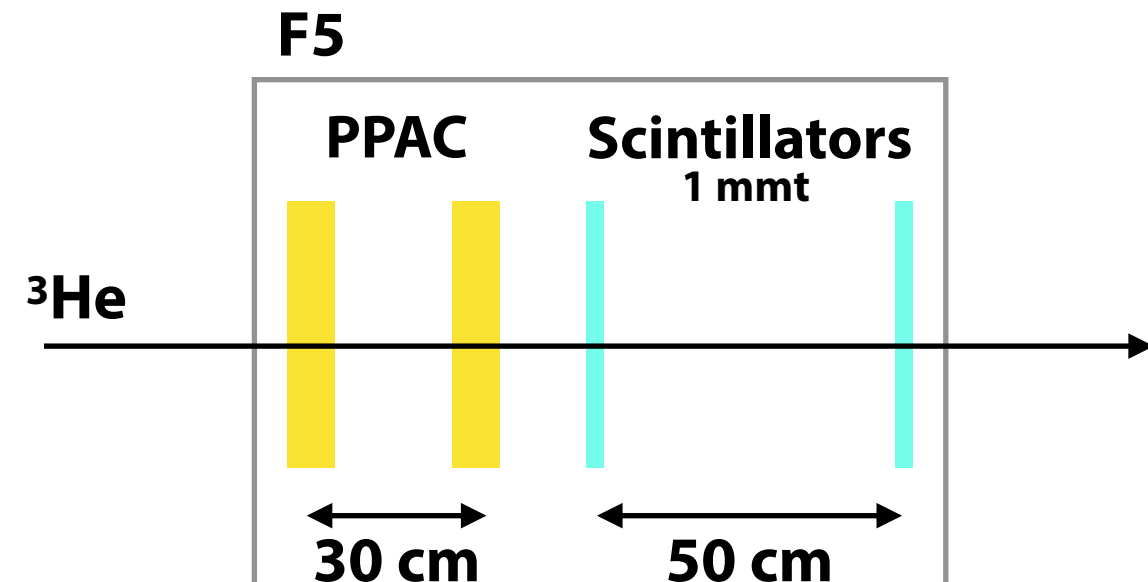
inverse kinematics reactions

We make use of BigRIPS
as spectrometer and
deduce MM by ^3He
momentum measurement

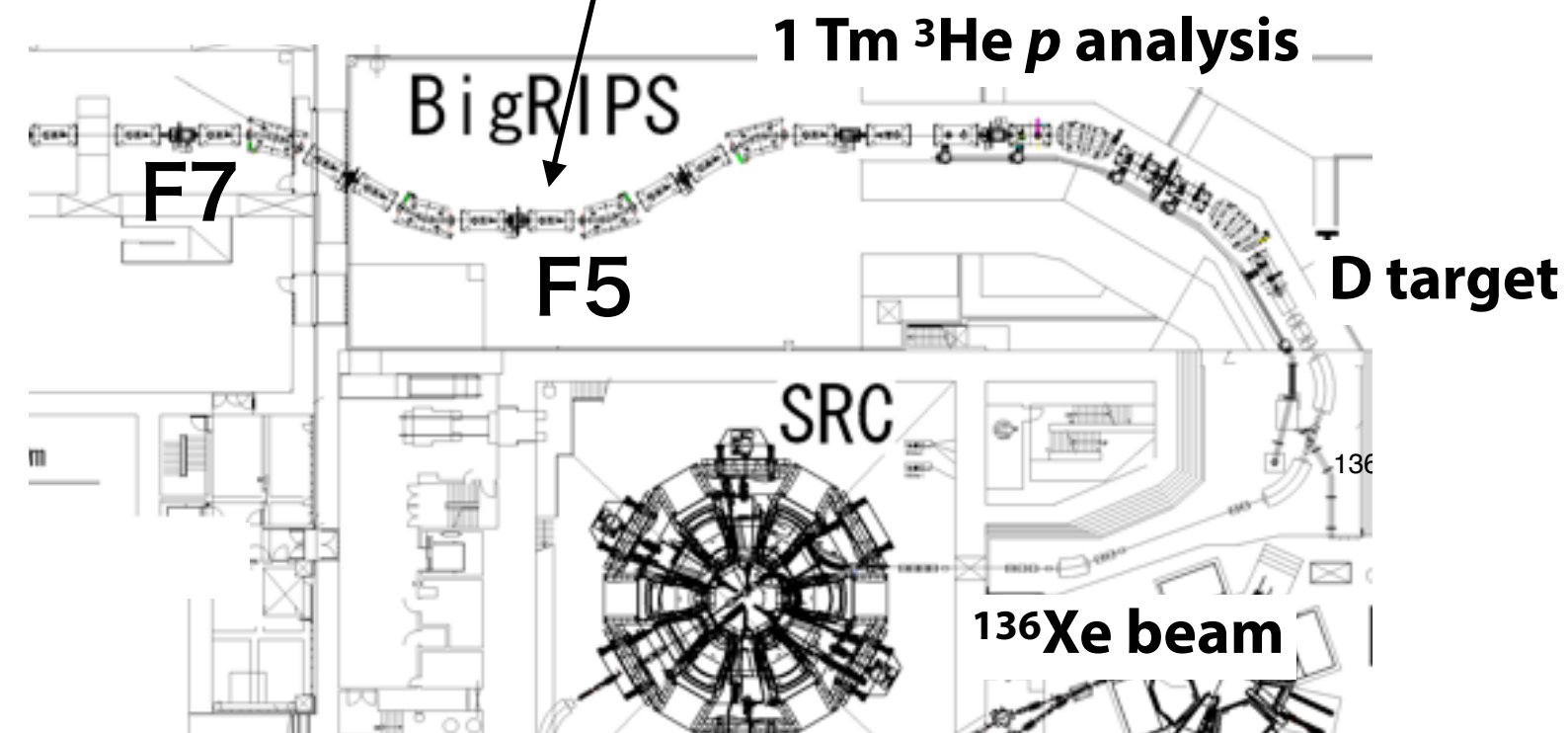


Experimental setup

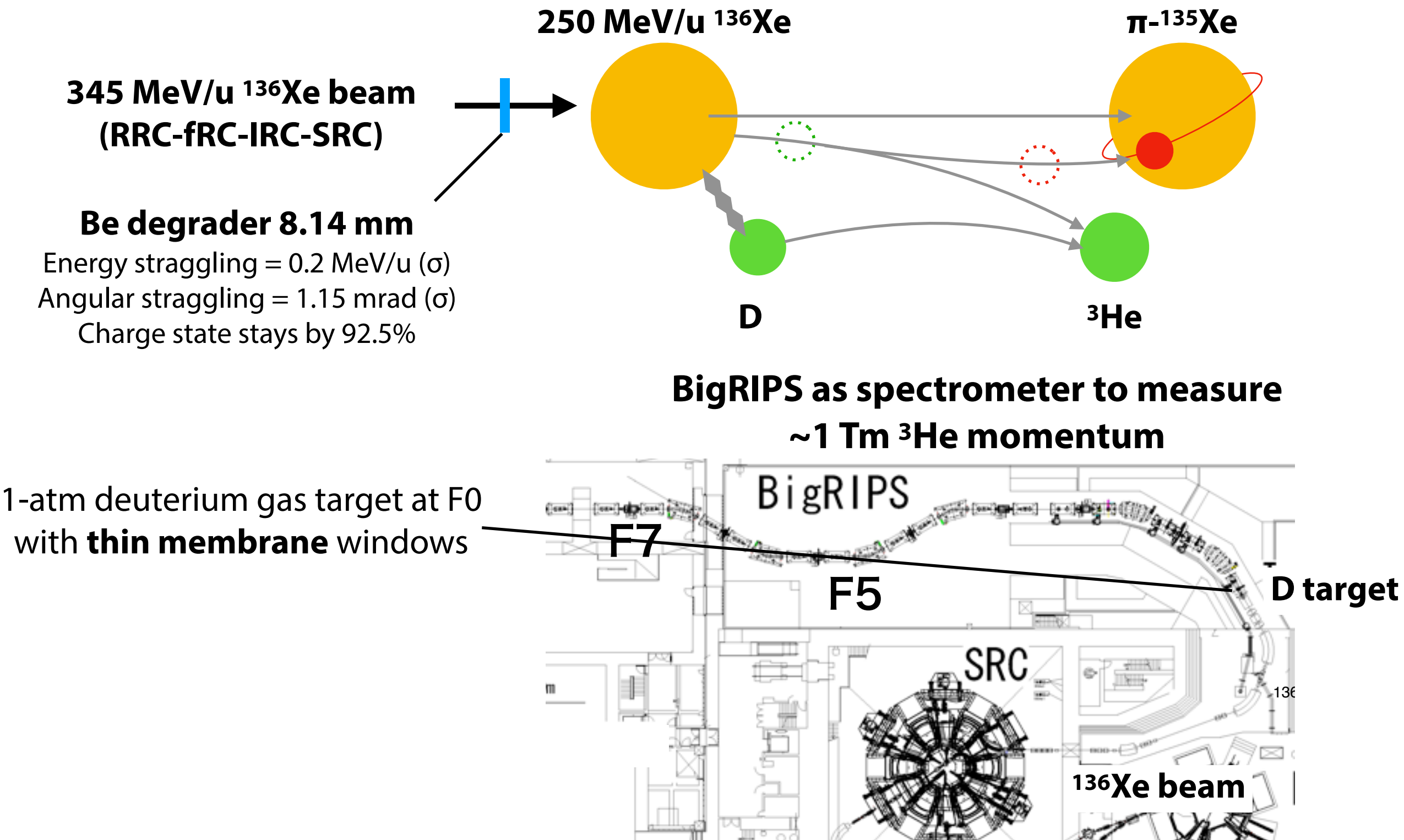
PPAC



${}^3\text{He}$ trigger by ΔE (and TOF)

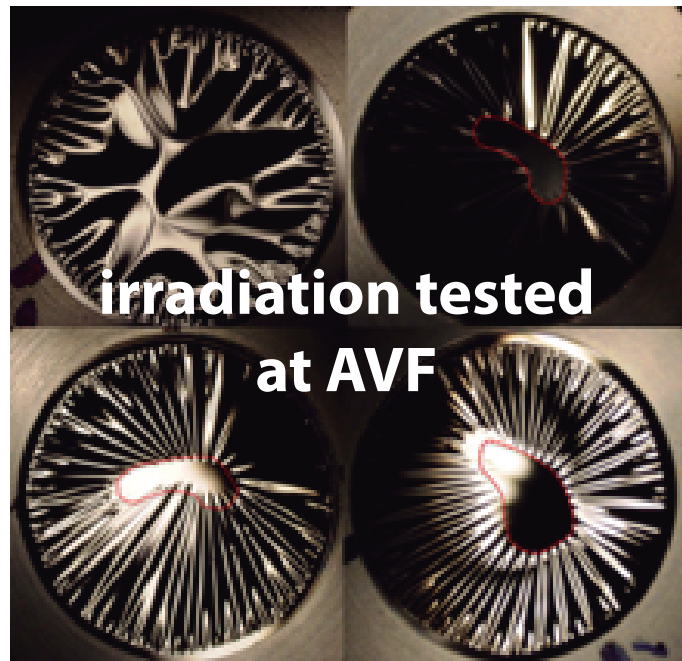


Experimental setup



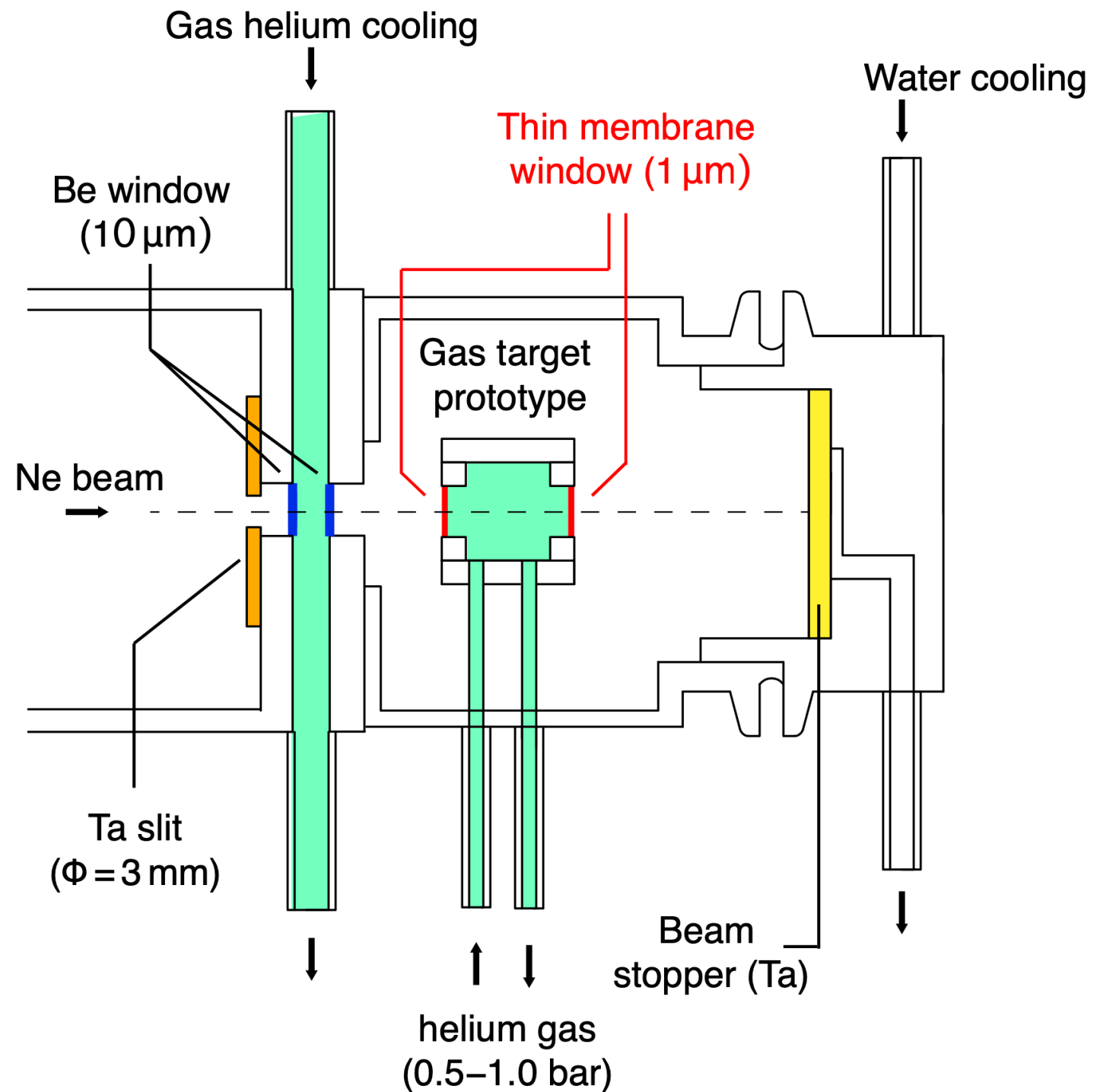
Deuterium gas target development

1 μm graphene foil
tested till breakdown
with 5 MeV Ne beam (2018)



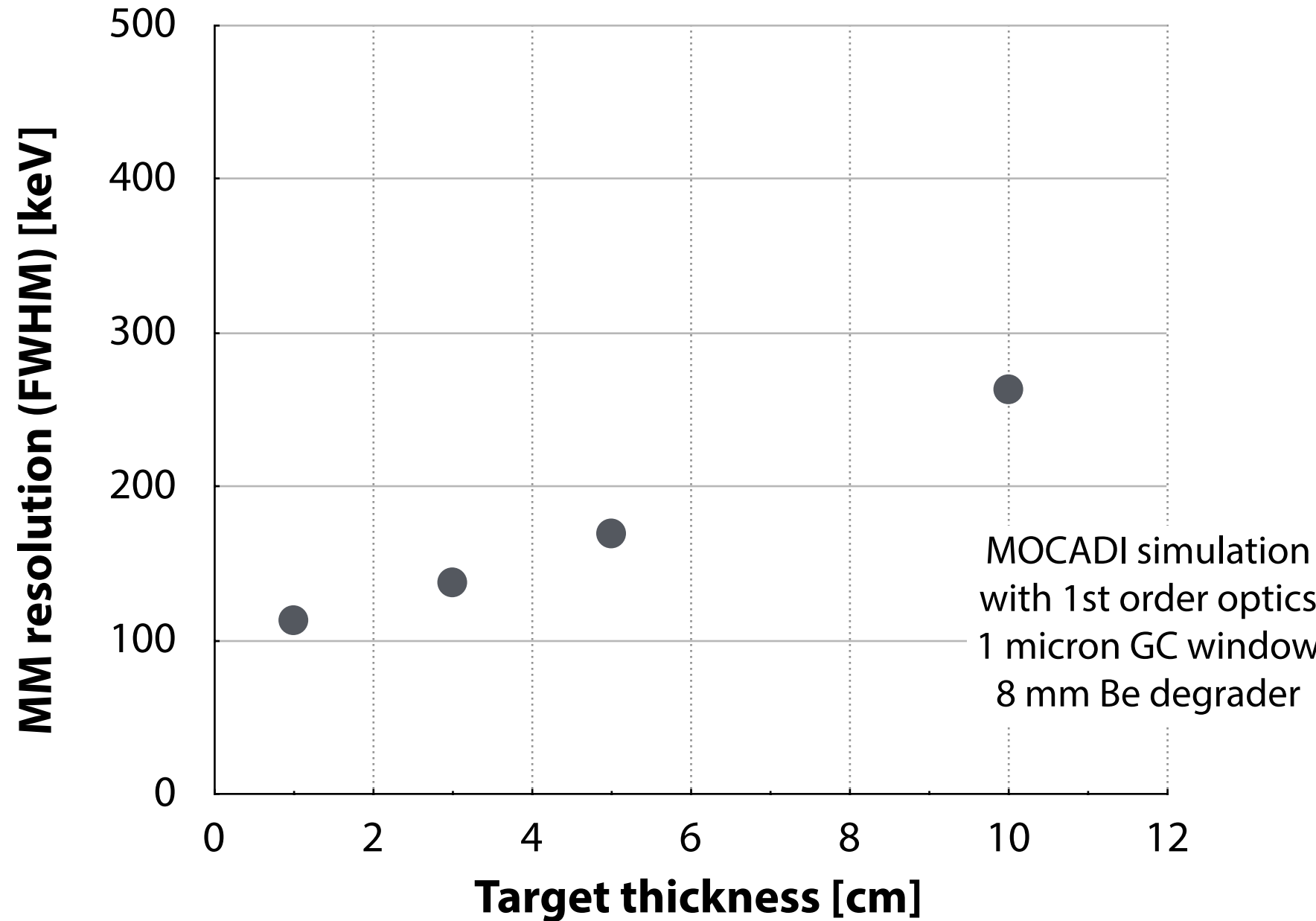
S. Purushothaman et al., APR **53**, 134 (2019)

**Beam test in 2024/4-5
to hold 0.5-1 atm He**

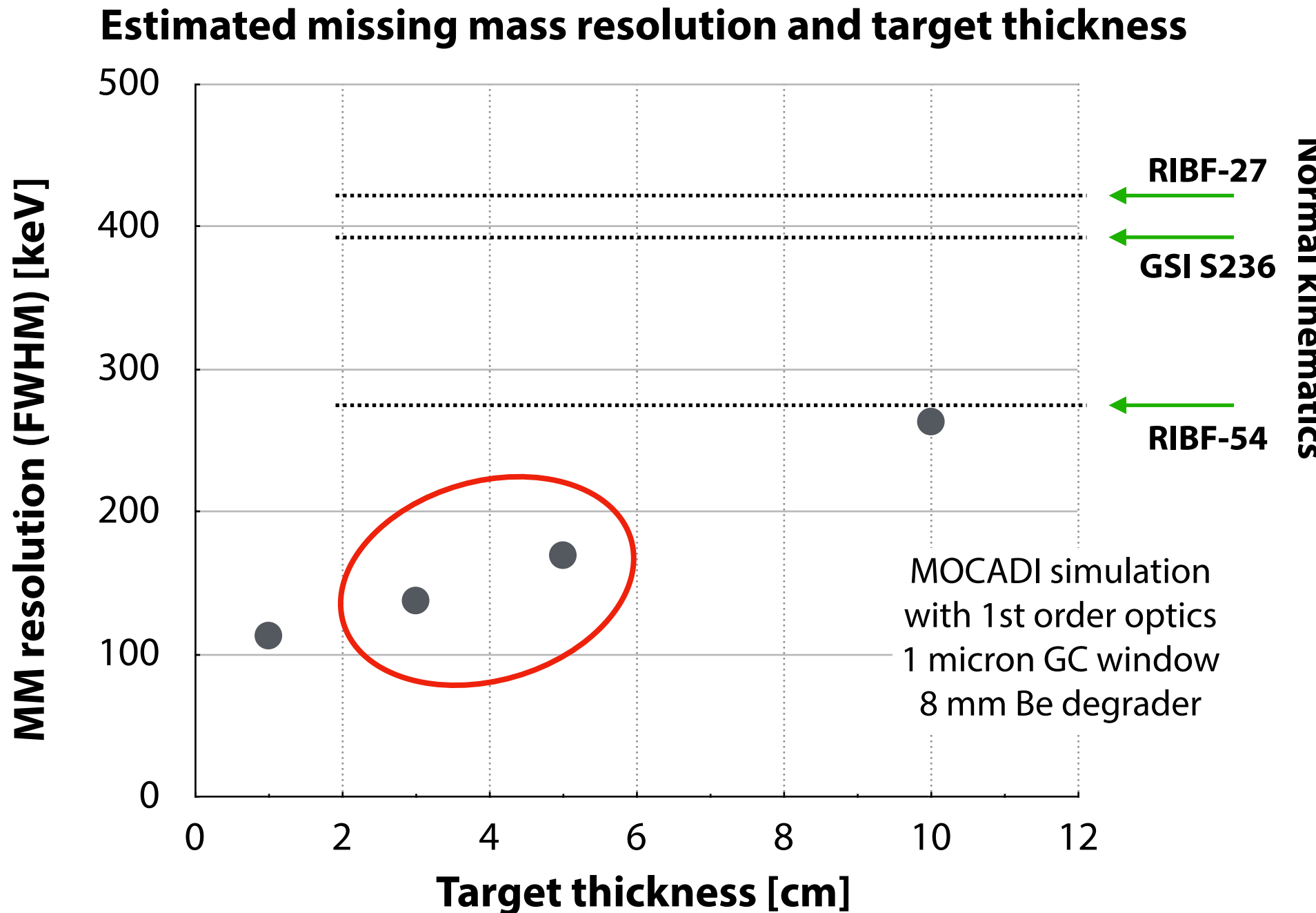


Missing mass resolution

Estimated missing mass resolution and target thickness



Missing mass resolution can be improved!

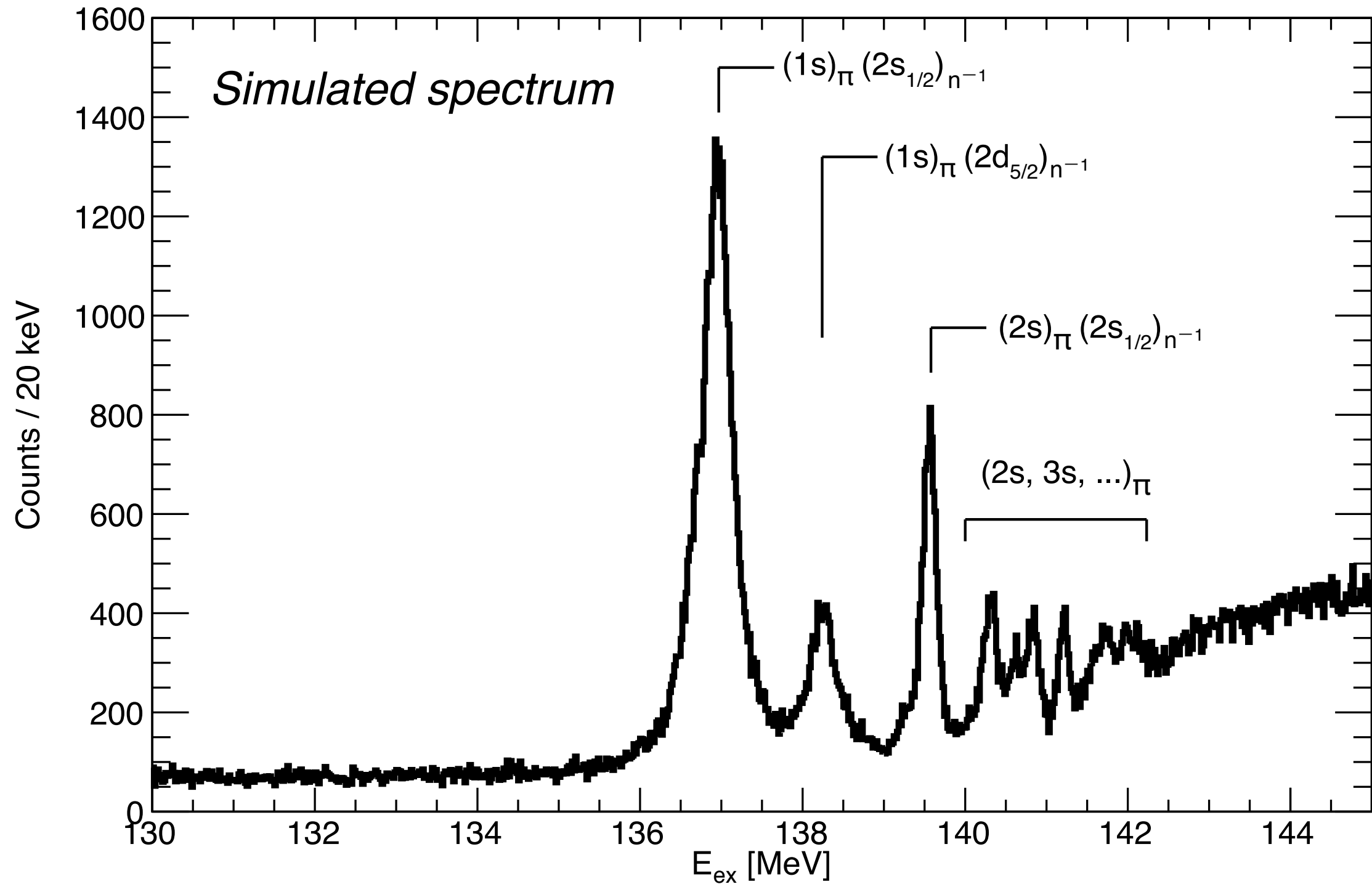


Unprecedented resolution can be achieved
 → Important for resolving higher orbitals and determine the widths

cf. For normal kinematics, resolution has been limited by beam properties.

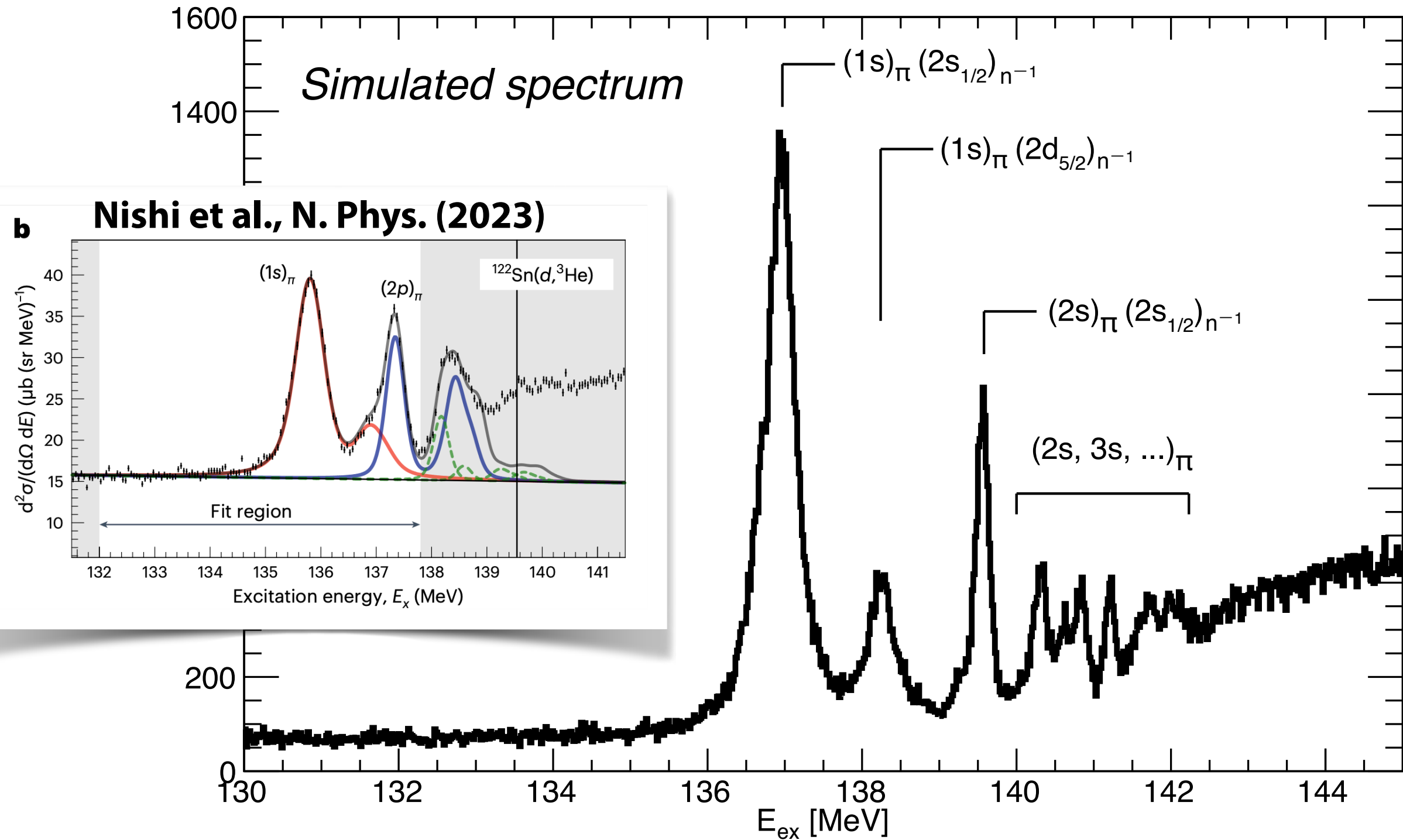
Striking spectrum with 150 keV resolution

36 hours with $10^{10}/\text{s}$ ^{136}Xe beam 4 cm target



Striking spectrum with 150 keV resolution

36 hours with $10^{10}/\text{s}$ ^{136}Xe beam 4 cm target



Summary

- Chiral condensate at ρ_e is evaluated to be reduced by $77 \pm 2\%$, which is linearly extrapolated to $60 \pm 3\%$ at the nuclear saturation density.
- The binding energies and widths of the pionic $1s$ and $2p$ states in Sn121 were determined with high precision. Taking difference between the $1s$ and $2p$ values drastically reduces the systematic errors.
- Recent theoretical progress was adopted to the $\langle qq \rangle$ deduction, which directly relates the chiral condensate and the pion-nucleus interaction.
- We calculated various corrections for the first time and applied them. The corrections made substantial effects. After the corrections, the chiral condensate ratio was deduced with much higher reliability.
- For future, we are analyzing data of systematic study of pionic Sn isotopes to achieve higher precision $\langle qq \rangle$.
- We also plan measurement in “inverse kinematics” reactions for pionic Xe 136. The resolution will be further improved. Now, we are aiming at determination of the $\pi N \sigma$ term.